



Title	REACTION MECHANISM OF F1-ATPASE
Author(s)	Matsuoka, Ichiro
Citation	Osaka University. 博士(理学)
Issue Date	1982-03-25
Doc URL	<a href="http://hdl.handle.net/2115/32903">http://hdl.handle.net/2115/32903</a>
Type	theses (doctoral)
File Information	matsuoka.pdf



[Instructions for use](#)

REACTION MECHANISM OF  $F_1$ -ATPASE

ICHIRO MATSUOKA

DEPARTMENT OF BIOLOGY, FACULTY OF SCIENCE, OSAKA UNIVERSITY

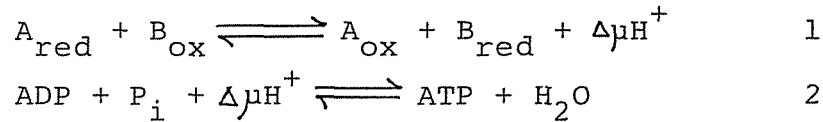
FEBRUARY 1982

## CONTENTS

GENERAL INTRODUCTION .....	2
ABBREVIATIONS .....	5
PART I. Reaction Mechanism of the ATPase Activity of Mitochondrial $F_1$ , Studied by Using a Fluorescent ATP Analog, 2'-(5-Dimethylaminonaphthalene-1- Sulfonyl) Amino-2'-DeoxyATP: Its Striking Resemblance to That of Myosin ATPase. ....	6
SUMMARY .....	7
INTRODUCTION .....	10
MATERIALS & METHODS .....	12
RESULTS .....	16
DISCUSSION .....	54
REFERENCES .....	63
PART II. Reactions of a Fluorescent ATP Analog, 2'-(5- Dimethylaminonaphthalene-1-Sulfonyl) Amino-2'- DeoxyATP, with <u>E.coli</u> $F_1$ -ATPase and Its Subunits.-	66
SUMMARY .....	67
INTRODUCTION .....	69
MATERIALS & METHODS .....	71
RESULTS .....	73
DISCUSSION .....	97
REFERENCES .....	104
ACKNOWLEDGMENTS .....	107
LIST OF PUBLICATIONS .....	108

## GENERAL INTRODUCTION

In oxidative phosphorylation and photophosphorylation, exergonic oxidation-reduction reactions are coupled to the endergonic synthesis of ATP. The chemiosmotic hypothesis of Peter Mitchell(1) best describes the manner in which energy is conserved during ATP synthesis; that is, a transmembrane electrochemical gradient serves as a required intermediate in the following energy conversion processes (Reaction 1 & 2).



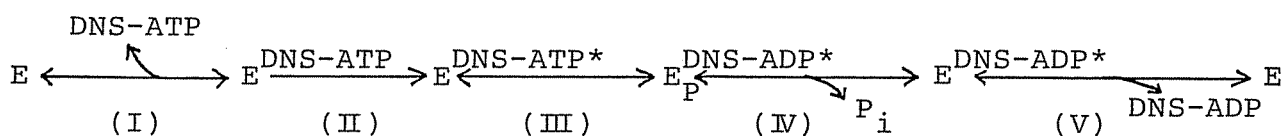
The vectorial transport of protons across the membrane associated with electron transport gives rise to a electrochemical gradient,  $\Delta\mu\text{H}^+$  (Reaction 1). The energy stored in this gradient is used by membrane-bound coupling factors,  $F_1-F_0$ , to drive the net synthesis of ATP (Reaction 2). As this reaction is reversible, the proton gradient is also formed during the net hydrolysis of ATP(1).

The complex of coupling factors that catalyzes Reaction 2 has two empirically defined components.  $F_0$  is an integral membrane complex of three distinct subunits, and has shown to play an essential role in the translocation of protons(2).  $F_1$  can be detached from the membrane as a water soluble complex of five subunits,  $\alpha$  to  $\epsilon$  (2). The enzyme,  $F_1$ , contains catalytic site for ATP synthesis and hydrolysis. However, the major question still to be answered is, How does the  $F_1-F_0$  complex catalyze the synthesis of ATP? When physically separated from membrane, soluble  $F_1$  is only capable of catalyzing the net hydrolysis of ATP. However, if we assume the mechanism of ATP synthesis is the

reversal of that of ATP hydrolysis, we can elucidate the mechanism of ATP synthesis from the detailed analysis on the mechanism of ATP hydrolysis catalyzed by soluble  $F_1$ . Thus, the reaction mechanism of  $F_1$ -ATPase is the subject of this thesis.

I attempted to clarify the reaction mechanism of  $F_1$ -ATPase using a fluorescent analog of ATP. Thus, 2'-(5-dimethylamino-naphthalene-1-sulfonyl) amino-2'-deoxyATP (DNS-ATP) was synthesized by Watanabe and coworkers(3). DNS-ATP has the following advantages for the present purpose. (1) The fluorescence intensity of DNS-ATP increases markedly on its bunding to  $F_1$ , and it reflects the environment of nucleotide binding site of  $F_1$ . (2) DNS-ATP is hydrolyzed by  $F_1$  very slowly, making kinetic measurements easier than with ATP. (3) DNS-AT<sup>32</sup>P can be easily synthesized enzymatically.

In this thesis, following conclusions were drawn from the analysis of the reactions of DNS-ATP with  $F_1$  (isolated from beef heart mitochondria) and  $EF_1$  (isolated from E. coli plasma membrane): (1)  $F_1$  contains two identical DNS-ATP binding sites. The affinity of the sites for DNS-ATP is very high, and the-DNS-ATP bound to this site is hydrolyzed according to the following reaction scheme:



This scheme is quite resembles that of myosin ATPase. (2) High concentrations of nucleotide, such as ATP, accelerate the steps (III), (IV), and (V) in the above scheme. Thus, the low affinity regulatory site(s) is suggested to exist, besides the high affinity catalytic sites. (3) DNS-ATP binds to  $\alpha$  subunit of  $EF_1$  with very high affinity and not to  $\beta$  subunit. The chemical modification of

$\beta$  subunit of  $EF_1$  with DCCD does not change the binding of DNS-ATP to  $EF_1$  (steps (I) and (II)), and does not inhibit the single turnover of DNS-ATP cleavage (step (III)). However, this modification leads to the inhibition of accelerating effect of ATP on the DNS-nucleotide release from  $EF_1$  (step (V)), and leads to the inhibition of  $EF_1$ -ATPase activity at steady state. Therefore, it is suggested that the high affinity catalytic site and low affinity regulatory site exist in the  $\alpha$  subunit and  $\beta$  subunit, respectively.

1. Mitchell, P. (1977) Ann. Rev. Biochem. 46, 996-1005
2. Kagawa, Y. (1978) Biochim. Biophys. Acta 505, 45-93
3. Watanabe, T., Inoue, A., Tonomura, Y., Uesugi, S., & Ikehara, M. (1981) J. Biochem. 90, 957-965

## ABBREVIATIONS

ATP	adenosinetriphosphate
ADP	adenosinediphosphate
AT <sup>32</sup> P	[ $\gamma$ - <sup>32</sup> P]ATP
DNS-ATP and DNS-ADP	2'-(5-dimethylaminonaphthalene-1-sulfonyl) amino- 2'-deoxyATP and -deoxyADP
DNS-AT <sup>32</sup> P	[ $\gamma$ - <sup>32</sup> P]DNS-ATP
CTP	cytidinetriphosphate
GTP	guanosinetriphosphate
ITP	inosinetriphosphate
NTP and NDP	nucleoside tri- and diphosphate
AMPPNP	adenylyl-5'-imidodiphosphate
F <sub>1</sub>	coupling factor 1 (soluble mitochondrial ATPase)
EF <sub>1</sub>	F <sub>1</sub> of <u>E. coli</u>
EDTA	ethylenediaminetetraacetic acid
DCCD	dicyclohexylcarbodiimido
PEP	phosphoenolpyruvate
SDS	sodium dodecyl sulfate
TCA	trichloroacetic acid
Tris	tris(hydroxymethyl)aminomethane
P <sub>i</sub>	inorganic phosphate
PP <sub>i</sub>	inorganic pyrophosphate

PART I.

Reaction Mechanism of the ATPase Activity of Mitochondrial  $F_1$ ,  
Studied by Using a Fluorescent ATP Analog, 2'-(5-Dimethylamino-  
naphthalene-1-Sulfonyl) Amino-2'-DeoxyATP: Its Striking  
Resemblance to That of Myosin ATPase.



## SUMMARY

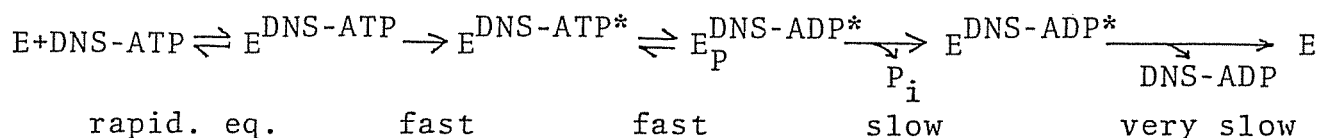
The reaction mechanism of beef heart mitochondrial  $F_1$ -ATPase was studied by using a fluorescent ATP analog, 2'-(5-dimethylamino-naphthalene-1-sulfonyl)amino-2'-deoxyATP (DNS-ATP), as a substrate. The following results were obtained.

1. In the presence of  $Mg^{2+}$ , 2 mol of DNS-ATP bind to 1 mol of  $F_1$  with an apparent dissociation constant of 0.44  $\mu M$ . Upon binding, the fluorescence emission spectrum of DNS-ATP shifted to shorter wavelengths, and the fluorescence intensity at 520 nm increased 4.8 fold. On the other hand, in the absence of  $Mg^{2+}$ , the apparent dissociation constant of  $F_1$ -DNS-ATP was 16  $\mu M$ , and the extent of fluorescence enhancement was 1.3- to 1.9-fold.

2. The initial rate of fluorescence enhancement,  $v_f$ , upon addition of  $Mg^{2+}$  to a mixture of  $F_1$  and DNS-ATP was given by the following equation:

$$v_f = \frac{V_f}{\left(1 + \frac{K_f}{[DNS-ATP]}\right)}$$

where  $V_f = 0.34 \text{ s}^{-1}$  and  $K_f = 3.3 \mu M$ . Following the fluorescence enhancement, TCA- $P_i$  and free  $P_i$  were liberated consecutively. The fluorescence intensity maintained its enhanced level even after the free  $P_i$  liberation and, on addition of an excess amount of EDTA, decreased slowly to the original level. From these findings, the following reaction mechanism for  $F_1$ -DNS-ATPase was proposed:



where an asterisk indicates the state of bound DNS-nucleotide with enhanced fluorescence, and  $\text{E}_P^{\text{DNS-ADP}^*}$  is a TCA-unstable reaction intermediate. This reaction mechanism resembles that of myosin ATPase. In accordance with the reaction mechanism and the stoichiometry of DNS-ATP binding, an initial burst of TCA- $\text{P}_i$  liberation of 2 mol/mol  $\text{F}_1$  was observed.

3. The addition of an excess of ATP to  $\text{F}_1$ -DNS-nucleotide in the presence of  $\text{Mg}^{2+}$  accelerated markedly the liberation of both TCA- $\text{P}_i$  and free  $\text{P}_i$ . ATP also accelerated the fluorescence decrease of  $\text{F}_1$ -DNS nucleotide. Direct measurements of released free DNS-nucleotide indicated that the fluorescence decrease was due to the release of DNS-ADP from  $\text{F}_1$ . ADP, AMPPNP, ITP, and GTP accelerated the  $\text{F}_1$ -DNS-ATPase reaction in a similar manner. On addition of these NTP, the release of DNS-ADP from  $\text{F}_1$  proceeded in rapid and slow steps. CTP and  $\text{PP}_i$  largely or completely failed to accelerate the conversion of  $\text{E}^{\text{DNS-ATP}^*}$  into  $\text{E}_P^{\text{DNS-ADP}^*}$ . Furthermore, CTP and  $\text{PP}_i$  induced only the slow release of DNS-ADP. Therefore, we concluded that several nucleotides including ATP bind to the regulatory site(s) on  $\text{F}_1$  to induce a conformational change at the catalytic sites and accelerate each of the following steps:  $\text{E}^{\text{DNS-ATP}^*} \rightleftharpoons \text{E}_P^{\text{DNS-ADP}^*} \xrightarrow[\text{P}_i]{\text{DNS-ADP}} \text{E}^{\text{DNS-ADP}^*} \xrightarrow[\text{DNS-ADP}]{} \text{E}$ . On the other hand,  $\text{PP}_i$  and CTP mainly accelerate the release of DNS-ADP from  $\text{E}^{\text{DNS-ADP}^*}$  by displacement. AMP did not affect the  $\text{F}_1$ -DNS-ATPase reaction.

4. The steady-state rate of  $F_1$ -DNS-ATPase,  $v_0$ , increased linearly with increase in the concentration of DNS-ATP and was  $1 \text{ s}^{-1}$  at  $200 \text{ }\mu\text{M}$  DNS-ATP exceeding than  $V_f$  ( $0.34 \text{ s}^{-1}$ ). The time course of ATP hydrolysis after addition of ATP to  $F_1$ -DNS-nucleotide showed no lag phase which corresponds to the release of DNS-ADP. These two findings indicate that  $F_1$ -NTPase can also occur through a reaction path in which  $E_p^{\text{NDP}}$  is not formed.

5.  $P_i$  enhanced the fluorescence of  $F_1$ -DNS-nucleotide and inhibited the displacement of bound DNS-ADP with ATP or  $PP_i$ . The extent of fluorescence enhancement by  $P_i$  was maximal at  $1 \text{ mol DNS-ATP/mol } F_1$ . This finding implies that the two DNS-ATP binding sites on  $F_1$  are heterogenous at least with respect to the interaction with  $P_i$ .

## INTRODUCTION

It is widely accepted that a mitochondrial  $F_1-F_0$  complex catalyzes the ATP synthesis in oxidative phosphorylation (for reviews see 1,2). When isolated from membrane,  $F_1$  catalyzes only the hydrolysis of ATP, although the reaction center of ATP synthesis is supposed to be remaining in the isolated enzyme.

Recently important information has been accumulated on the structure and function of each subunit in  $F_1$ -ATPase [EC 3.6.1.3] from thermophilic bacteria (2) and E. coli (3) by use of a reconstitution technique. Furthermore, many features of nucleotide binding to  $F_1$  were reported by Slater (4) and others (for review see 5). Boyer and coworkers (6) investigated the reaction mechanism of  $F_1$ -ATPase mainly utilizing the oxygen exchange reaction, and Slater and coworkers (7) analyzed kinetic properties of the presteady state of ATP hydrolysis. Several authors (6-10) suggested regulatory effects of ATP and ADP on the reaction rate, nucleotide binding, and  $P_i$  binding to  $F_1$ . Boyer and coworkers (11) have proposed a possible catalytic cooperativity among subunits in the reaction of  $F_1$ -ATPase.

Boyer and coworkers (11) suggested that there was a similarity between  $F_1$ -ATPase and myosin ATPase in their reaction mechanisms. In myosin ATPase, each reaction step is identified and conformational change of the enzyme induced by nucleotide binding is directly measured (12-15). On the other hand, details of the reaction mechanism of  $F_1$ -ATPase are not known despite numerous efforts as mentioned above. Therefore, we attempted to clarify the reaction mechanism of  $F_1$ -ATPase by using the methods developed

in the research of myosin ATPase (12-15). One of them was to use a fluorescent analog of ATP, 2'-(5-dimethylaminonaphthalene-1-sulfonyl) amino-2'-deoxyATP (DNS-ATP) which was synthesized by substituting the 2'-hydroxy group of ATP with an amino group and introducing a dimethyl amino naphthalene sulfonyl group (16). DNS-ATP has the following advantages serving the present purpose: (1) The fluorescence intensity of DNS-ATP increases markedly on its binding to  $F_1$ , and the extent of enhancement depends on experimental conditions. (2) DNS-ATP is hydrolyzed by  $F_1$  very slowly, enabling easier kinetic measurements than using ATP. (3) DNS-AT<sup>32</sup>P can be easily synthesized enzymatically.

## MATERIALS AND METHODS

Materials — DNS-ATP and DNS-ADP were synthesized as described previously (16). DNS-AT<sup>32</sup>P was synthesized by the same enzymatic method as described by Glynn and Chapell for AT<sup>32</sup>P synthesis (17). Specific radioactivity of DNS-AT<sup>32</sup>P was about 2  $\mu$ Ci/nmol. Adequate purity of DNS-ATP, DNS-ADP, and DNS-AT<sup>32</sup>P was confirmed by paper electrophoresis run in 50 mM triethylamine bicarbonate at pH 7.6 (16).

Pyruvate kinase [EC 2.7.1.40] was prepared according to the method of Tietz and Ochoa (18). Luciferase [EC 1.13.12.7] was prepared from firefly lantern as described previously (19). ATP, ADP, and AMP were purchased from Khojin Ltd.(Tokyo). AMPPNP, ITP, GTP, PEP, and luciferin were purchased from Sigma Chemicals Co.(St. Louis). [<sup>3</sup>H]Glucose was purchased from New England Nuclear Co.(London). All other chemicals were of reagent grade purity.

Purification of F<sub>1</sub>— Submitochondrial particles were prepared from beef heart mitochondria as described by Beyer (20). F<sub>1</sub> was extracted from submitochondrial particles with chloroform as described by Beechy et al. (21). After 30-60% ammonium sulfate fractionation, the concentrated extract was subjected to gel filtration on a Sephacryl S-300 Superfine column (3.2x75 cm) equilibrated with 100 mM Tris-HCl, 5mM EDTA, and 50% glycerol at pH 8.0 and 20°C. The eluted enzyme was concentrated by ultrafiltration on an Amicon Diaflo XM-100A membrane, and stored at 0°C. The protein concentration of purified F<sub>1</sub> was determined by the biuret method (22) with bovine serum

albumin ( $A_{279 \text{ nm}} = 0.667 \text{ cm}^2 \cdot \text{mg}^{-1}$ ) as a standard. The concentration of  $F_1$  was calculated by using a molecular weight of 360,000 (1). The purified enzyme was subjected to SDS-gel electrophoresis on 10% polyacrylamide gel according to the method of Weber and Osborne (23).

The nucleotide content of purified  $F_1$  was measured as follows: To 0.5 ml of  $F_1$  solution at 22 mg/ml, 0.5 ml of 8%  $\text{HClO}_4$  was added. After centrifugation at 2000 x g for 20 min, the supernatant was neutralized to pH 7.6 with 4 N KOH. Total nucleotide content was determined spectrophotometrically by using  $\epsilon_{259 \text{ nm}} = 15.4 \text{ mM}^{-1} \text{ cm}^{-1}$  for adenine nucleotides, since the UV absorption spectrum of the supernatant was the same as that for adenine nucleotides. The contents of ATP and ADP were determined by the firefly luciferase system, as described by Furukawa *et al.* (19), after conversion of ADP to ATP by 0.1 mg/ml pyruvate kinase and 4 mM PEP.

Fluorescence Measurement — Usually measurement solutions were prepared by addition of reagents in 5-20  $\mu\text{l}$  portions to 2.0 ml of 50 mM Tris-HCl, pH 8.0 containing 2 mM EDTA. The measurements were performed at 30°C. To initiate a reaction, a reagent was stirred into a cuvette containing the rest of a reaction mixture with the aid of a magnetic stirrer (mixing time  $\leq 0.2$  s). Fluorescence intensity was measured on a Hitachi MPF-4 spectrofluorometer equipped with a thermostated cuvette holder. The slit widths on the excitation and emission monochrometers were 6 and 8 nm, respectively. The fluorescence intensity at 520 nm of DNS-ATP and DNS ADP was measured with excitation at 340 nm.

Partial Reaction of  $F_1$ -DNS-ATPase — All the concentrations were expressed in terms of final concentrations, unless otherwise stated, throughout the text and figure legends. The composition of a reaction mixture was 5 mM  $MgCl_2$ , 2 mM EDTA, 50 mM Tris-HCl at pH 8.0 and appropriate concentrations of DNS-ATP and  $F_1$ . After adding 0.1 ml of  $F_1$  solution to 0.85 ml of a solution containing EDTA and DNS-AT $^{32}P$  in Tris-HCl, it was incubated for 30 s at 30°C. The  $F_1$ -DNS-ATPase reaction was started by addition of 0.05 ml of 100 mM  $MgCl_2$ . At appropriate intervals the reaction was stopped by addition of 1 ml of 10% TCA. After centrifugation,  $^{32}P_i$  in the supernatant (TCA- $^{32}P_i$ ) was measured as described by Nakamura and Tonomura (24).

The concentration of total free  $^{32}P$  (free  $^{32}P_i$  + free DNS-ATP $^{32}P$ ) was measured by a double membrane filtration method developed by Yamaguchi and Tonomura (25). By using a set of two membrane filters (upper Amicon Diaflo XM-100A membrane; lower Millipore filter, pore size 0.8  $\mu m$ ), this technique enabled the separation of free  $^{32}P$  remaining on the Millipore filter from the  $F_1$ -bound form on the Amicon membrane. The diameter of both membranes was 10 mm. The reaction mixture was the same as used in the TCA- $^{32}P_i$  measurement, except that 10 mM [ $^3H$ ]glucose was added to measure the volume of a filtrate. At appropriate times, 50  $\mu l$  of the reaction mixture was withdrawn and applied on the upper membrane and filtrated by vacuum sucking for 4 s. A small volume (0.5-3  $\mu l$ ) of filtrate remained on the Millipore filter was dried, and the residues were solubilized in 1 ml of dimethyl formamide. The concentration of total free  $^{32}P$  in the filtrate was determined from the ratio of radioactivities,  $^{32}P/^3H$  (25).



The reaction mixture for measurement of the concentration of free DNS-nucleotide was the same as that for the TCA- $^{32}\text{P}_i$  measurement, except that 10 mM [ $^3\text{H}$ ]glucose was added and DNS-ATP was used instead of DNS-AT $^{32}\text{P}$ . The diameter of the membranes was 25 mm, and the volume of a reaction mixture applied on the membranes was 500  $\mu\text{l}$ , leaving 10-30  $\mu\text{l}$  on the Millipore filter after sucking. The dried Millipore filter was solubilized by 2 ml of dimethyl formamide.

The amount of free DNS-nucleotide in the filtrate was determined by measuring the fluorescence intensity at 530 nm after correcting the fluorescence due to Millipore filter solubilized by dimethyl formamide. The volume of the filtrate was determined from the radioactivity of [ $^3\text{H}$ ]glucose.

ATPase Activity — The ATPase activity of  $F_1$  was measured in the presence of a pyruvate kinase system (0.1 mg/ml pyruvate kinase and 4 mM PEP) as a feeder, and the amount of  $P_i$  liberated was measured by the method of Fiske and Subbarow (26).

## RESULTS

Properties of Purified  $F_1$  — The specific activity of purified  $F_1$  measured in the presence of 5 mM ATP at pH 8.0 and 30 °C was 120-150 U/mg, which was similar to that already reported (7). When kept in 50% glycerol,  $F_1$  was quite stable. At 0 °C the activity did not change at all for more than three months. As is widely accepted, purified  $F_1$  was composed of 5 subunits (Fig. 1), and the intrinsic inhibitor protein which is usually seen between  $\delta$  and  $\epsilon$  subunits in SDS-gel electrophoresis (27) was completely removed by gel filtration on Sephacryl S-300. The adenine nucleotide content calculated from  $\Delta A$  at 259 nm was 2.4 mol/mol  $F_1$ . The ATP content of the sample measured by the luciferin-luciferase method was 2.3 mol/mol  $F_1$ . The ADP content was less than 0.3 mol/mol  $F_1$ .

Fluorescence Change of DNS-ATP on Its Binding to  $F_1$  — Figure 2 shows that the addition of 1.5  $\mu$ M  $F_1$  to 3.2  $\mu$ M DNS-ATP in the presence of 2 mM EDTA increased the fluorescence intensity at 520 nm 24% from the level of free DNS-ATP, and that this increase consisted of an initial rapid change and the following slow one. This fluorescence increase was completely reversed by addition of 0.2 mM ATP, 0.2 mM ADP, 1 mM  $PP_i$  or 1 mM  $P_i$  (data not shown). On further addition of 5 mM  $MgCl_2$  to the above mixture of  $F_1$  and DNS-ATP, the fluorescence was markedly enhanced with a halftime of about 10 s, and reached a plateau within about 1 min. The  $Mg^{2+}$ -dependent fluorescence enhancement was observed only in the presence of  $F_1$ . Subsequent addition of  $P_i$  slowly enhanced the fluorescence intensity as will be

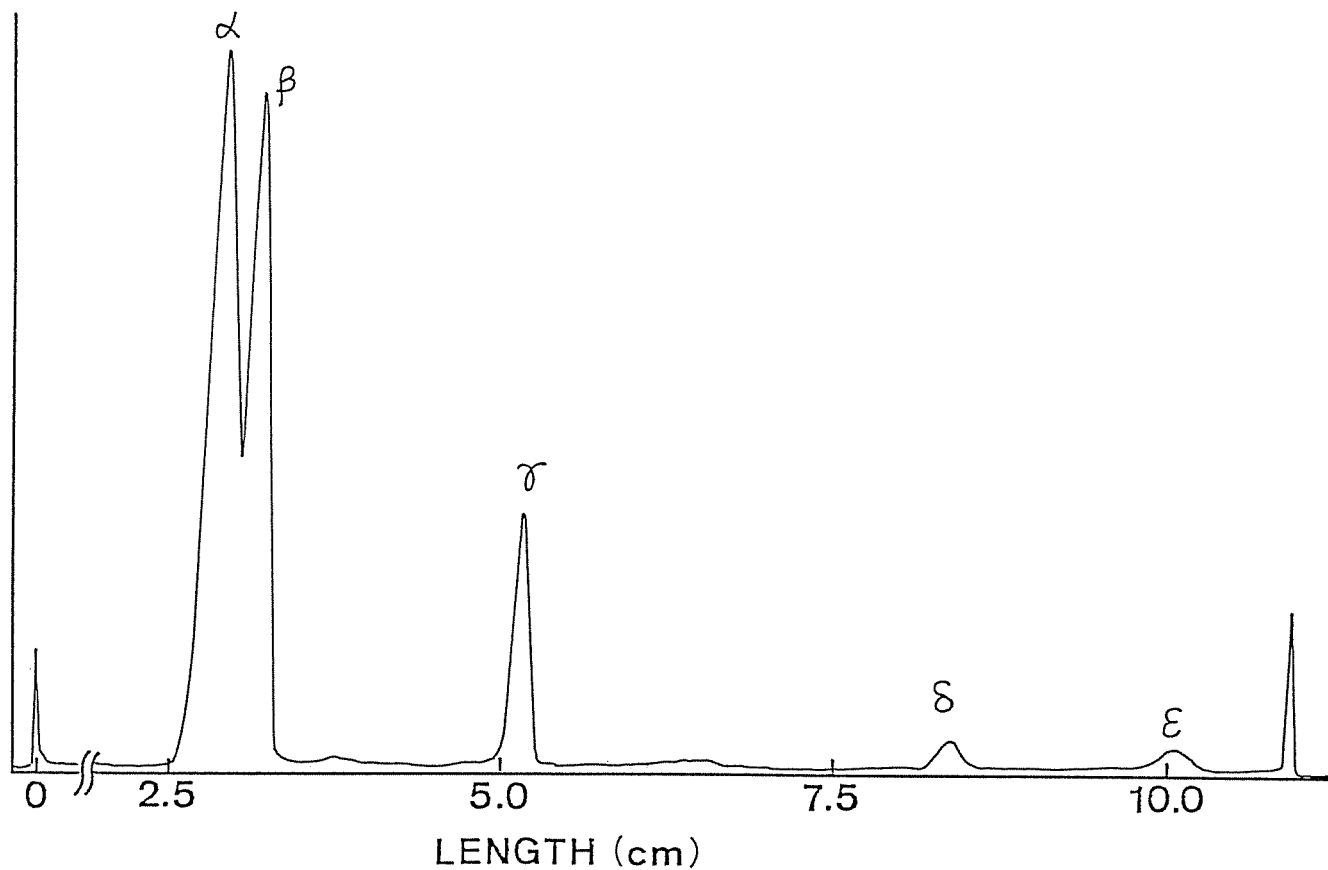


Fig. 1. SDS-gel electrophoretic pattern of purified F<sub>1</sub>-ATPase. The amount of the applied protein was 5 μg. The length is the migration distance from the origin. The gel was stained by Coomassie Brilliant Blue, and scanned at 550 nm at 0.05 mm slit width.

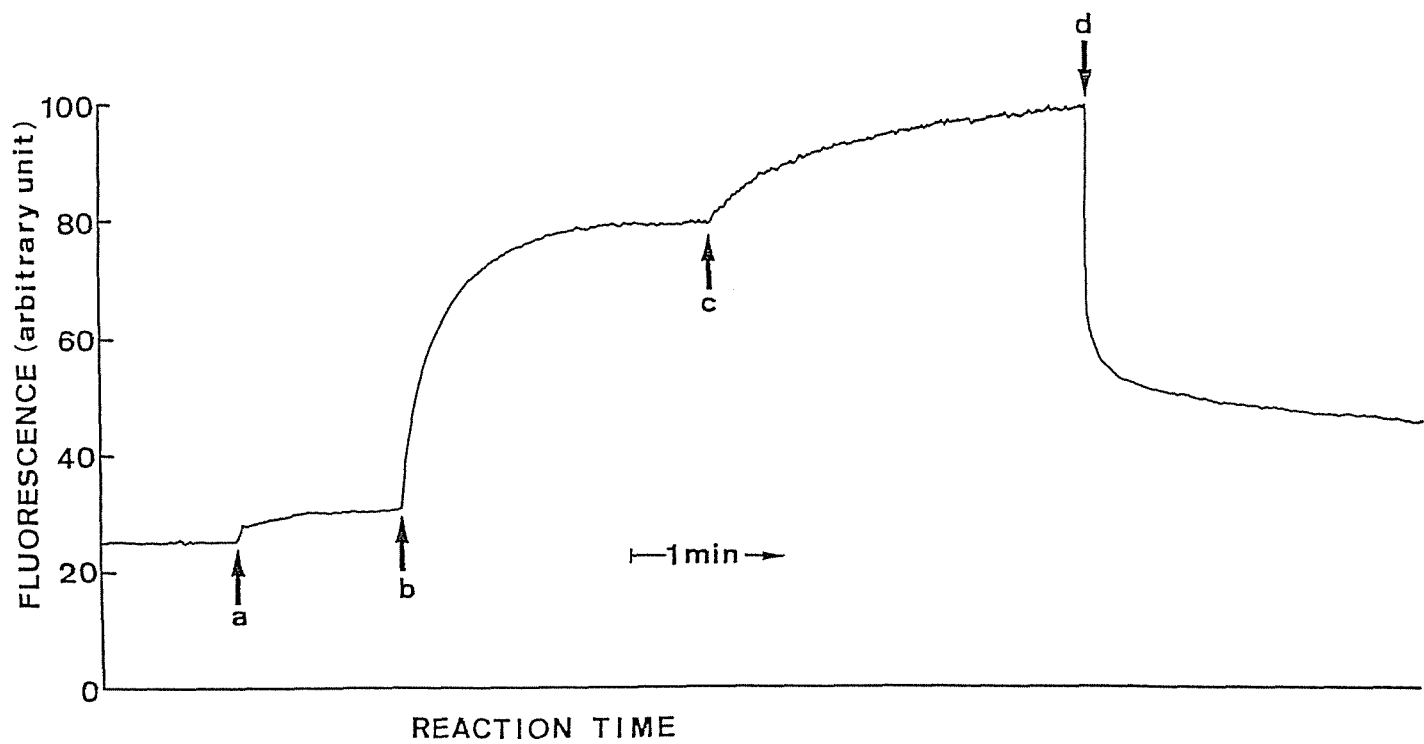


Fig. 2. Fluorescence intensity change of DNS-ATP on its binding to  $F_1$ . To mixture containing 3.2  $\mu\text{M}$  DNS-ATP and 2 mM EDTA in 50 mM Tris-HCl, pH 8.0, following additions were made: a, 1.5  $\mu\text{M}$   $F_1$ ; b, 5 mM  $\text{MgCl}_2$ ; c, 4 mM  $\text{K-P}_i$ ; d, 0.2 mM ATP.

detailed later. During this series of reaction, fluorescence emission spectra were recorded at various stages as shown in Fig. 3. DNS-ATP in 2 mM EDTA had an emission peak at around 555 nm (trace a) (16), which shifted to 545 nm with a slight increase in fluorescence intensity by addition of  $F_1$  (trace b). Addition of 5 mM  $MgCl_2$  markedly enhanced the fluorescence the maximum shifting to 525 nm (trace c). Finally by addition of 2mM Pi, the fluorescence maximum shifted to 520 nm with an intensity increase (trace d). As reported previously (12), addition of dioxane to an aqueous solution of DNS-ATP enhanced its fluorescence and caused a blue shift reflecting a hydrophobic interaction. Therefore hydrophobicity of the DNS-ATP binding site in  $F_1$  was suggested to be very high (see Table I in DISCUSSION).

When  $F_1$  was added to DNS-ATP in the presence of 2 mM EDTA at pH 6.5 or 7.5 (Fig. 4, arrow a), the fluorescence intensity increased rapidly followed by a slow decrease (Fig. 4). The fluorescence intensities at 1 min after addition of  $F_1$  were 1.8- and 2.1-fold greater than those of free DNS-ATP at pH 7.5, and 6.5, respectively. At pH 8.0 this increase was 1.3-fold. The extent and time course of the fluorescence enhancement on addition of 5 mM  $MgCl_2$  (arrow b) were almost the same at these pHs. All the following experiments were carried out at pH 8.0, where the fluorescence of DNS-ATP changed only slightly on addition of  $F_1$  in the absence of  $Mg^{2+}$ .

The stoichiometry of DNS-ATP binding to  $F_1$  was determined by fluorometric titration of 0.75 or 1.5  $\mu M$   $F_1$  with DNS-ATP in the presence of  $Mg^{2+}$  (Fig. 5.). The data were analyzed based on the quadratic equation:

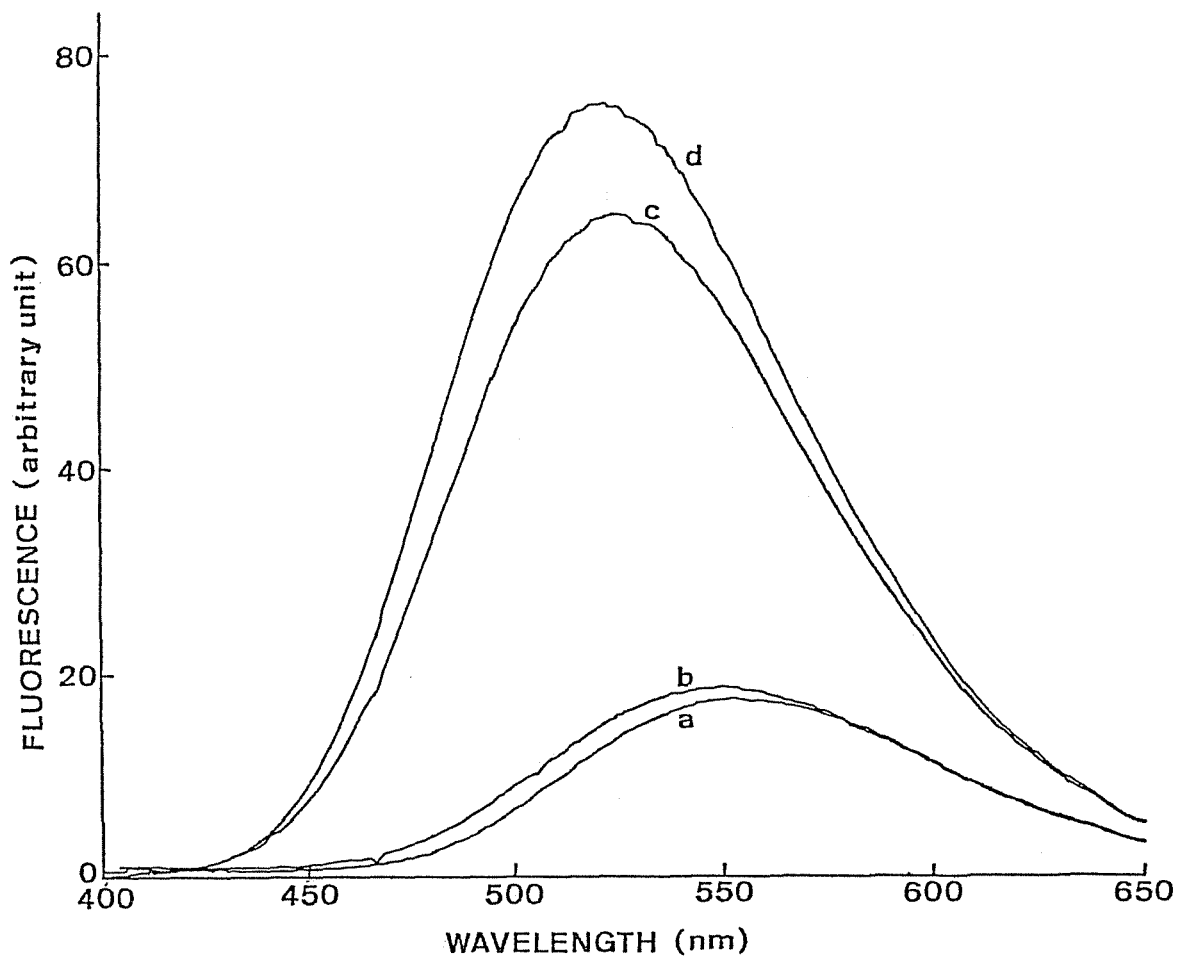


Fig. 3. Fluorescence emission spectra recorded during a course of reaction of DNS-ATP with  $F_1$ . Spectra were recorded in the following order; curve a, 2.1  $\mu$ M DNS-ATP alone; curve b, 1 min after addition of 2.3  $\mu$ M  $F_1$ ; curve c, 2 min after addition of 5 mM  $MgCl_2$ ; curve d, 2 min after addition of 2 mM K- $P_i$ . The excitation wavelength was 340 nm.

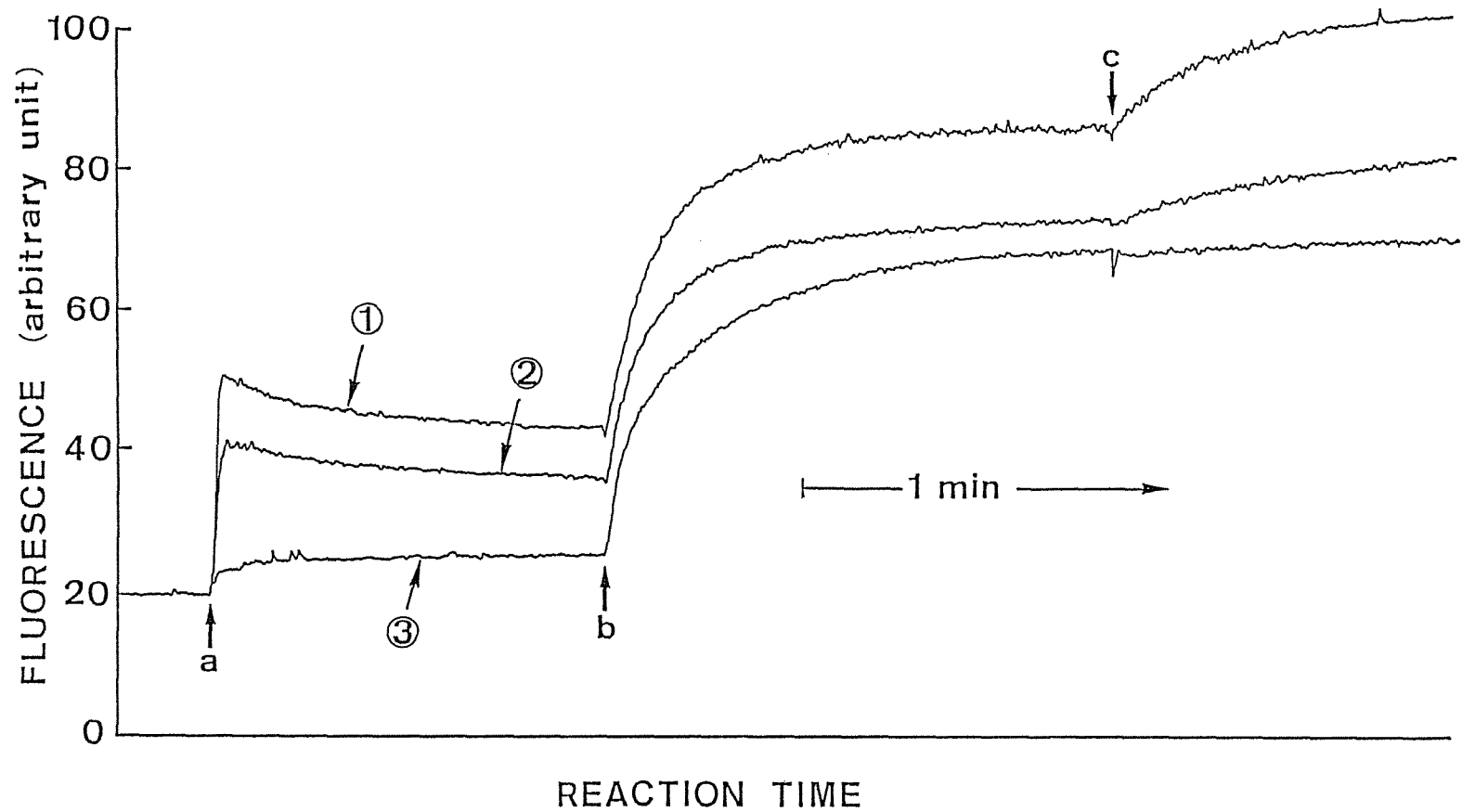


Fig. 4. pH Dependence of reaction of DNS-ATP with  $F_1$ . The pH of a mixture containing  $2.1 \mu\text{M}$  DNS-ATP and  $2 \text{ mM}$  EDTA at  $30^\circ\text{C}$  was adjusted to 6.5 with  $50 \text{ mM}$  Tris-acetate (curve 1), 7.5 with  $50 \text{ mM}$  Tris-HCl (curve 2) and 8.0 with  $50 \text{ mM}$  Tris-HCl (curve 3). Following additions were made; a,  $1.5 \mu\text{M}$   $F_1$ ; b,  $5 \text{ mM}$   $\text{MgCl}_2$ ; c,  $50 \mu\text{M}$   $\text{K-P}_i$ .

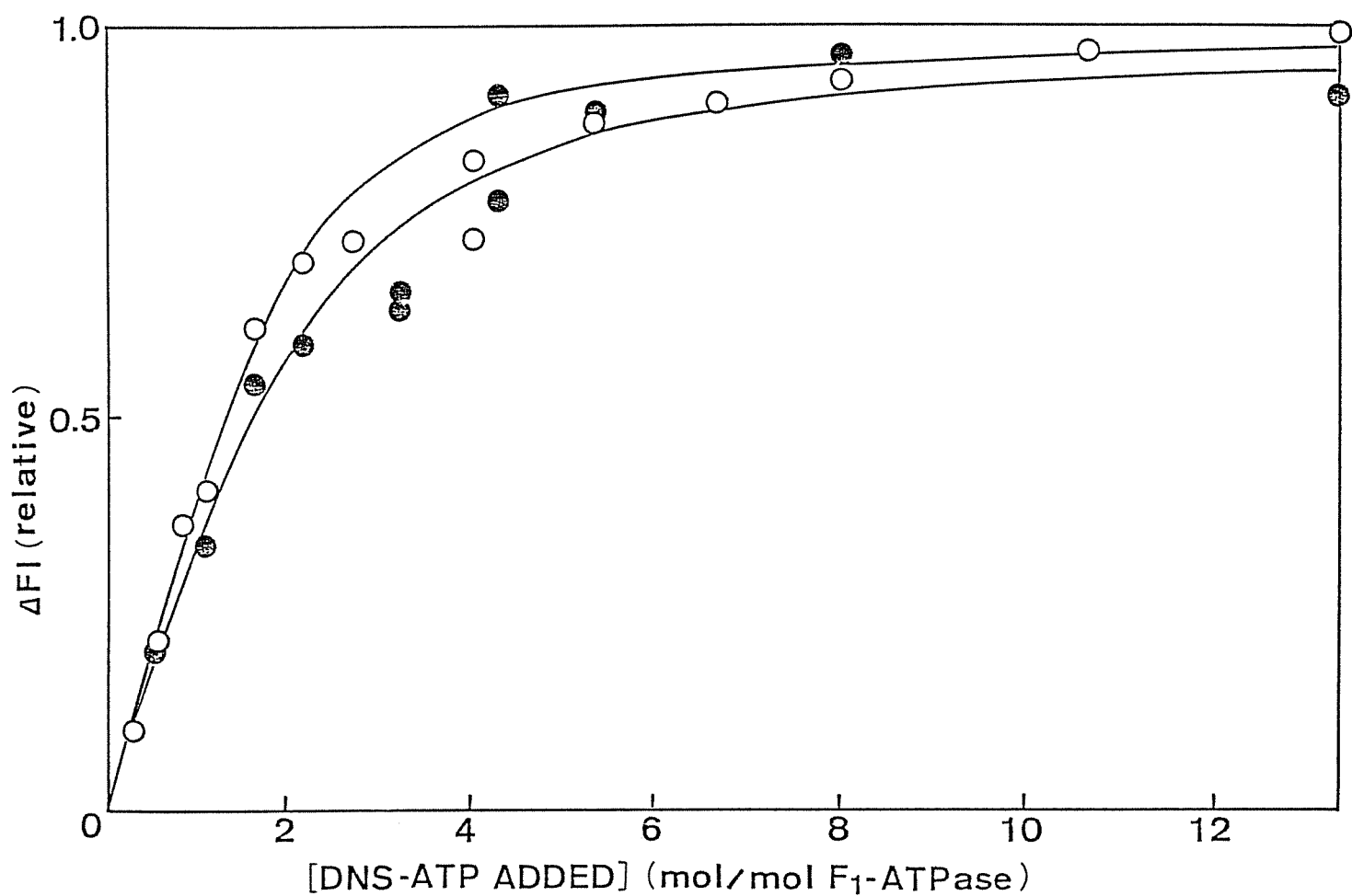


Fig. 5. Fluorometric titration of  $F_1$  by DNS-ATP in the presence of  $MgCl_2$ . The extent of fluorescence enhancement 2 min after addition of 5 mM  $MgCl_2$  was plotted against the amount of DNS-ATP added. The reaction mixture contained 0.75 (●) or 1.5  $\mu M$  (○)  $F_1$  in 2 mM EDTA, 50 mM Tris-HCl at pH 8.0. The solid lines are the theoretical curves (see text). The upper is for 1.5  $\mu M$   $F_1$ , and the lower for 0.75  $\mu M$   $F_1$ .



$$\Delta F = \frac{R}{2} \left\{ (nE_0 + S_0 + \phi_{\text{DNS-ATP}}) - [(nE_0 + S_0 + \phi_{\text{DNS-ATP}})^2 - 4nE_0S_0]^{1/2} \right\} \quad (1)$$

where  $\Delta F$  is the extent of fluorescence enhancement, and is assumed to be proportional to the amount of the  $F_1$ -DNS-nucleotide.

$R$  is the fluorescence parameter dependent upon experimental conditions,  $n$  is the number of independent and equivalent binding sites of DNS-ATP on  $F_1$ ,  $E_0$  and  $S_0$  are the total concentrations of  $F_1$  and DNS-ATP, respectively, and  $\phi_{\text{DNS-ATP}}$  is the dissociation constant for the complex. It was also postulated that the fluorescence intensity of DNS-ATP during the course of interaction did not change. The curves in Fig. 5 are the best fits of the data to Eqn. 1 with  $n = 2$  and  $\phi_{\text{DNS-ATP}} = 0.44 \mu\text{M}$ . With  $n$  values other than 2, the fit was poor.

When  $\text{PP}_i$  had been added to the  $F_1$ -DNS-ATP system in advance, the extent of fluorescence enhancement on addition of  $\text{Mg}^{2+}$  decreased with increasing concentration of  $\text{PP}_i$  (Fig. 6). The results were explained by a competitive binding of  $\text{PP}_i$  to the DNS-ATP binding site on  $F_1$ :

$$\phi'_{\text{DNS-ATP}} = \phi_{\text{DNS-ATP}} \left( 1 + \frac{[\text{PP}_i]}{\phi_{\text{PP}_i}} \right) \quad (2)$$

where  $\phi'_{\text{DNS-ATP}}$  is the apparent dissociation constant for  $F_1$ -DNS-nucleotide in the presence of  $\text{PP}_i$  and  $\phi_{\text{PP}_i}$  is the dissociation constant for  $F_1$ - $\text{PP}_i$ . The data in Fig. 6 were analyzed based on Eqn. 1, where  $\phi_{\text{DNS-ATP}}$  was replaced by  $\phi'_{\text{DNS-ATP}}$  of Eqn. 2. The curve in Fig. 6 is the best fit to the data obtained with  $\phi_{\text{PP}_i} = 39 \mu\text{M}$ .

DNS-ADP was also bound to  $F_1$  and brought about similar fluorescence changes as DNS-ATP. In Fig. 7, the extents of

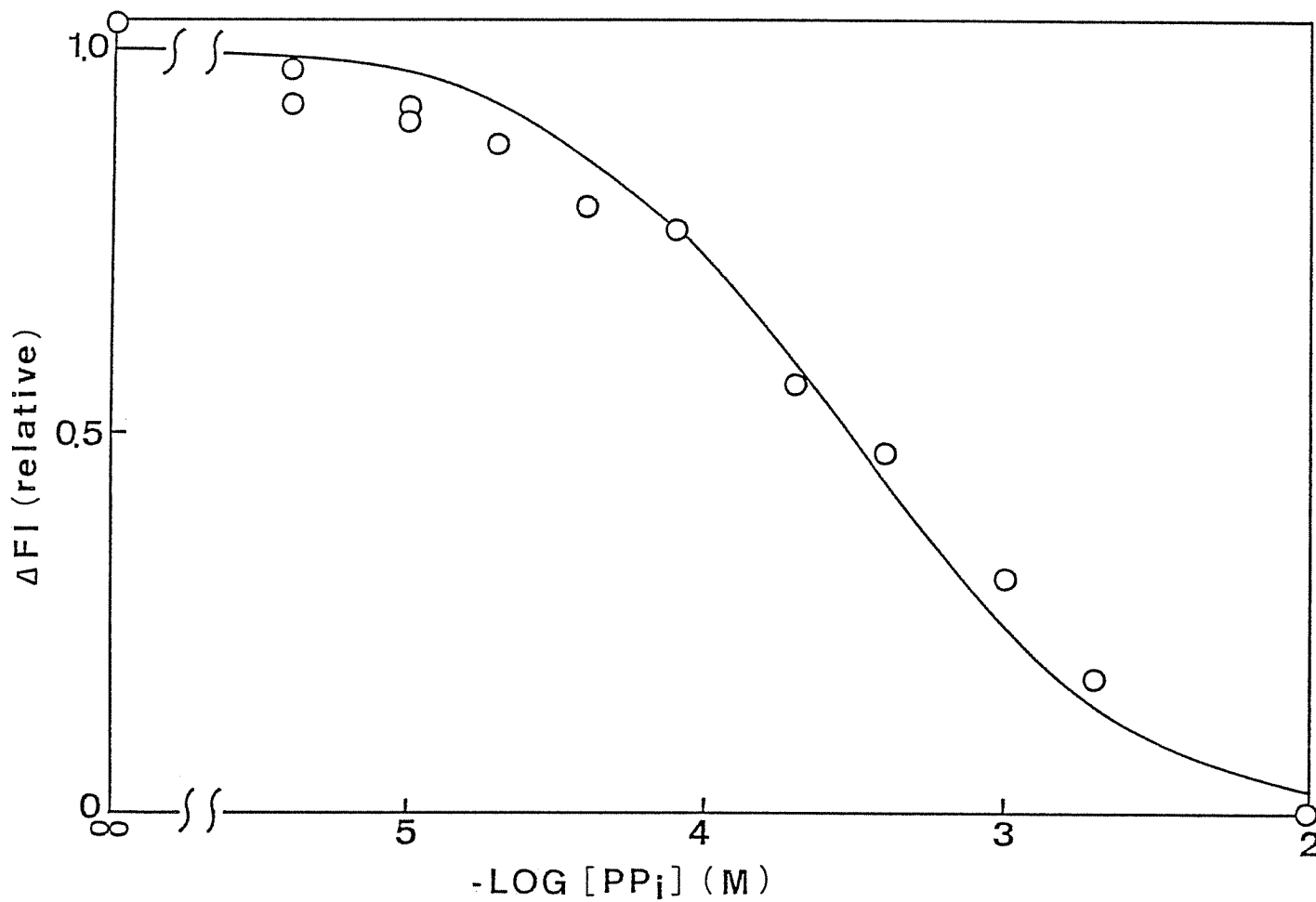


Fig. 6. Competitive binding of  $PP_i$  to the DNS-ATP binding site on  $F_1$ . The extent of fluorescence enhancement of DNS-ATP after addition of 5 mM  $MgCl_2$  was plotted against the concentration of  $PP_i$ . The reaction mixture contained 3.2  $\mu\text{M}$  DNS-ATP and 0.75  $\mu\text{M}$   $F_1$ . The solid line is the theoretical curve (see text).

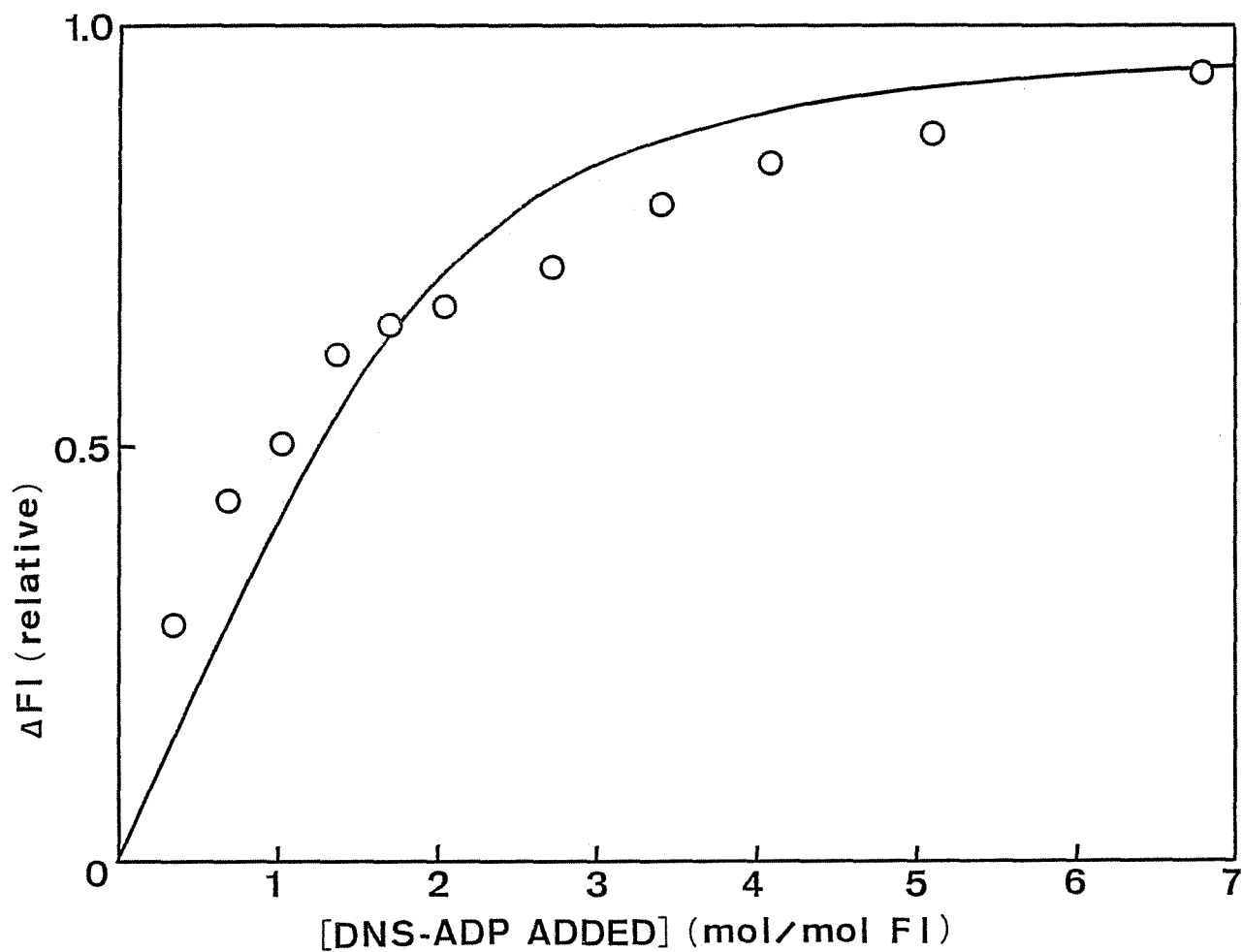
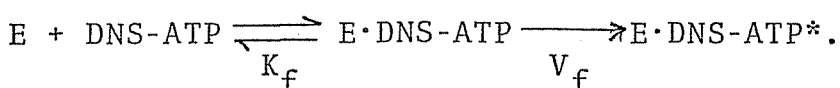


Fig. 7. Fluorometric titration of  $F_1$  with DNS-ADP in the presence of  $MgCl_2$ . The extent of fluorescence enhancement 2 min after addition of 5 mM  $MgCl_2$  was plotted against the amount of DNS-ADP added. The reaction mixture contained 1.5  $\mu M$   $F_1$ . The solid line is the theoretical curve (see text).

fluorescence enhancement on addition of 5 mM MgCl<sub>2</sub> to mixtures containing 1.5 μM F<sub>1</sub> and various amounts of DNS-ADP were plotted against the amounts of DNS-ADP added. The theoretical curve was obtained by using Eqn. 1, where parameters for DNS-ATP were taken as those for DNS-ADP, with n = 2 and φ<sub>DNS-ADP</sub> = 0.4 μM. However, the measured values deviated somewhat from the curve.

Reaction Sequence of F<sub>1</sub>-DNS-ATPase — We measured the initial rates of fluorescence enhancement, v<sub>f</sub>, on addition of 5 mM MgCl<sub>2</sub> to mixtures containing 1.5 μM F<sub>1</sub> and various concentrations of DNS-ATP. The double reciprocal plot of v<sub>f</sub> against the concentration of DNS-ATP gave a straight line as shown in Fig. 8. This result may be explained by the following reaction scheme,



By assuming that the first step is in rapid equilibrium (see DISCUSSION), we obtain

$$v_f = \frac{V_f}{1 + \frac{K_f}{[\text{DNS-ATP}]}} \quad (3)$$

where K<sub>f</sub> is the dissociation constant of E·DNS-ATP, V<sub>f</sub> is the rate constant of the fluorescence enhancement, and an asterisk indicates a complex with an enhanced fluorescence intensity. The values of K<sub>f</sub> and V<sub>f</sub> were estimated as 3.3 μM and 0.34 s<sup>-1</sup>, respectively, from the results in Fig. 8.

In Fig. 9, the initial phase of fluorescence enhancement on addition of 5 mM MgCl<sub>2</sub> to a mixture of 4.28 μM DNS-AT<sup>32</sup>P and 6.78 μM F<sub>1</sub> is compared with the TCA-<sup>32</sup>P<sub>i</sub> liberation

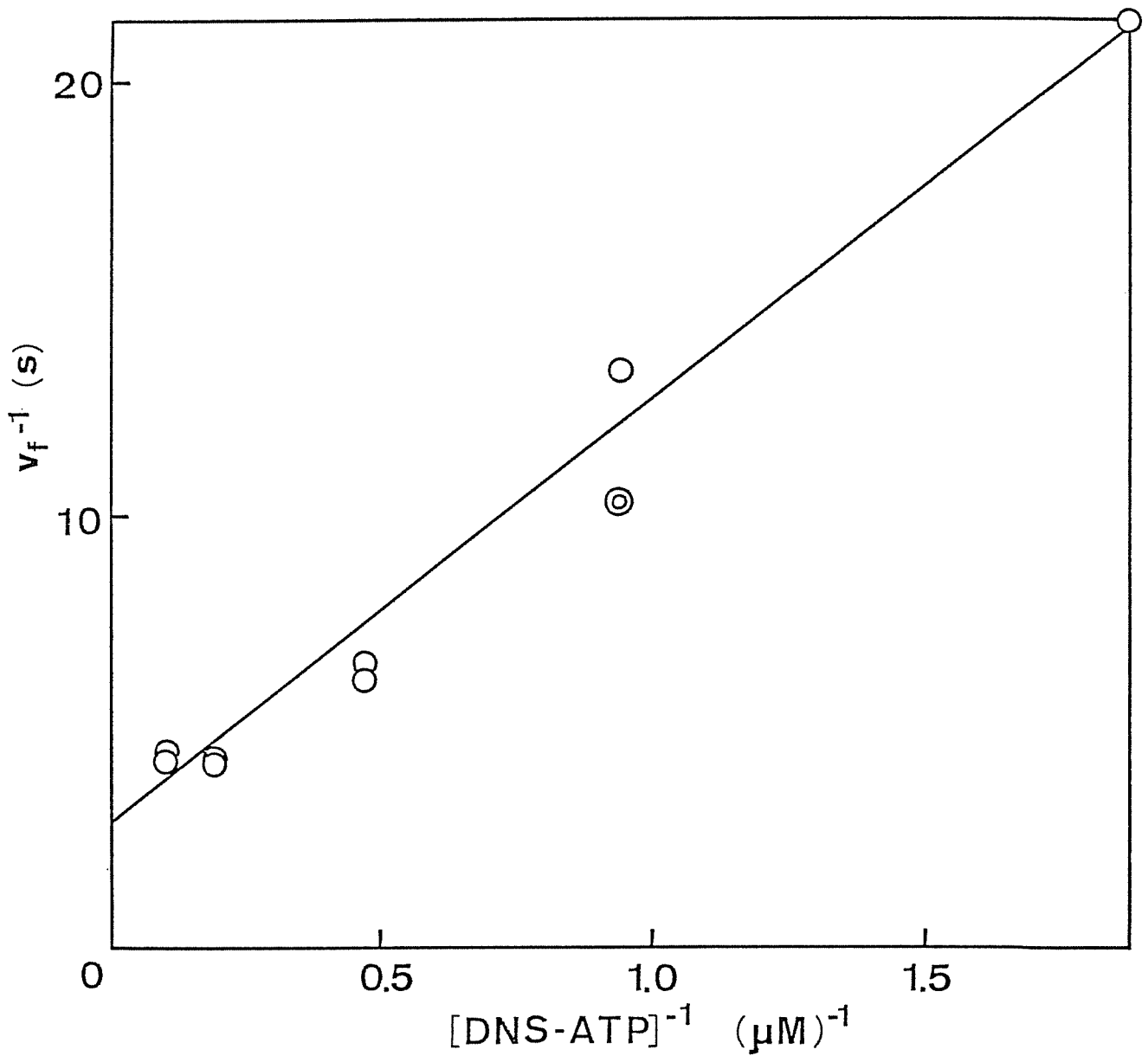


Fig. 8. Double reciprocal plot of the initial rate of fluorescence enhancement against DNS-ATP concentration. The reciprocal of the initial rate of fluorescence enhancement of DNS-ATP on addition of 5 mM  $\text{MgCl}_2$ ,  $v_f$ , was plotted against the reciprocal of the concentration of DNS-ATP added. The concentration of  $F_1$  was 1.5  $\mu\text{M}$ .

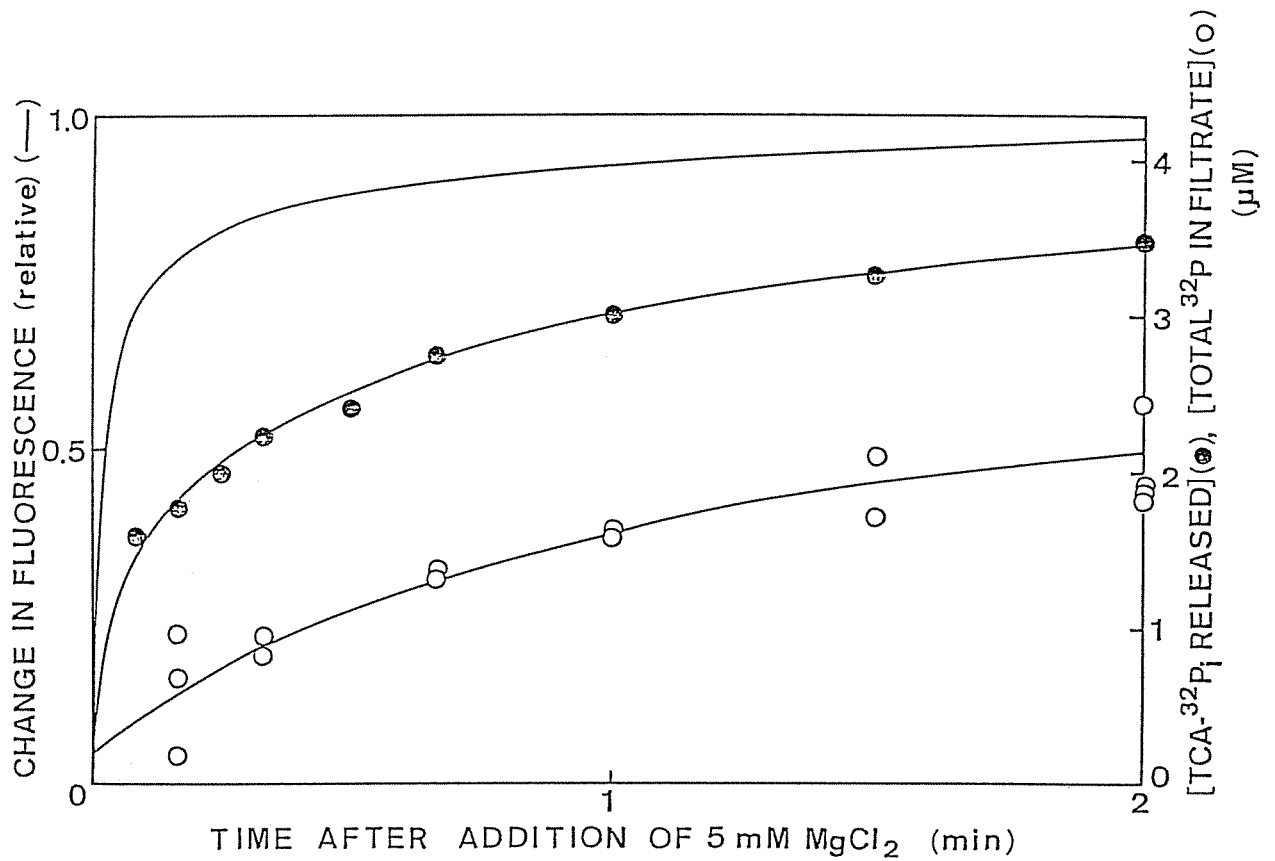


Fig. 9. Time course of fluorescence enhancement, TCA-<sup>32</sup>P<sub>i</sub> liberation and total free <sup>32</sup>P liberation in the initial phase of the reaction of DNS-AT<sup>32</sup>P with F<sub>1</sub>. The reaction mixture contained 4.28 μM DNS-AT<sup>32</sup>P, 6.78 μM F<sub>1</sub>, and 10 mM [<sup>3</sup>H]glucose in 2 mM EDTA and 50 mM Tris-HCl at pH 8.0. The reaction was started by addition of 5 mM MgCl<sub>2</sub>, and stopped by addition of 5% TCA (TCA-<sup>32</sup>P<sub>i</sub>) or filtration through an XM-100A membrane (total free <sup>32</sup>P) at the indicated time. The time course of fluorescence enhancement was measured separately under the same conditions.

and release of total  $^{32}\text{P}$  into the filtrate of the reaction mixture (see MATERIALS and METHODS). The percentages of DNS-AT $^{32}\text{P}$  bound to  $F_1$  immediately after addition of  $\text{Mg}^{2+}$  and at the steady state were calculated by using  $K_f = 3.3 \mu\text{M}$  [Eqn. (3)] and  $\phi_{\text{DNS-ATP}} = 0.44 \mu\text{M}$  [Eqn. (1)] to be 73% and 95%, respectively. Even if the initial concentration of free DNS-AT $^{32}\text{P}$  is 27%, this is expected to decrease rapidly corresponding to an initial rapid increase in the fluorescence intensity. Therefore, we concluded that the amount of total  $^{32}\text{P}$  in the filtrate was almost equal to or slightly higher than the amount of free  $^{32}\text{P}_i$  released from  $F_1$  to the medium. Thus, after the addition of 5 mM  $\text{MgCl}_2$  the fluorescence enhancement, liberation of TCA- $^{32}\text{P}_i$  due to hydrolysis of DNS-ATP, and liberation of free  $^{32}\text{P}_i$  seem to occur sequentially in this order. Since the fluorescence intensity maintained its enhanced level for most of the reaction, it is clear that DNS-ADP formed by hydrolysis of DNS-AT $^{32}\text{P}$  was still bound to  $F_1$  and that the release of DNS-ADP from  $F_1$  was very slow.

Figure 10A shows the time courses of TCA- $^{32}\text{P}_i$  liberation after addition of 2.83, 5.65 or 11.3 mol DNS-AT $^{32}\text{P}$ /mol  $F_1$  to  $0.75 \mu\text{M } F_1$ . In Fig. 10B, the logarithm of the remaining fraction of DNS-AT $^{32}\text{P}$ ,  $([\text{total } ^{32}\text{P}] - [\text{TCA-}^{32}\text{P}_i])/[\text{total } ^{32}\text{P}]$ , was plotted against time after addition of 5 mM  $\text{MgCl}_2$ . At all DNS-AT $^{32}\text{P}$  concentrations examined, the time course of TCA- $^{32}\text{P}_i$  liberation deviated from a single exponential curve, exhibiting rapid and subsequent slow phases. The amount of TCA- $^{32}\text{P}_i$  liberated during the rapid phase was estimated by extrapolating the second

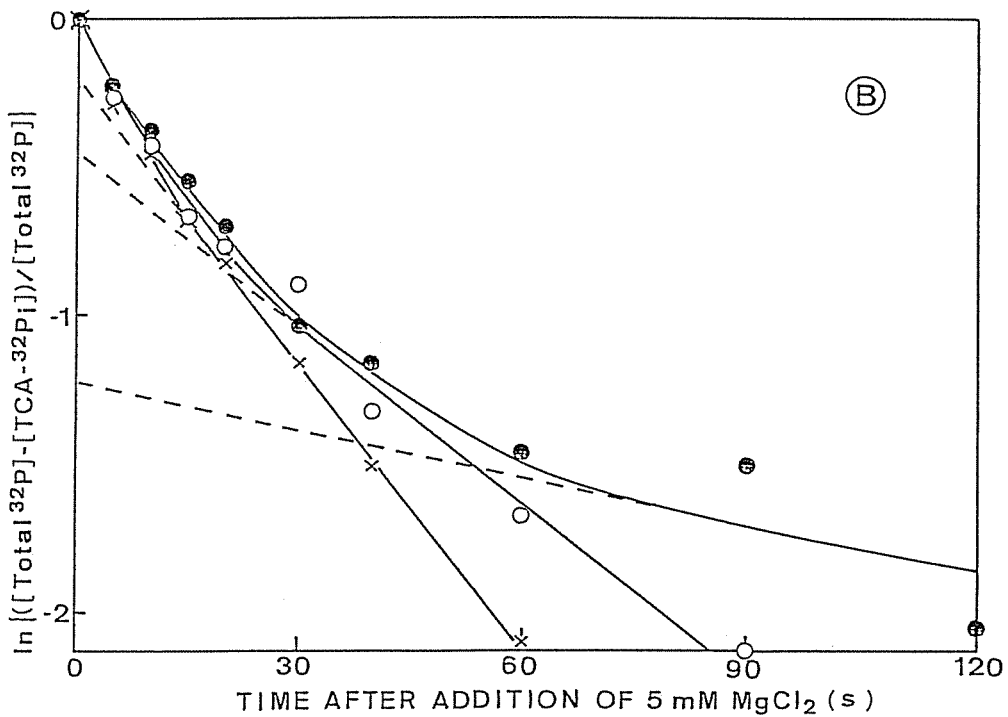
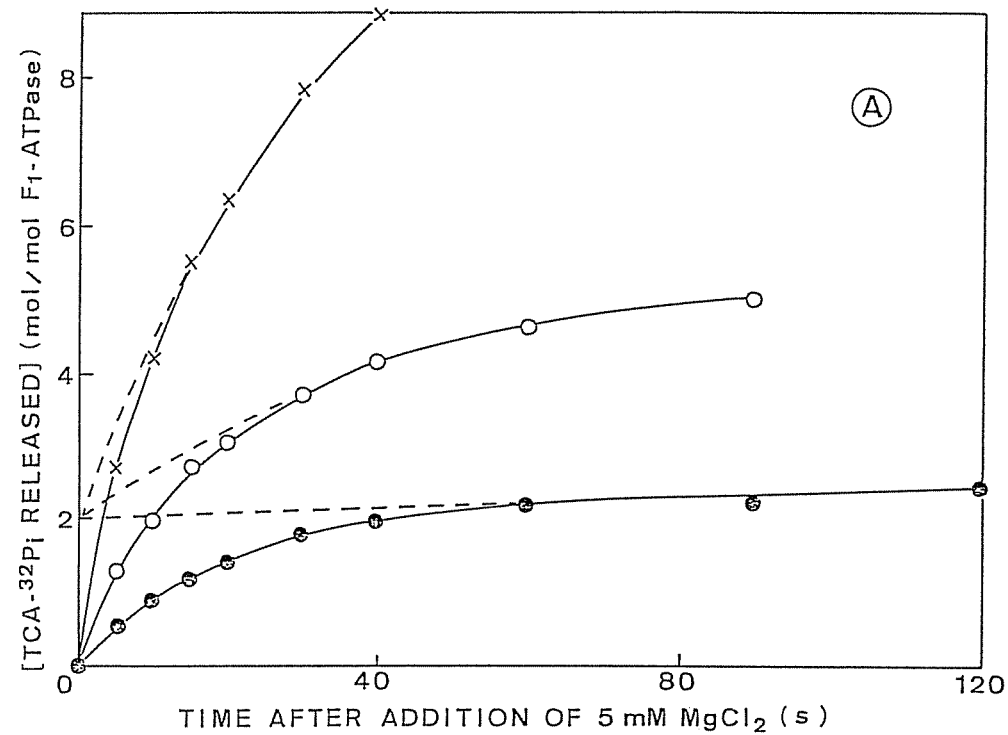


Fig. 10. Initial phase of TCA- $^{32}\text{P}_i$  liberation from DNS-AT $^{32}\text{P}$  by  $\text{F}_1$ . A: The reaction mixture contained 2.83 (●), 5.65 (○) or 11.3 (×) mol DNS-AT $^{32}\text{P}$ /mol  $\text{F}_1$  and  $0.75 \mu\text{M}$   $\text{F}_1$ . The reaction was started by addition of 5 mM  $\text{MgCl}_2$ . B: The data in A were plotted as the logarithm of the fraction of remaining amount of DNS-AT $^{32}\text{P}$  versus reaction time. The  $\text{P}_i$ -burst size was obtained by extrapolating the linear portion of a slow change to time 0 (broken line).



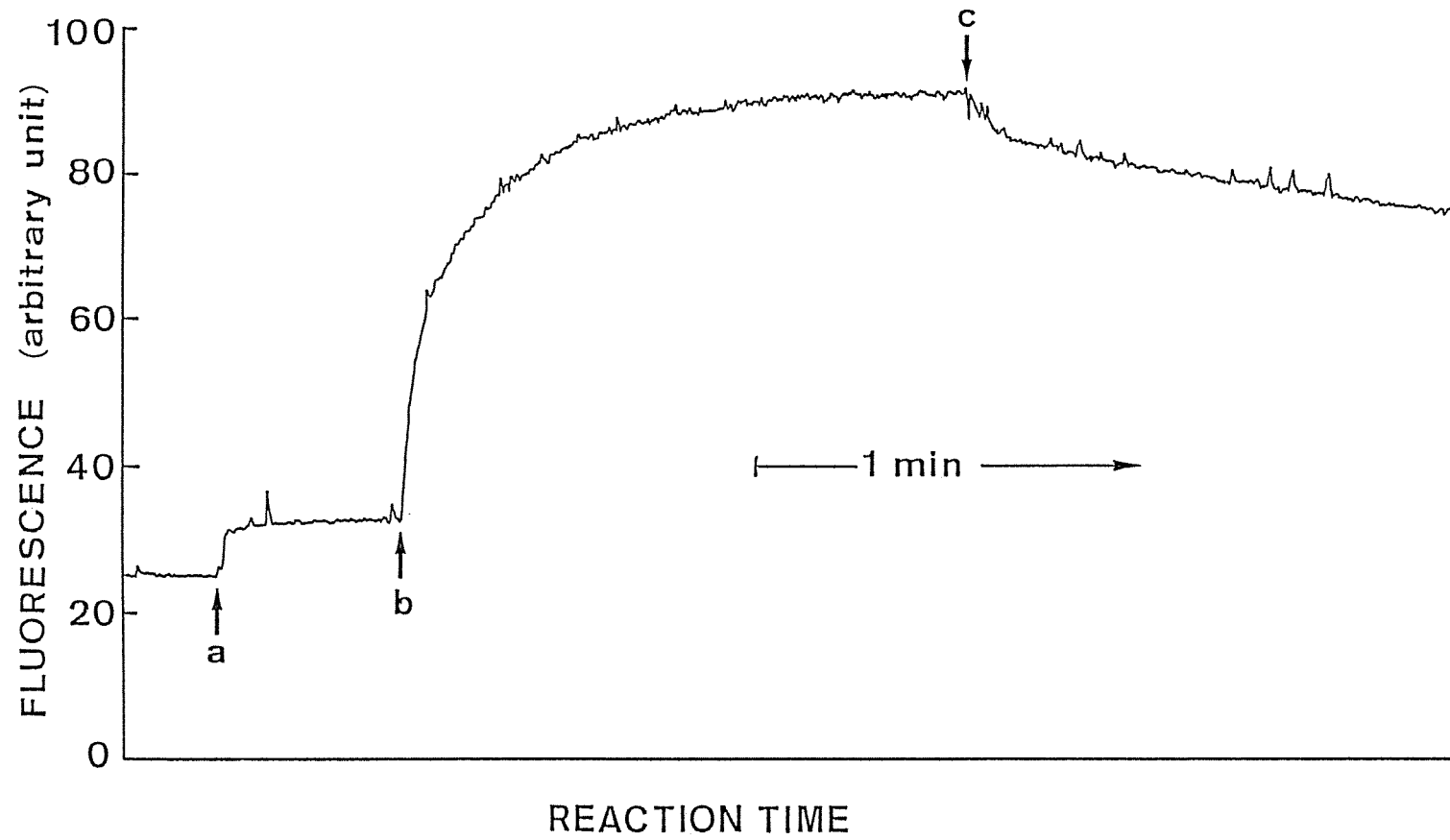


Fig. 11. Fluorescence decay on addition of EDTA to  $F_1$ -DNS-nucleotide. The reaction mixture contained 2.12  $\mu$ M DNS-ATP in 2 mM EDTA, 50 mM Tris-HCl at pH 8.0. Following additions were made; a, 1.36  $\mu$ M  $F_1$ ; b, 4 mM  $MgCl_2$ ; c, 7 mM EDTA.

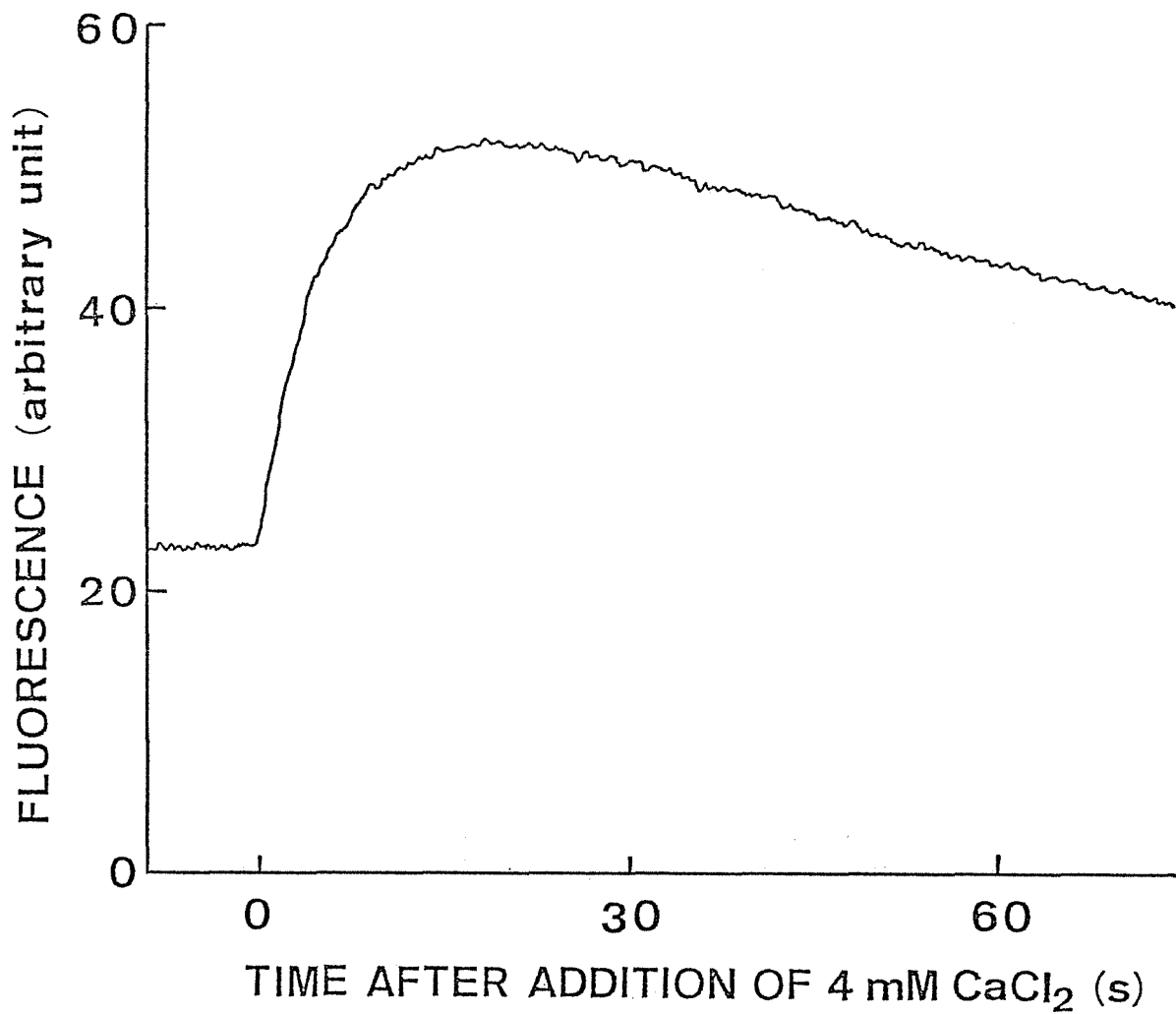


Fig. 12. Time course of change in fluorescence on reaction of DNS-ATP with  $F_1$  in the presence of  $CaCl_2$ . The reaction mixture contained  $1.1 \mu M$  DNS-ATP and  $1.1 \mu M$   $F_1$ . The reaction was started by addition of  $4 mM$   $CaCl_2$ .

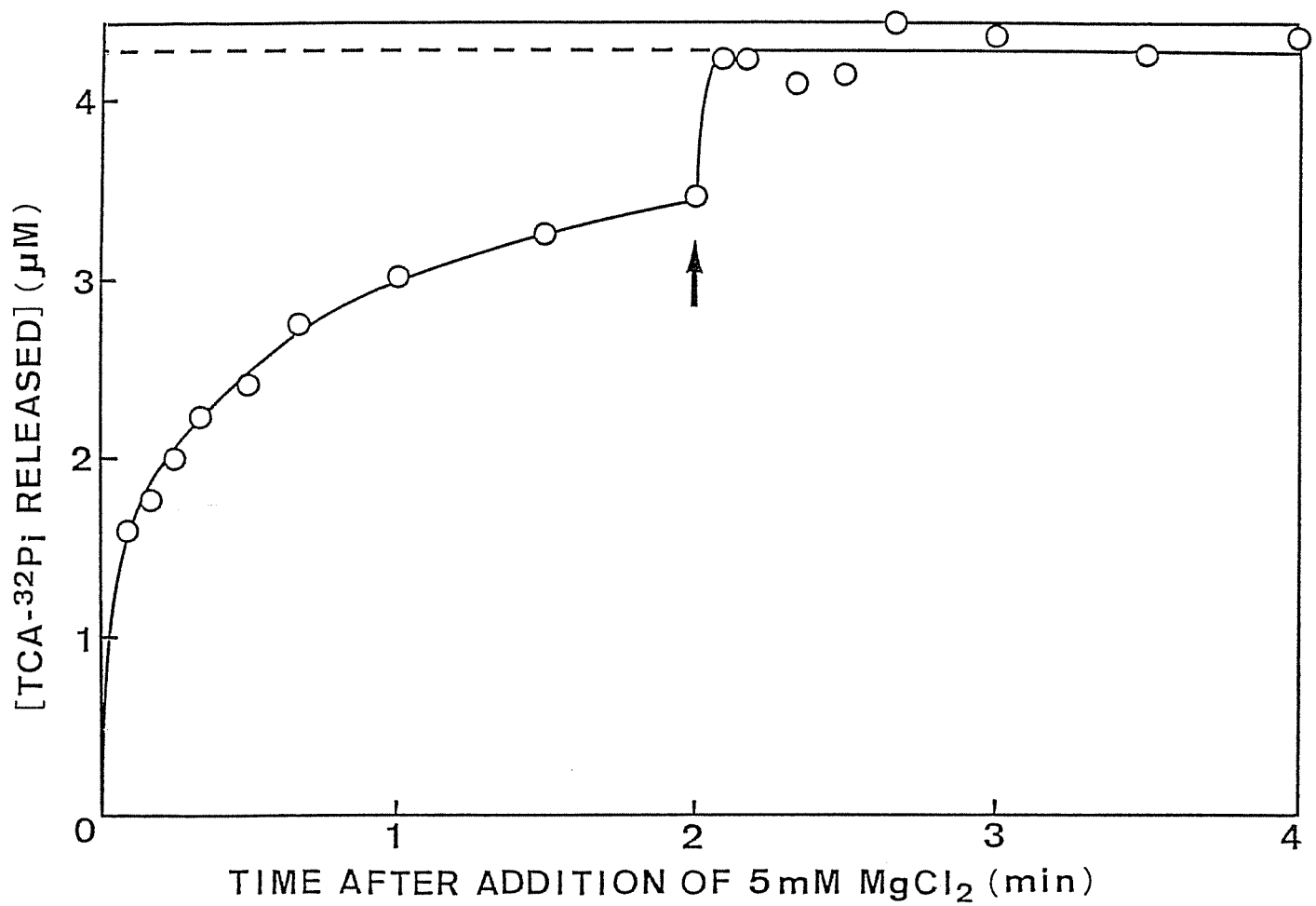


Fig. 13. Acceleration by ATP of TCA-<sup>32</sup>P<sub>i</sub> liberation from the F<sub>1</sub>-DNS-AT<sup>32</sup>P system. The reaction mixture contained 4.28 µM DNS-AT<sup>32</sup>P and 6.78 µM F<sub>1</sub>. The reaction was started by addition of 5 mM MgCl<sub>2</sub>. At the arrow (2 min) 0.2 mM ATP was added. The broken line shows the level of 4.28 µM.

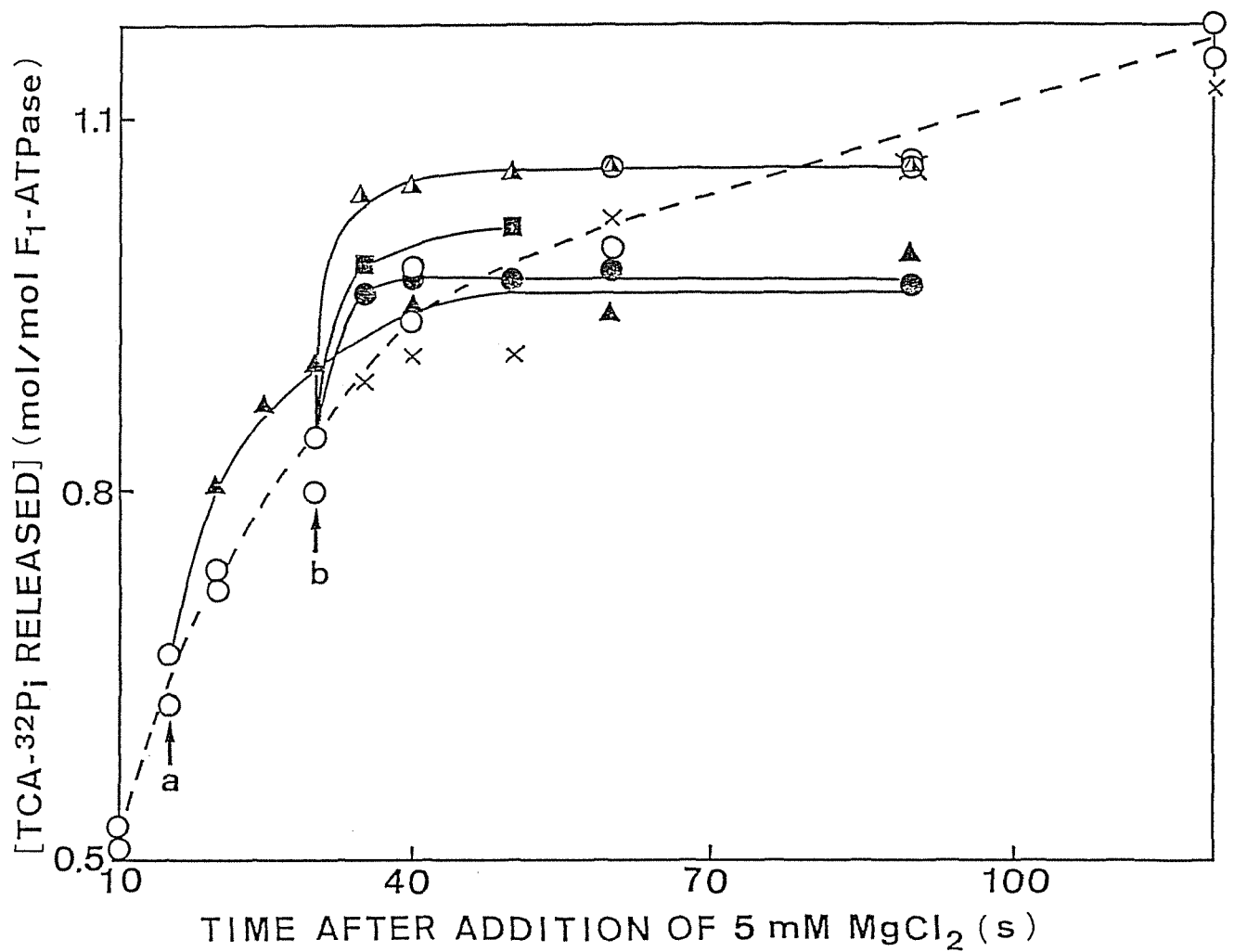


Fig. 14. Acceleration by various phosphate compounds of TCA-<sup>32</sup>P<sub>i</sub> liberation from the F<sub>1</sub>-DNS-AT<sup>32</sup>P system. The reaction mixture contained 1.8 μM DNS-AT<sup>32</sup>P and 1.22 μM F<sub>1</sub>. The reaction was started by addition of 5 mM MgCl<sub>2</sub>. At the arrow a (15 s) 0.2 mM ATP (▲) was added. At the arrow b (30 s) 0.2 mM ATP (▲), 0.2 mM AMPPNP (■), 0.2 mM ADP (●) or 1 mM PP<sub>i</sub> (×) was added. The control (○) is also indicated.

calculated by using  $\phi_{\text{DNS-ATP}} = 0.44 \mu\text{M}$ . The rate of TCA- $^{32}\text{P}_i$  liberation also increased by addition of 0.2 mM ADP or 0.2 mM AMPPNP but to a lesser extent. Addition of 0.2 mM  $\text{PP}_i$  showed no effect. The results in Figs. 13-15 clearly demonstrate that DNS-AT $^{32}\text{P}$  bound to  $\text{F}_1$  is hydrolyzed very rapidly on addition of 0.2 mM ATP, and that  $[\gamma\text{-}^{32}\text{P}]$ phosphoryl group is rapidly released as free  $^{32}\text{P}_i$ .

Acceleration of DNS-ADP Release from  $\text{F}_1$ -DNS-Nucleotide Complex by Addition of High Concentration of ATP — A decrease in fluorescence intensity and release of DNS-nucleotide occurred concomitantly on addition of 0.2 mM ATP to a mixture of 8.6  $\mu\text{M}$  DNS-ATP, 9.2  $\mu\text{M}$   $\text{F}_1$ , and 5 mM  $\text{Mg}^{2+}$ , which had been incubated for 2 min (Fig. 16). The fluorescence intensity decreased rapidly to about 50% of the original level within the response time of apparatus ( $\lesssim 0.5$  s), followed by a slow decrease approaching the level of free DNS-ATP. Since  $\text{F}_1$ -DNS-ATP was readily converted into  $\text{F}_1$ -DNS-ADP +  $\text{P}_i$  by addition of ATP as mentioned above, the observed changes correspond to the release of DNS-ADP from  $\text{F}_1$ -DNS-ADP.

When increasing concentrations of ATP were added to  $\text{F}_1$ -DNS-nucleotide, the extent of the first rapid decrease of the fluorescence increased with an increase in the rate of slow change (Fig. 17), but did not reach 100% even on addition of 0.2 mM ATP.

Acceleration of DNS-ADP Release from  $\text{F}_1$ -DNS-Nucleotide Complex by Addition of Various Phosphate Compounds — ATP, ADP, AMPPNP, ITP, and GTP, 0.2 mM each, added to  $\text{F}_1$ -DNS-nucleotide induced a fluorescence decrease consisting of rapid and slow

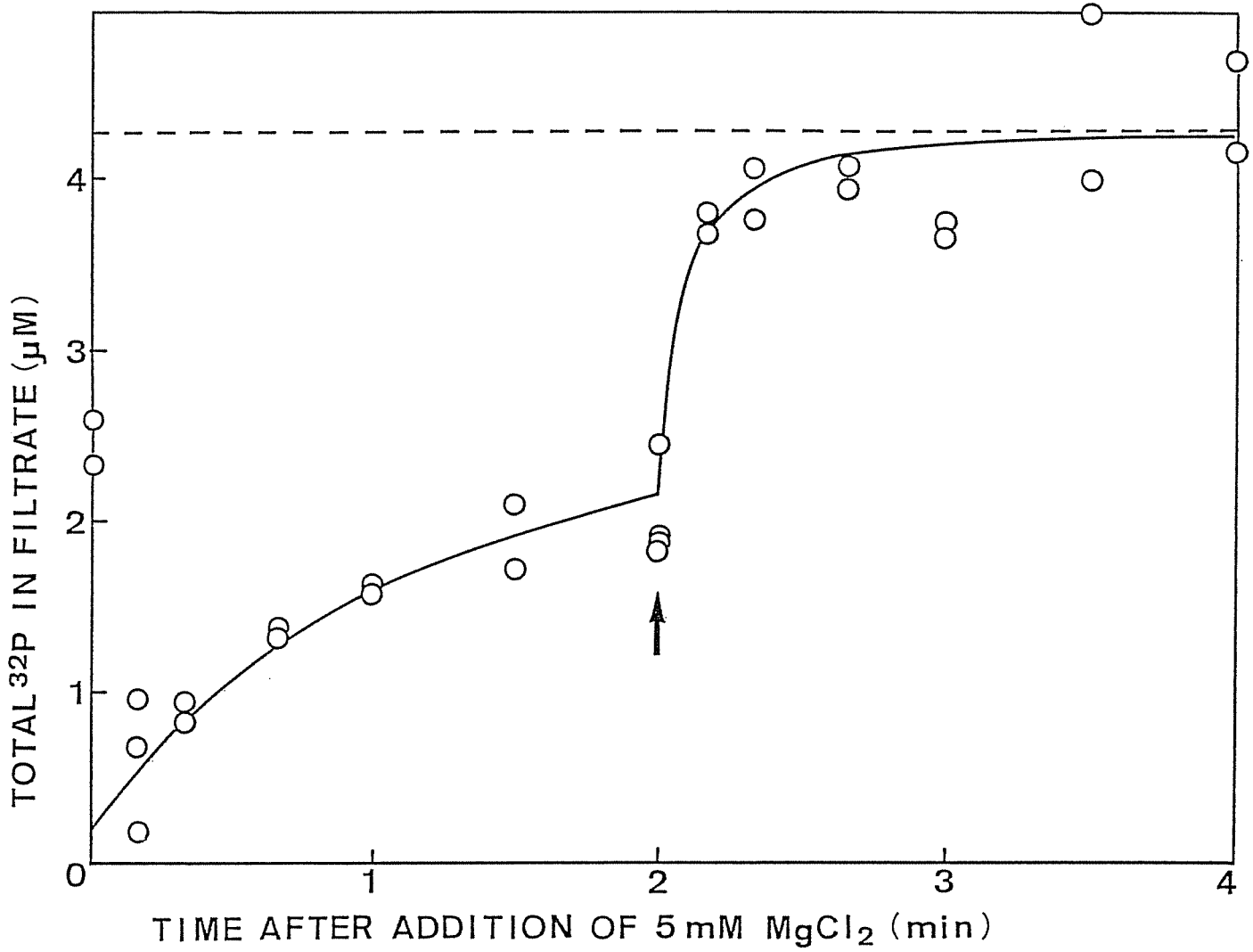


Fig. 15. Acceleration by ATP of free <sup>32</sup>P liberation from the F<sub>1</sub>-DNS-AT<sup>32</sup>P system. The reaction was carried out under the identical conditions as described in the legend to Fig. 13 except that the reaction was stopped by filtration through an XM-100A membrane.

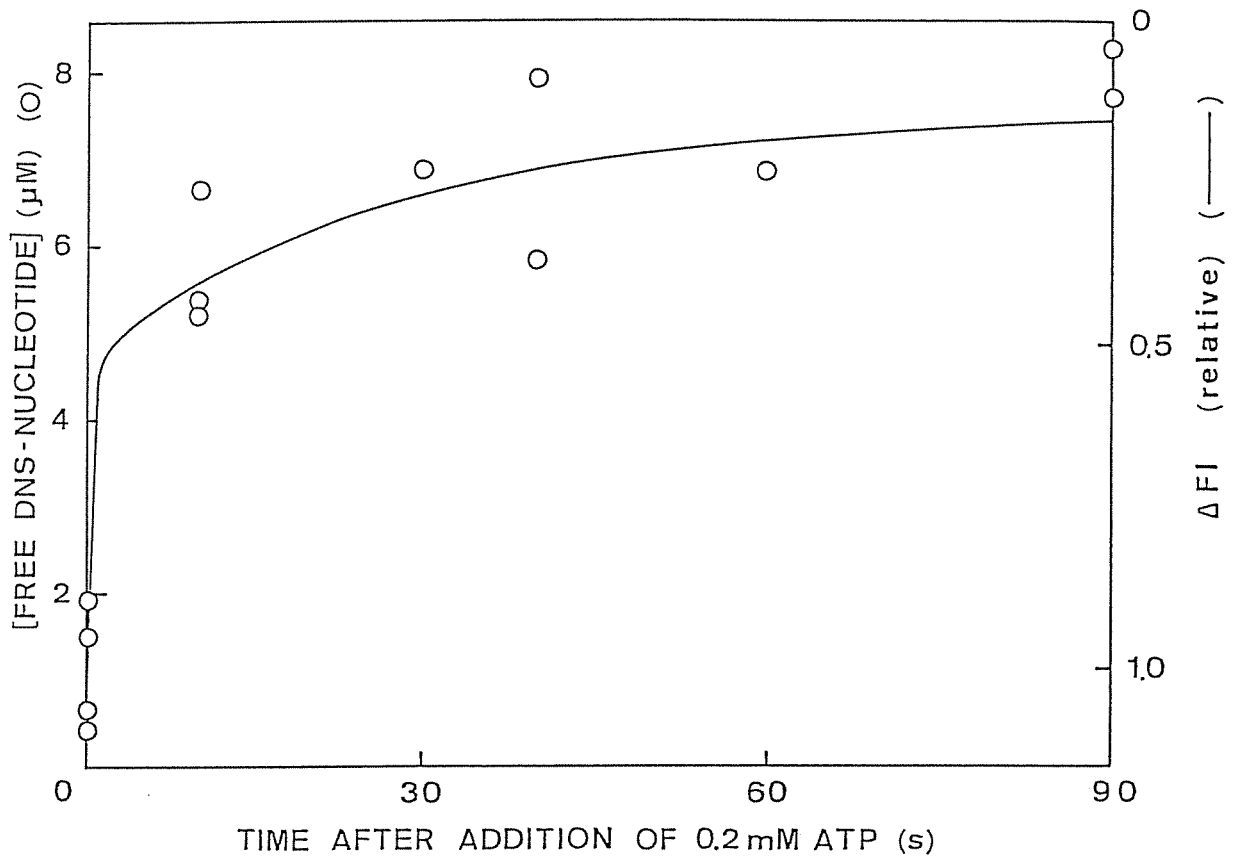


Fig. 16. Comparison of the time course of a decrease in fluorescence with that of release of DNS-nucleotide on addition of ATP to  $F_1$ -DNS-ATP. A mixture containing 8.6  $\mu$ M DNS-ATP, 9.2  $\mu$ M  $F_1$ , and 10 mM [ $^3$ H]glucose was incubated with 5 mM  $MgCl_2$  for 90 s, and then 0.2 mM ATP was added. The reaction was stopped by filtration through an XM-100A membrane at the time indicated. The extent of a decrease in fluorescence intensity,  $\Delta FI$ , is plotted as relative to difference between the intensity before addition of 0.2 mM ATP (1.0) and that of free DNS-ADP (0).

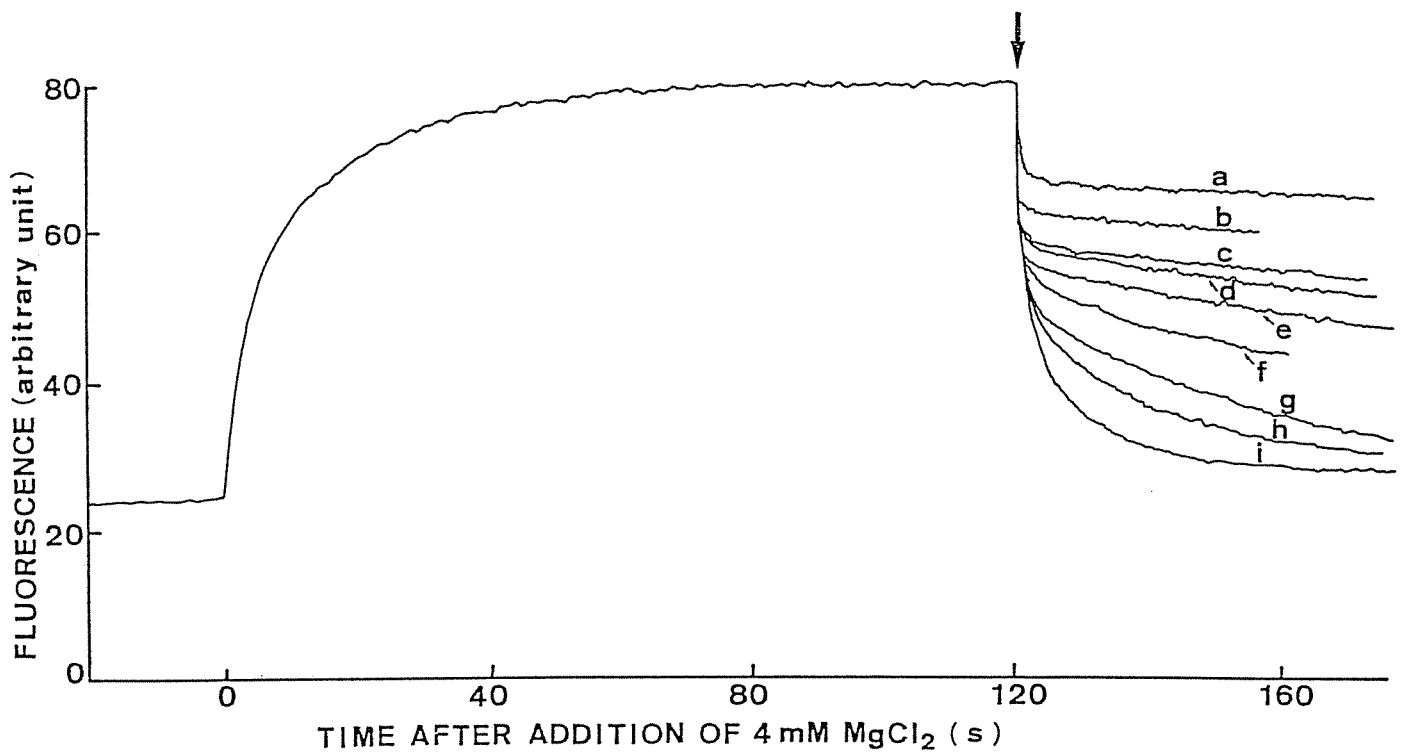


Fig. 17. Fluorescence decay on addition of various concentrations of ATP to  $F_1$ -DNS-nucleotide. The reaction mixture contained  $1.1 \mu\text{M}$  DNS-ATP and  $1.1 \mu\text{M}$   $F_1$  in  $2 \text{ mM}$  EDTA,  $50 \text{ mM}$  Tris-HCl at pH 8.0. At the arrow (2 min), following concentrations of ATP were added;  $0.5 \mu\text{M}$  (a),  $1.0 \mu\text{M}$  (b),  $1.5 \mu\text{M}$  (c),  $2.0 \mu\text{M}$  (d),  $5.0 \text{ uM}$  (e),  $10 \mu\text{M}$  (f),  $40 \mu\text{M}$  (g),  $80 \mu\text{M}$  (h),  $0.2 \text{ mM}$  (i).



phases (Fig. 18). CTP at 0.2 mM yielded only a slow phase, and its rate was of the same order of magnitude as the second slow phase observed with 0.2 mM ATP. At the same time, the rate of TCA- $^{32}\text{P}_i$  liberation from  $\text{F}_1$ -DNS-nucleotide (Fig. 19) was accelerated slightly.

On addition of 7 mM EDTA to  $\text{F}_1$ -DNS-nucleotide in the presence 4 mM  $\text{MgCl}_2$ , the fluorescence intensity decreased very slowly as previously shown in Fig. 11 (Fig. 20). Further addition of 0.1 mM ATP or 0.1 mM ADP markedly increased the rate of the fluorescence decrease. The time course of the fluorescence decrease induced by 0.1 mM ADP followed simple kinetics, whereas that induced by 0.1 mM ATP showed both rapid and slow phases as in the presence of  $\text{Mg}^{2+}$  (Fig. 17).

As previously described,  $\text{PP}_i$  binds to  $\text{F}_1$  competitively with DNS-ATP but with a much lower affinity than that of DNS-ATP. As shown in Fig. 21, the fluorescence intensity of  $\text{F}_1$ -DNS-nucleotide decreased on addition of  $\text{PP}_i$  with a single slow phase, and the extent of the fluorescence change increased with increasing concentration of  $\text{PP}_i$ . The rate of the fluorescence decrease in the presence of 10 mM  $\text{PP}_i$  was almost equal to that induced by 0.2 mM ATP in its slow phase. Furthermore, 1 mM  $\text{PP}_i$  did not accelerate TCA- $^{32}\text{P}_i$  liberation from  $\text{F}_1$ -DNS-nucleotide (see Fig. 14). AMP at 0.2 mM had no effect on the fluorescence intensity of  $\text{F}_1$ -DNS-nucleotide in the presence of  $\text{Mg}^{2+}$  (Fig. 22), did not change the rate of TCA- $^{32}\text{P}_i$  liberation from  $\text{F}_1$ -DNS-nucleotide (Fig. 19).

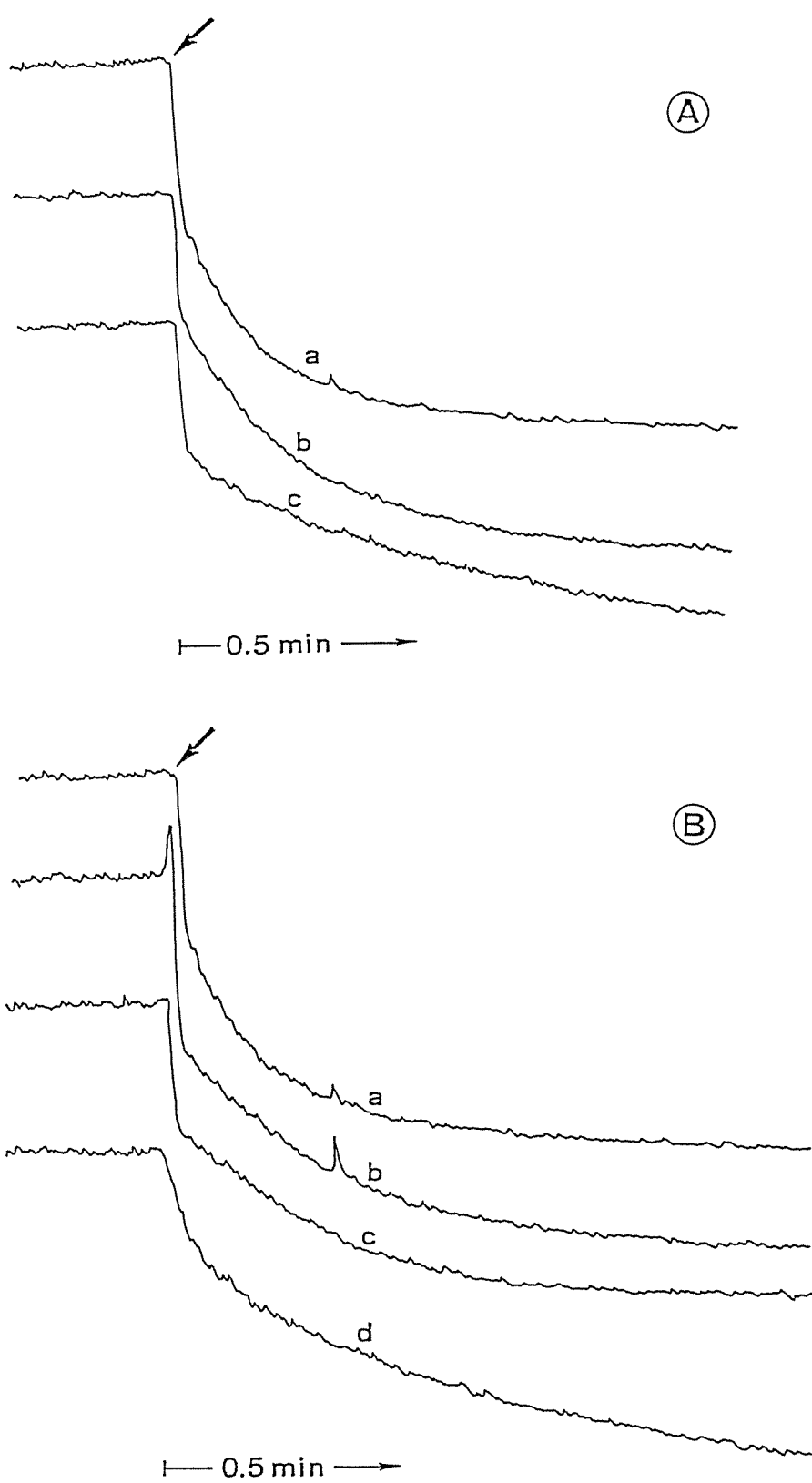


Fig. 18. Fluorescence decay on addition of various nucleotides to  $F_1$ -DNS-nucleotide. A mixture containing  $2.1 \mu\text{M}$  DNS-ATP and  $1.5 \mu\text{M}$   $F_1$  was incubated in the presence of  $5 \text{ mM}$   $\text{MgCl}_2$  for 2 min, and then (at the arrow) following additions were made. A:  $0.2 \text{ mM}$  ATP (a);  $0.2 \text{ mM}$  ADP (b);  $0.2 \text{ mM}$  AMPPNP (c). B:  $0.2 \text{ mM}$  ATP (a);  $0.19 \text{ mM}$  GTP (b);  $0.22 \text{ mM}$  ITP (c);  $0.18 \text{ mM}$  CTP (d).

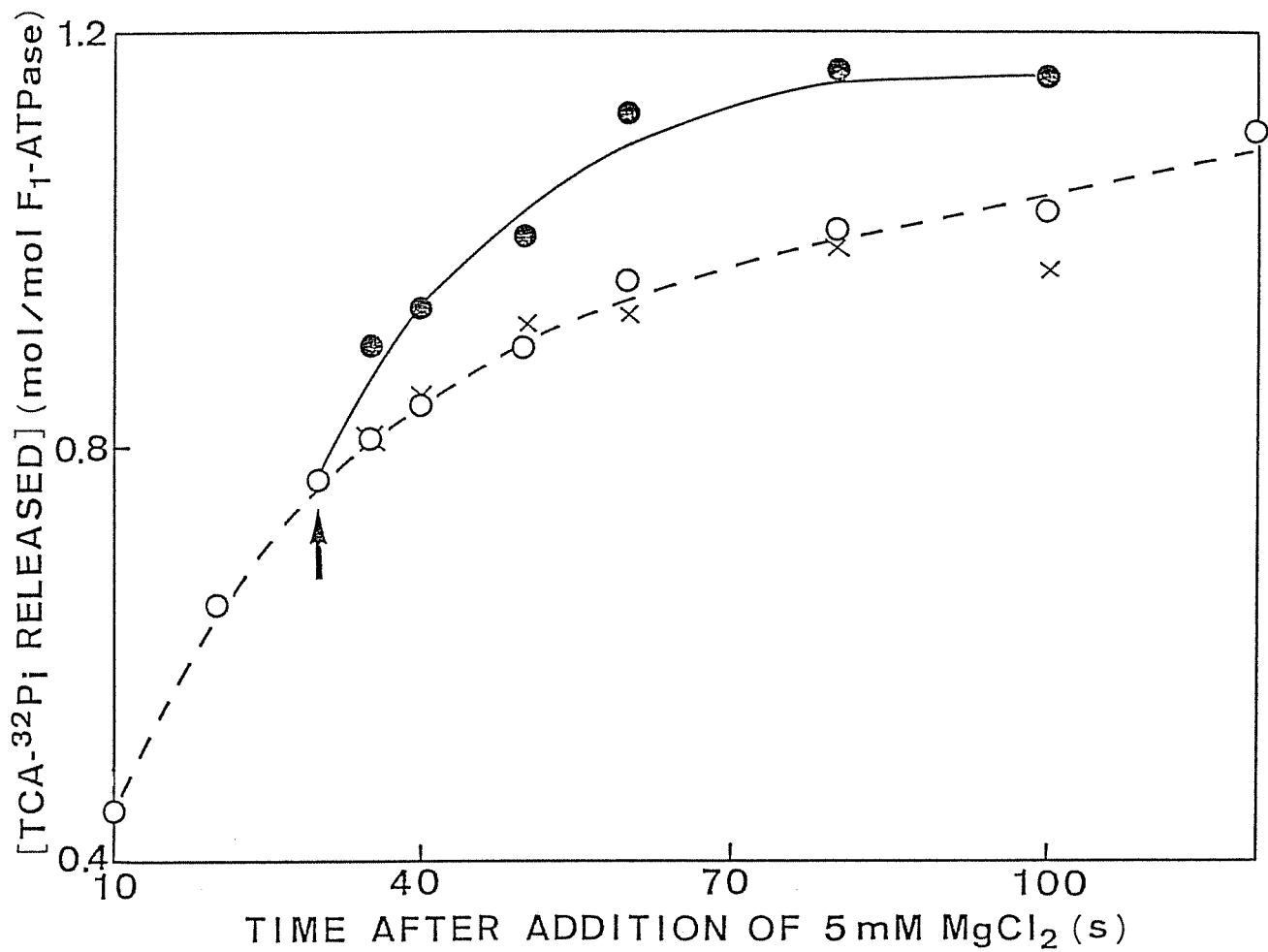


Fig. 19. Effect of CTP and AMP on TCA-<sup>32</sup>P<sub>i</sub> liberation from the F<sub>1</sub>-DNS-AT<sup>32</sup>P system. The reaction mixture contained 1.8 μM DNS-AT<sup>32</sup>P and 1.2 μM F<sub>1</sub> in 2 mM EDTA, 50 mM Tris-HCl at pH 8.0. The reaction was started by addition of 5 mM MgCl<sub>2</sub>. At the arrow (30 s), 0.2 mM CTP (●) or 0.2 mM AMP (X) was added. The control (O) is also indicated.

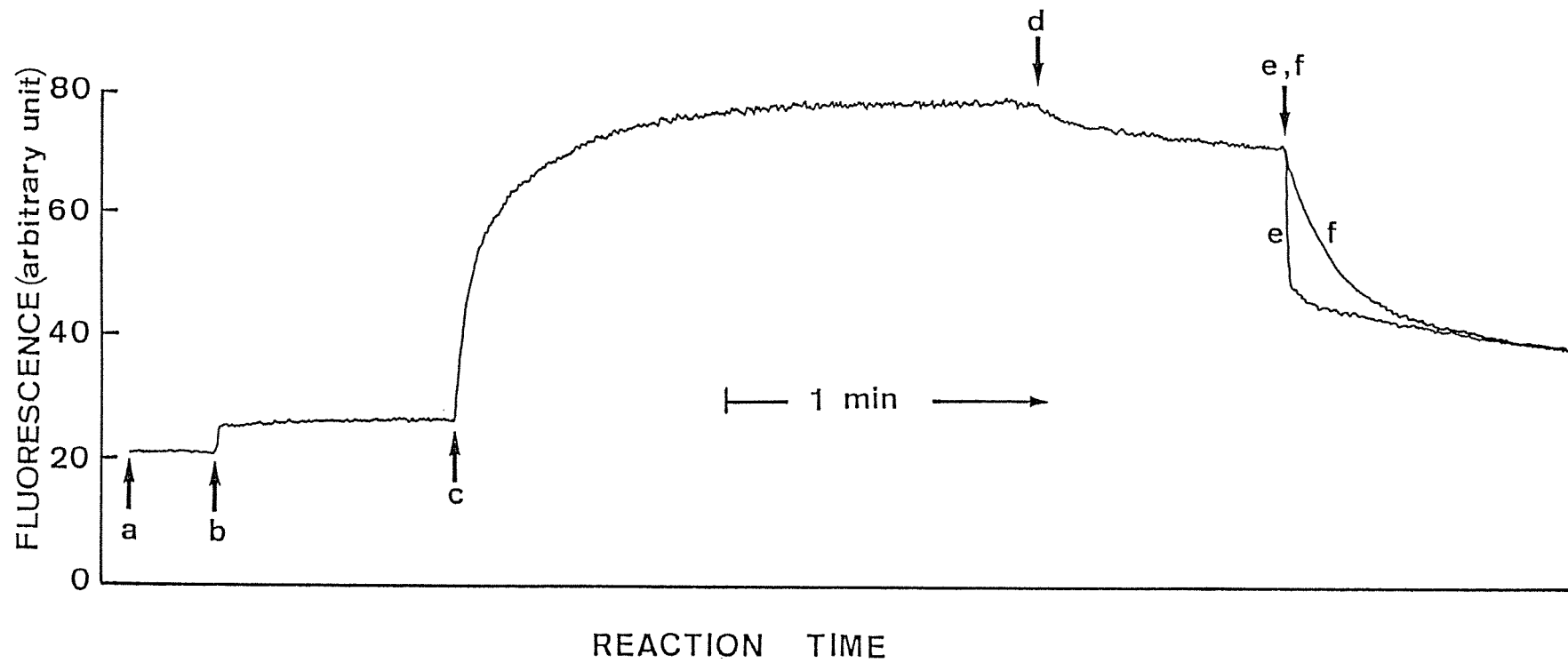


Fig. 20. Fluorescence decay of  $F_1$ -DNS-nucleotide on addition of ATP or ADP in the presence of EDTA. To a mixture containing 2 mM EDTA and 50 mM Tris-HCl at pH 8.0, following additions were made; a, 2.1  $\mu$ M DNS-ATP; b, 1.4  $\mu$ M  $F_1$ ; c, 4 mM  $MgCl_2$ ; d, 7 mM EDTA (final concentration); e, 0.1 mM ATP; f, 0.1 mM ADP.

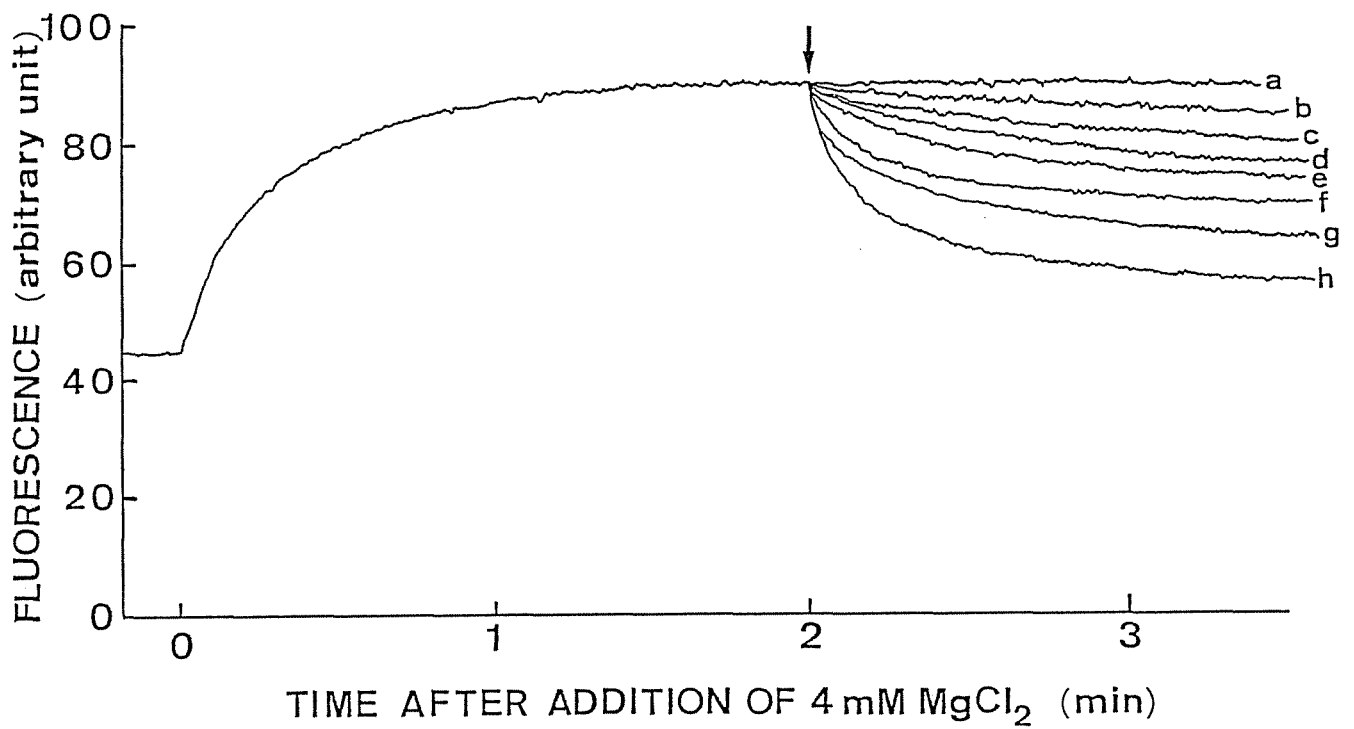


Fig. 21. Fluorescence decay of  $F_1$ -DNS-nucleotide on addition of various concentrations of  $PP_i$ . The reaction mixture contained  $4.0 \mu\text{M}$  DNS-ATP and  $0.75 \mu\text{M}$   $F_1$ . At the arrow (2 min), following concentrations of  $PP_i$  were added; 0 (a),  $4 \mu\text{M}$  (b);  $10 \mu\text{M}$  (c);  $40 \mu\text{M}$  (d);  $100 \mu\text{M}$  (e);  $400 \mu\text{M}$  (f);  $4 \text{mM}$  (g);  $10 \text{mM}$  (h).

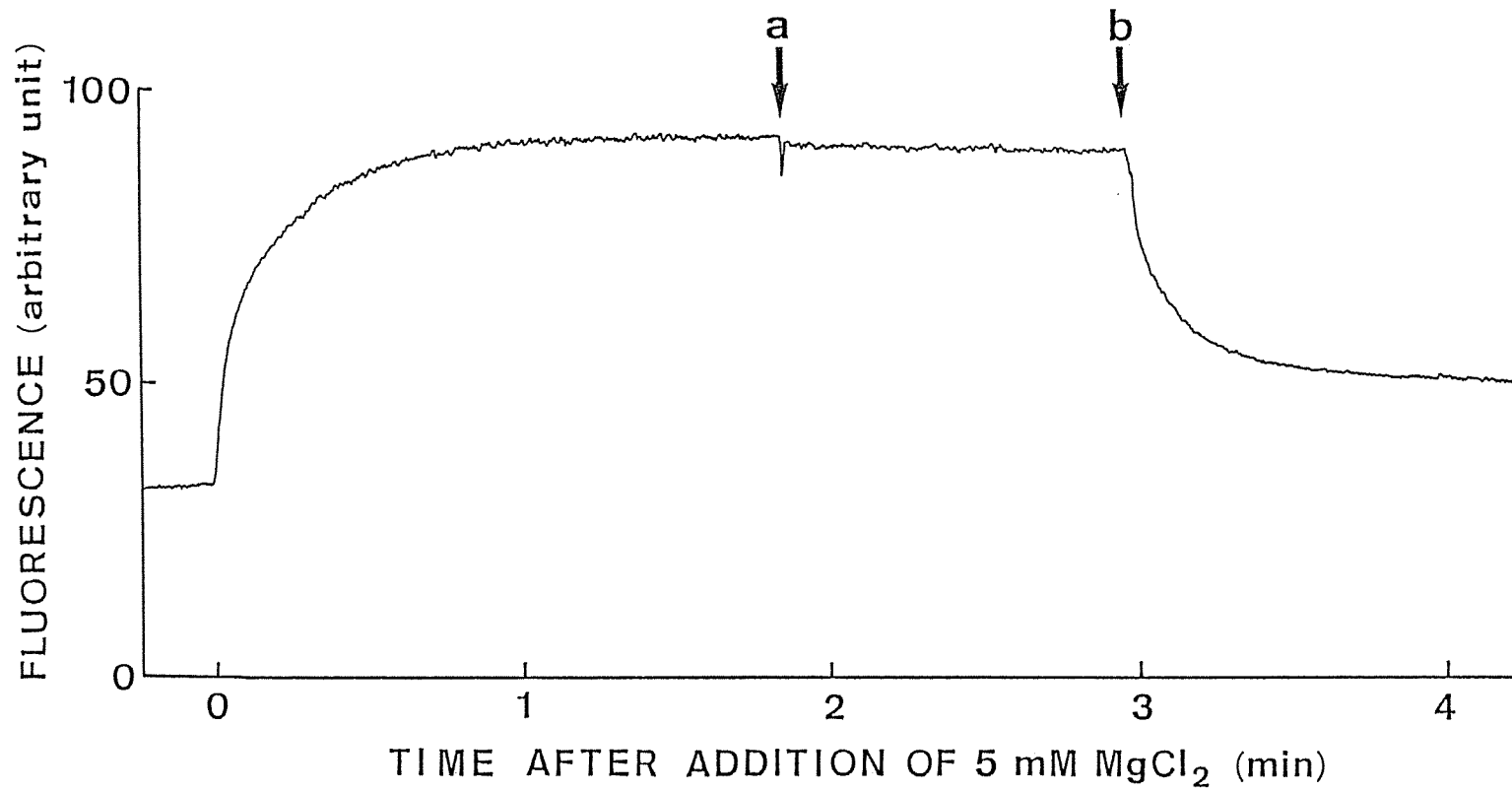


Fig. 22. Effect of AMP on fluorescence of  $F_1$ -DNS-nucleotide. The reaction mixture contained  $2.1 \mu\text{M}$  DNS-ATP and  $1.5 \mu\text{M}$   $F_1$ . After addition of  $5 \text{ mM}$   $\text{MgCl}_2$ , following additions were made; a,  $0.2 \text{ mM}$  AMP; b,  $0.2 \text{ mM}$  ATP.

Dependence of the Steady-State Rate of  $F_1$ -DNS-ATPase on Substrate Concentration---As shown in Fig. 23, the steady-state rate,  $v_o$ , increased in proportion to the DNS-AT<sup>32</sup>P concentration up to 200  $\mu$ M, where the  $v_o$  value was 1.0 s<sup>-1</sup> accounting for about 0.5% of that of  $F_1$ -ATPase reaction at 200  $\mu$ M ATP (cf. Fig. 24). If we assume that the  $F_1$ -DNS-ATPase reaction at the steady state follows a simple Michaelis-Menten kinetics, this result indicates that the values of  $K_m$  for DNS-ATP and  $V_{max}$  are much larger than 200  $\mu$ M and 1 s<sup>-1</sup>, respectively.

Comparison of Time Course of ATP Hydrolysis with That of DNS-ADP Release from  $F_1$ -DNS-Nucleotide Complex after Addition of ATP — DNS-ATP (6.42  $\mu$ M) was allowed to react with  $F_1$  (0.3  $\mu$ M) in the presence of Mg<sup>2+</sup>, PEP, and pyruvate kinase for 90 s. It was confirmed that ADP but not DNS-ADP can be converted into NTP by pyruvate kinase (16). Then 0.2 mM ATP was added, and both fluorescence decrease and TCA-P<sub>i</sub> liberation were followed in parallel experiments. Under the condition used, almost all TCA-P<sub>i</sub> was derived by ATP hydrolysis. At the moment of the ATP addition, more than 95% of  $F_1$  added was estimated to have bound DNS-nucleotide on the basis of  $\phi_{DNS-ATP} = 0.44 \mu$ M. As shown in Fig. 24, the fluorescence intensity decreased in two phases. If we assume that ATP is mainly hydrolyzed at the same site(s) where DNS-nucleotides bind to  $F_1$ , the TCA-P<sub>i</sub> liberation should have a lag phase corresponding to the release of DNS-ADP (about 3.5 min). However, no such lag phase was observed.

Effect of P<sub>i</sub> on Fluorescence of  $F_1$ -DNS-Nucleotide Complex — As already shown in Fig. 2, the fluorescence of  $F_1$ -Mg<sup>2+</sup>-DNS-nucleotide was further enhanced by addition of P<sub>i</sub>. Figure 25A

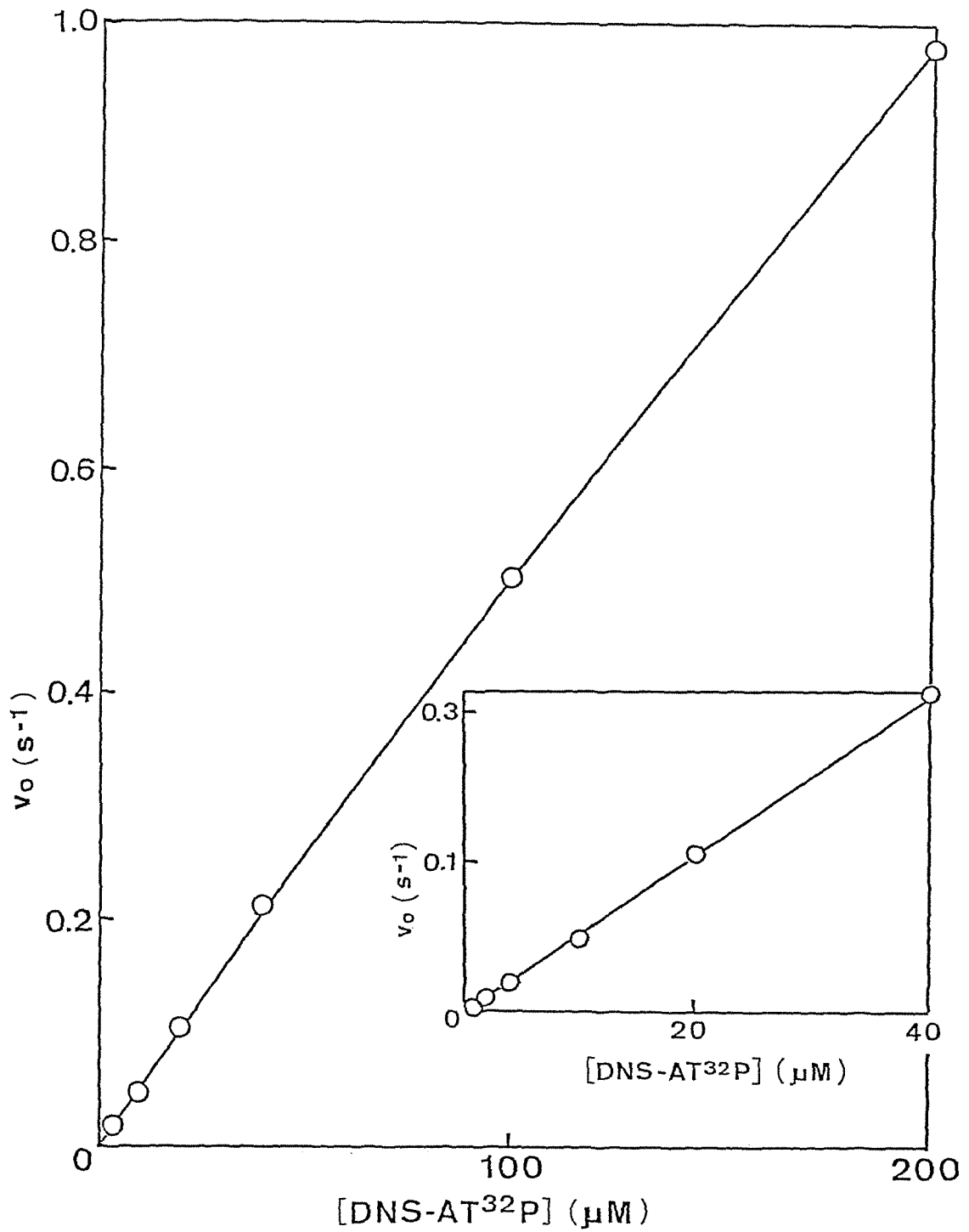


Fig. 23. Dependence on DNS-ATP concentration of the steady-state rate of  $F_1$ -DNS-ATPase reaction. The reaction mixture contained  $0.30 \mu\text{M}$   $F_1$ , various concentrations of DNS-AT<sup>32</sup>P,  $2.5 \text{ mM}$   $\text{MgCl}_2$ , and  $50 \text{ mM}$  Tris-HCl at pH 8.0 and  $30^\circ\text{C}$ . The reaction was started by addition of DNS-AT<sup>32</sup>P.



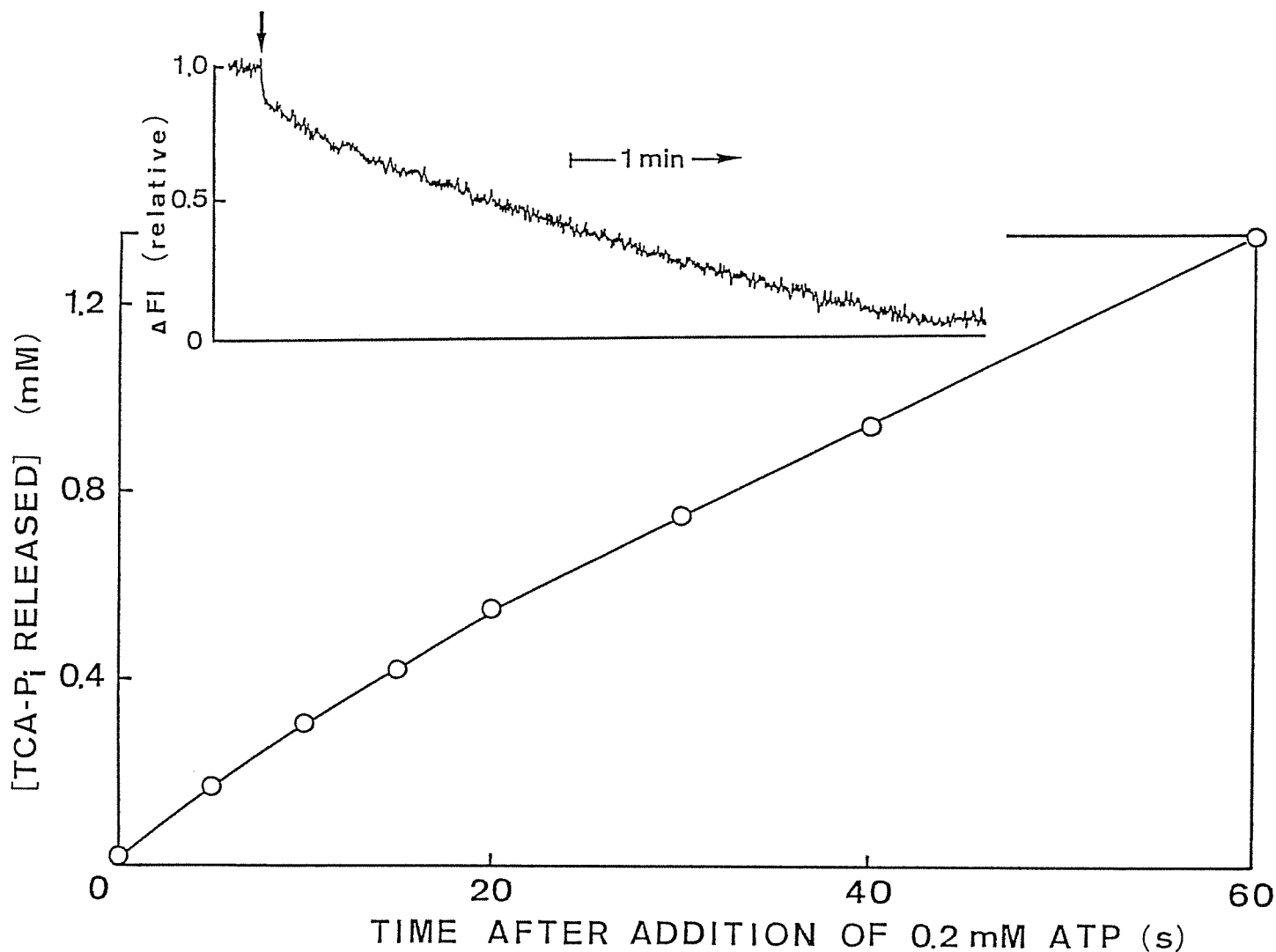


Fig. 24. Comparison of the time course of ATP hydrolysis with that of the DNS-ADP release from F<sub>1</sub>-DNS-nucleotide after addition of ATP. A mixture containing 6.42  $\mu$ M DNS-ATP, 0.31  $\mu$ M F<sub>1</sub>, 0.48 mg/ml pyruvate kinase, and 4 mM PEP in 2 mM EDTA, 50 mM Tris-HCl at pH 8.0 was incubated with 5 mM MgCl<sub>2</sub> for 90 s, and 0.2 mM ATP was added. The reaction was stopped by addition of 5% TCA at the time indicated. The time course of the DNS-ADP release was measured separately as a fluorescence change under the same conditions (inset). The arrow in the inset shows the time of addition of 0.2 mM ATP.

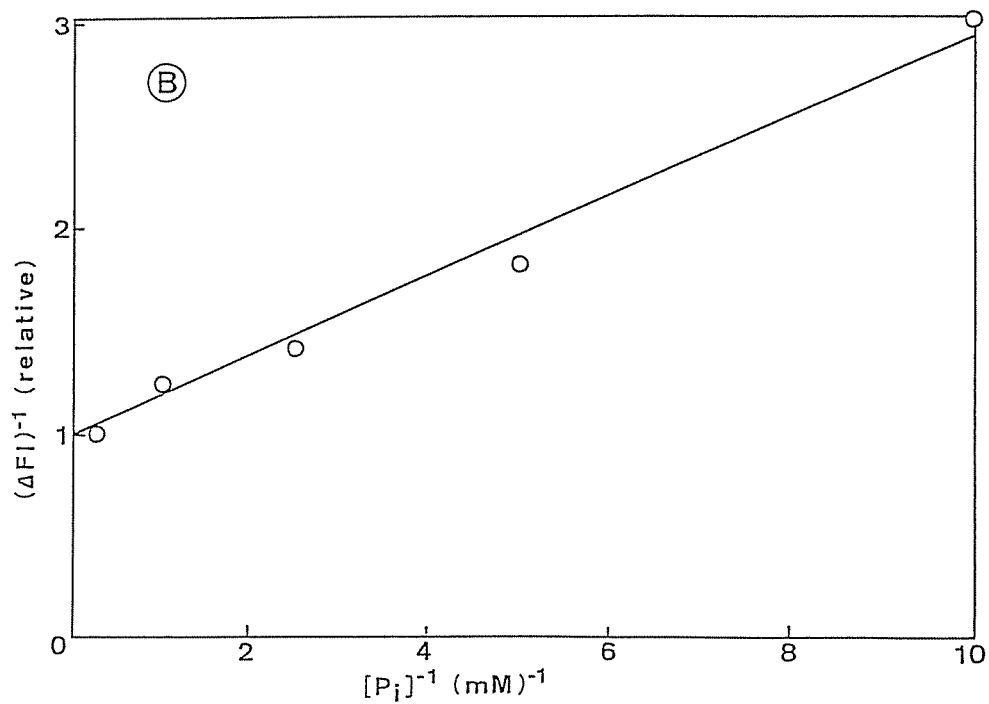
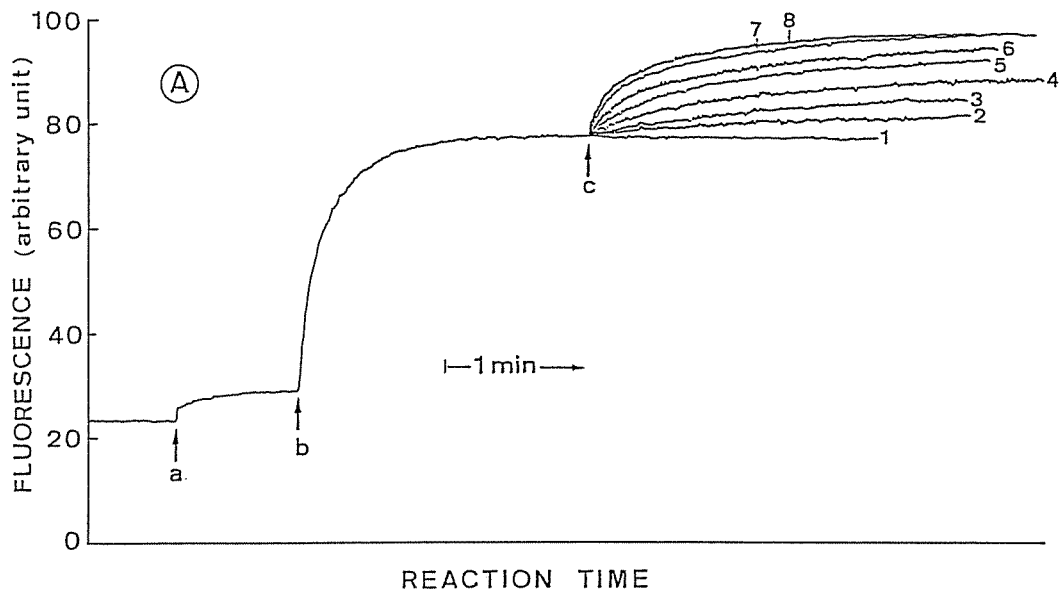


Fig. 25. Fluorescence enhancement of  $F_1$ -DNS-nucleotide on addition of  $P_i$ . The concentration of DNS-ATP added was  $3.2 \mu\text{M}$ . A: Following additions were made; a,  $1.5 \mu\text{M } F_1$ ; b,  $5 \text{ mM } \text{MgCl}_2$ ; c, K- $P_i$  at concentrations of 0 (1),  $40 \mu\text{M}$  (2),  $0.1 \text{ mM}$  (3),  $0.2 \text{ mM}$  (4),  $0.4 \text{ mM}$  (5),  $1 \text{ mM}$  (6),  $4 \text{ mM}$  (7),  $10 \text{ mM}$  (8). B: The reciprocal of the extent of fluorescence enhancement at 2 min after K- $P_i$  addition ( $\Delta F$ ) was plotted against the reciprocal of the concentration of K- $P_i$  added.

shows the time courses of the fluorescence enhancement of  $F_1$ -DNS-nucleotide on addition of various concentrations of  $P_i$  at pH 8.0. With increasing concentrations of  $P_i$ , the extent of the fluorescence enhancement increased, and was saturated at about 4 mM  $P_i$ . Figure 25B shows a double reciprocal plot of the extent of the fluorescence enhancement at 2 min after  $P_i$  addition and the  $P_i$  concentration. A single straight line enabled an estimation of an apparent dissociation constant of  $P_i$  from  $F_1$ -DNS-nucleotide ( $\phi_{P_i}$ ) as 195  $\mu$ M. The affinity of  $F_1$ -DNS-nucleotide for  $P_i$  increased with decreasing pH (Fig. 4). At pH 6.5 the fluorescence enhancement was saturated at least with 50  $\mu$ M  $P_i$  (data not shown). The rate of DNS-AT<sup>32</sup>P hydrolysis in the presence of 4.3  $\mu$ M DNS-AT<sup>32</sup>P, 1.7  $\mu$ M  $F_1$ , and 5 mM MgCl<sub>2</sub> was unaffected by the addition of 1 mM  $P_i$  (data not shown).

We also examined effects of various anions on the fluorescence intensity of  $F_1$ -DNS-nucleotide (Fig. 26). These anions are known to accelerate the  $F_1$ -ATPase activity (28). The fluorescence intensity was almost unaffected by 5 mM HCO<sub>3</sub><sup>-</sup> or 2 mM maleate, and slightly increased on addition of 0.5 mM HSO<sub>3</sub><sup>-</sup>. The effect of HSO<sub>3</sub><sup>-</sup> was maximal at 2 mM.

#### Binding of DNS-Nucleotide to $F_1$ in the Presence of $P_i$ —

The fluorescence intensity of DNS-ATP after addition of  $F_1$ , MgCl<sub>2</sub>,  $P_i$ , and ATP, as added in this order, was measured in the presence of different concentrations of DNS-ATP (see Fig. 2), and the fluorescence intensities at each step were plotted against the DNS-ATP concentration (Fig. 27A). The extent of the fluorescence enhancement induced by  $P_i$  was replotted in

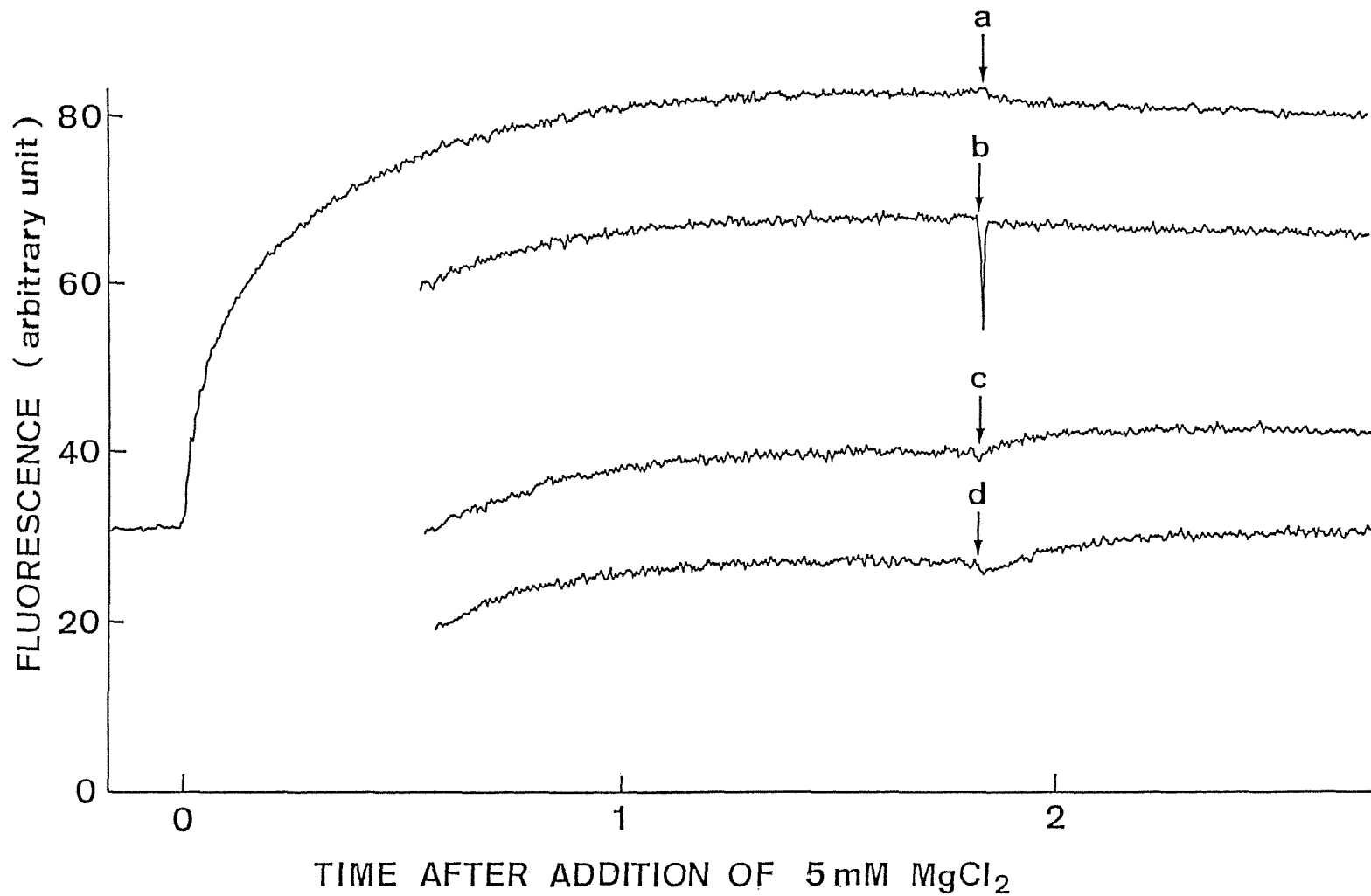


Fig. 26. Fluorescence change of F<sub>1</sub>-DNS-nucleotide induced by various anions. The reaction mixture contained 2.1 μM DNS-ATP and 1.5 μM F<sub>1</sub>. After addition of 5 mM MgCl<sub>2</sub>, following additions were made; a, 5 mM HCO<sub>3</sub><sup>-</sup>; b, 2 mM maleate; c, 0.5 mM HSO<sub>3</sub><sup>-</sup>; d, 2 mM HSO<sub>3</sub><sup>-</sup>.

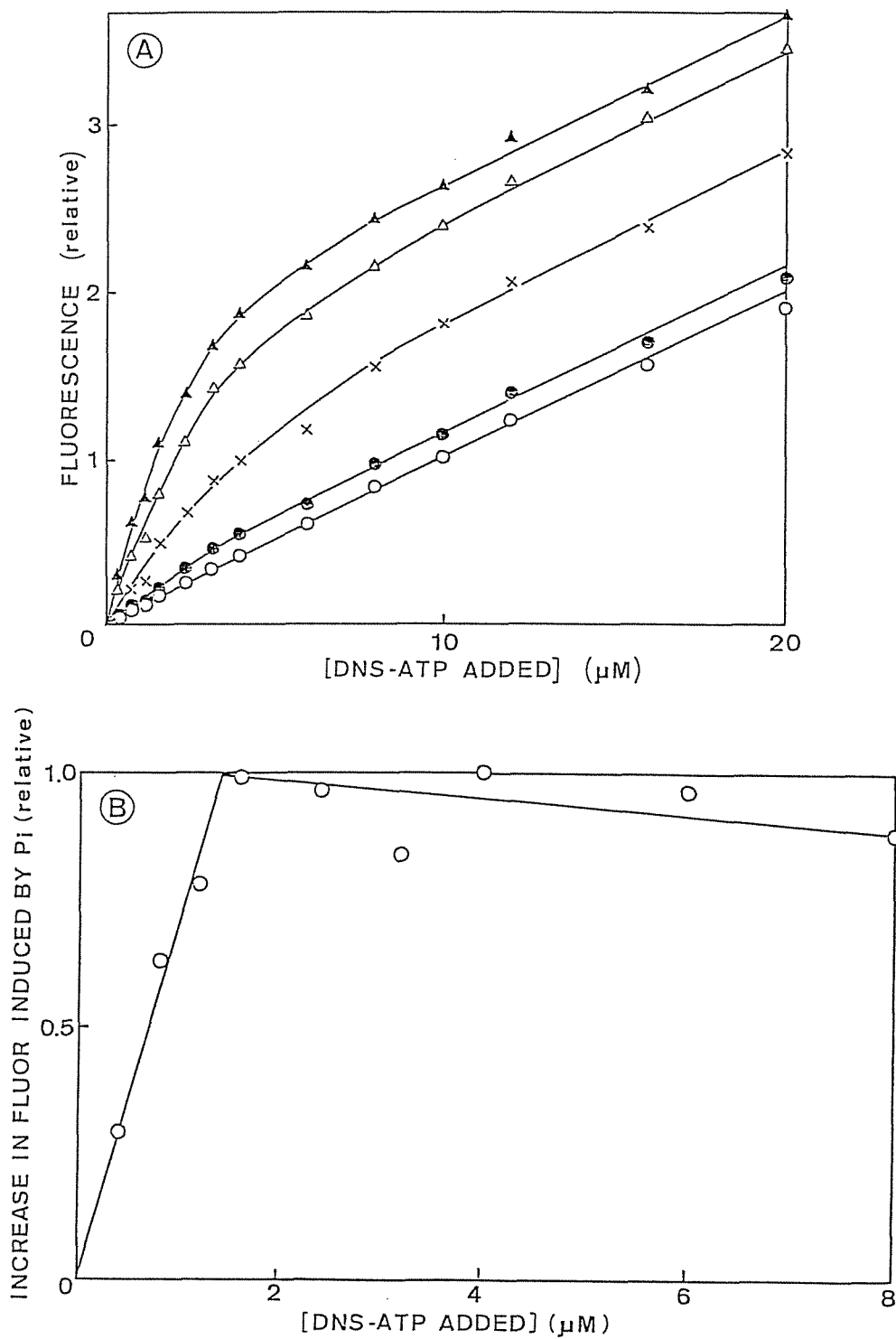


Fig. 27. Fluorometric titration of  $F_1$  by DNS-ATP in the presence of  $P_i$ . A: The fluorescence intensity was measured sequentially as follows; DNS-ATP alone (O); 1 min after addition of  $1.5 \mu\text{M}$   $F_1$  ( $\odot$ ); 2 min after addition of  $5 \text{ mM}$   $\text{MgCl}_2$  ( $\Delta$ ); 2 min after addition of  $8 \text{ mM}$   $\text{K-P}_i$  ( $\blacktriangle$ ); the level decreased rapidly on addition of  $0.2 \text{ mM}$  ATP ( $\times$ ). B: The extent of fluorescence enhancement after addition of  $8 \text{ mM}$   $\text{K-P}_i$  ( $\blacktriangle$  minus  $\Delta$ ) was plotted against the concentration of DNS-ATP added.

Fig. 27B. With an equimolar concentration of DNS-ATP to  $F_1$  (1.5  $\mu$ M), the enhancement was saturated.

Figure 28 shows the effect of 4 mM  $P_i$  on the release of DNS-nucleotide from  $F_1$  induced by  $PP_i$  (A) or ATP (B). The fluorescence decrease on addition of 1 mM  $PP_i$  showed only a slow phase, as already mentioned (cf. Fig. 21), and its rate was remarkably reduced by addition of 4 mM  $P_i$ .  $P_i$  also inhibited the second slow change of the DNS-ADP release on addition of ATP. After the fluorescence intensity of  $F_1$ -DNS-nucleotide was enhanced by addition of 4 mM  $P_i$ , 0.2 mM ATP was added. The fluorescence decreased in two phases as observed in the absence of  $P_i$ . However, the extent of the rapid phase was larger and the rate of the second slow phase was much smaller than those in the absence of  $P_i$ .

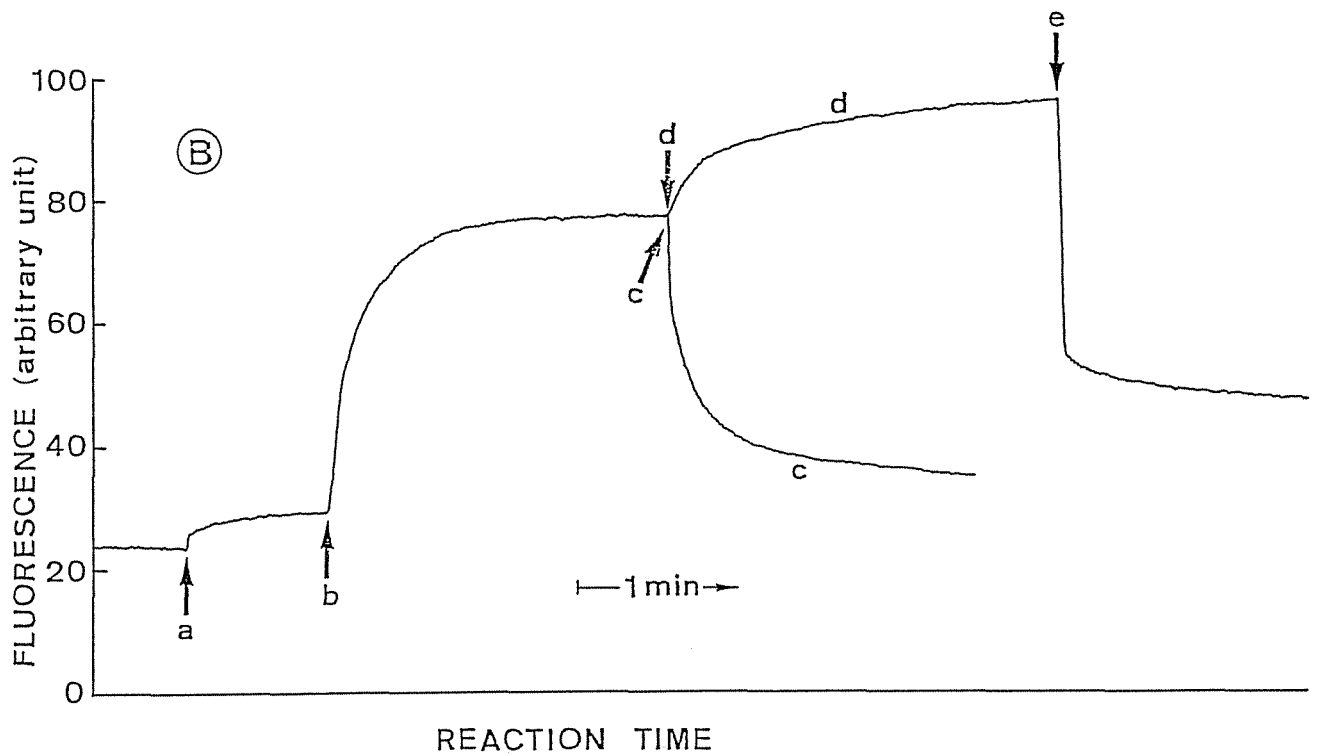
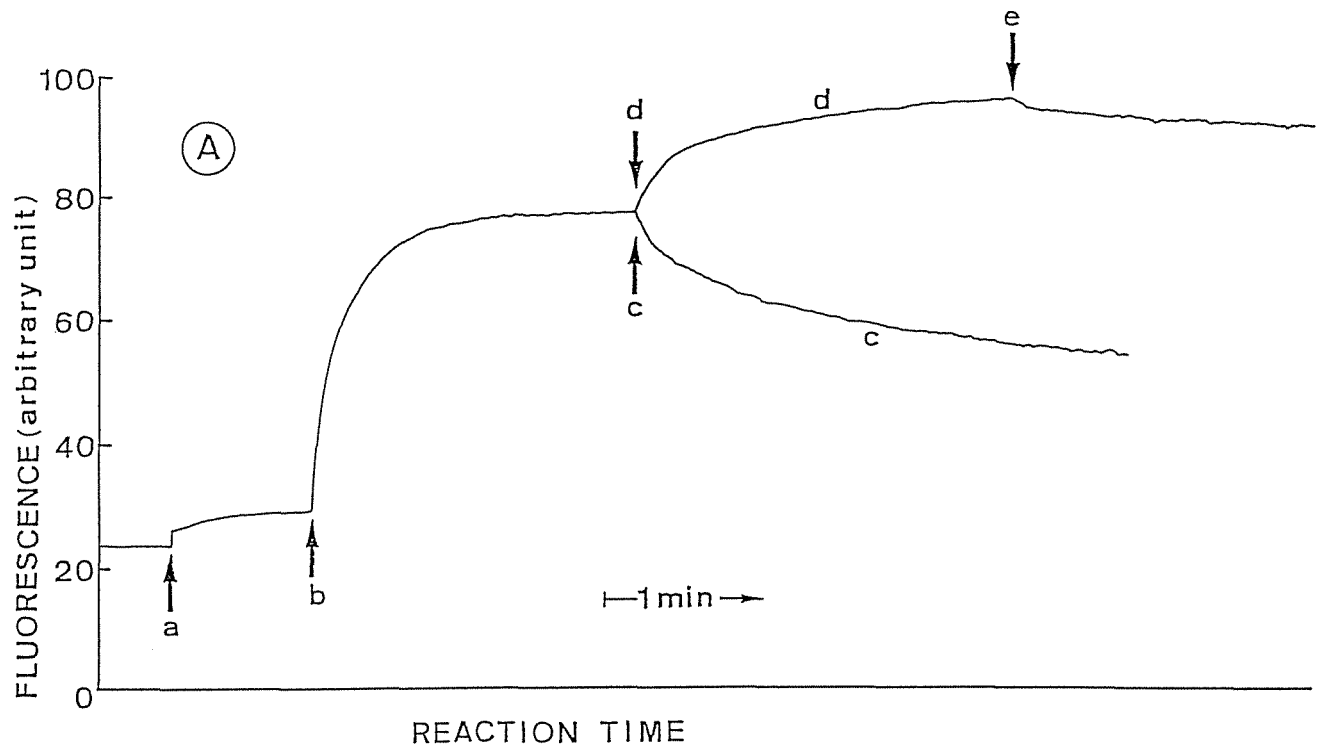


Fig. 28. Time course of a decrease in fluorescence of  $F_1$ -DNS-nucleotide in the presence and absence of  $P_i$  on addition of  $PP_i$  or ATP. The concentration of DNS-ATP added was  $3.2 \mu\text{M}$ .  
 A: Following additions were made; a,  $1.5 \mu\text{M } F_1$ ; b,  $5 \text{ mM } \text{MgCl}_2$ ; c,  $1 \text{ mM } PP_i$ ; d,  $4 \text{ mM } \text{K-}P_i$ ; e,  $1 \text{ mM } PP_i$ . B: Following additions were made; a,  $1.5 \mu\text{M } F_1$ ; b,  $5 \text{ mM } \text{MgCl}_2$ ; c,  $0.2 \text{ mM } \text{ATP}$ ; d,  $4 \text{ mM } \text{K-}P_i$ ; e,  $0.2 \text{ mM } \text{ATP}$ .

## DISCUSSION

Recently, Slater et al. reported that purified  $F_1$  contains 2 mol of unexchangeable ATP/mol  $F_1$  and proposed that these ATP are indispensable in maintaining the conformation of  $F_1$  (4). The amount of ATP tightly bound to our purified  $F_1$  preparation was 2.3 mol/mol  $F_1$ . In this paper, we assumed that these tightly bound ATP were not directly involved in the  $F_1$ -DNS-ATPase reaction (4). Our purified  $F_1$  preparation contained no intrinsic ATPase inhibitor protein (Fig. 1, 27).

So far there are several reports that the nucleotide binding sites on energy-transducing ATPases form hydrophobic clefts (29-31). Upon binding to  $F_1$ , DNS-ATP showed a similar change in fluorescence emission spectrum as when it was brought into dioxane (see Fig. 3 and also Table I). This change was reversed by adding several nucleotides including ATP. Therefore, we concluded that the nucleotide binding site of  $F_1$  was in a hydrophobic cleft. The present fluorometric titration studies of  $F_1$  by DNS-ATP in the presence of  $Mg^{2+}$  indicated that 2 mol of DNS-ATP were bound to 1 mol of  $F_1$  with an apparent dissociation constant of 0.44  $\mu M$  (Fig. 5). This finding is consistent with the  $\alpha_2 \beta_2$  stoichiometry of  $F_1$  subunits reported by Vershoor et al. (32). However, we cannot deny the possibility that our purified  $F_1$  preparation was partially inactivated, so that the  $\alpha_3 \beta_3$  stoichiometry (33) cannot be ruled out.

Binding of various phosphate compounds to  $F_1$  are affected markedly by divalent cations and pH (34,35). The properties of fluorescence emission spectra of various complexes of DNS-ATP



with  $F_1$  are summarized in Table I. The apparent dissociation constant of DNS-ATP bound to  $F_1$  in the absence of  $Mg^{2+}$  was about  $16 \mu M$  (Fig. 15), which was much higher than the  $\phi$  value of  $0.44 \mu M$  in the presence of  $Mg^{2+}$ . In Table I, the dioxane concentrations giving the same fluorescence emission peak and intensity at 520 nm that were obtained with free DNS-ATP and  $F_1$ -DNS-ATP in aqueous solution are also included. Thus, the hydrophobicity of environment around the DNS group in E-DNS-ATP and  $E \cdot Mg^{2+} \cdot DNS-ATP$  was equivalent to that of 20-30 and 58-76% dioxane, respectively. It is also suggested that  $Mg^{2+}$  increases both the affinity of  $F_1$  for DNS-nucleotide and the hydrophobicity of the DNS-nucleotide binding site on  $F_1$ . A further increase in the extent of the fluorescence enhancement of DNS-ATP by reaction with  $F_1$  in the absence of  $Mg^{2+}$  by lowering the pH (Fig. 4) suggests that the conformation around the nucleotide binding site on  $F_1$  is altered by changing pH.

DNS-ADP was also bound to  $F_1$  with a high affinity in the presence of  $Mg^{2+}$ , but the titration curve showed some heterogeneity (Fig. 7). One possibility is that two molecules of DNS-ADP bound to  $F_1$  are not equivalent in terms of fluorescence intensity even if there is no interaction between them.

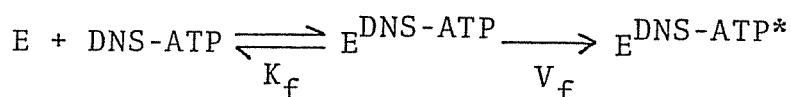
In this study, various elementary steps in the  $F_1$ -DNS-ATPase reaction were identified. The initial rate of fluorescence enhancement on addition of  $Mg^{2+}$  to  $F_1$  increased with increasing concentration of DNS-ATP, following typical Michaelis-Menten kinetics (Fig. 8). Thus, we assumed the following reaction scheme to explain the formation of a complex of DNS-ATP and  $F_1$  having enhanced fluorescence intensity ( $E^{DNS-ATP*}$ ):

Table I. Properties of fluorescence emission spectra of various complexes of DNS-ATP and  $F_1$ . All the indicated values are for the bound forms of DNS-ATP except for free DNS-ATP.

Complex	Fluor. Max. (nm)	Fluor. Intensity at 520 nm (relative)	$\phi$ ( $\mu$ M)	Dioxane (v/v %) <sup>b</sup>	
				Position of Peak	Intensity at 520 nm
Free DNS-ATP	555	1.0	—	0	0
E·DNS-ATP <sup>a</sup>	545	1.3-1.9	16 <sup>a</sup>	20	30
E·Mg <sup>2+</sup> ·DNS-ATP	525	4.8	0.44	58	76
P <sub>i</sub> ·E·Mg <sup>2+</sup> ·DNS-ATP	520	5.8	—	66	100

<sup>a</sup> The  $\phi$  value was calculated from the data of Fig. 15. Fluorescence intensity at 520 nm was calculated from the data of Figs. 2 and 15.

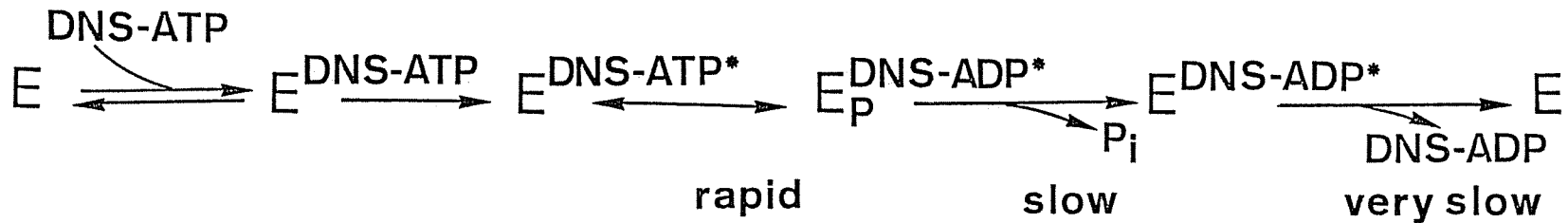
<sup>b</sup> Concentration of dioxane which induces the same change in fluorescence properties of free DNS-ATP as that induced by formation of complex with  $F_1$ .



On addition of  $\text{Mg}^{2+}$  to a mixture containing DNS-ATP and  $F_1$  the enhancement of fluorescence intensity of DNS-ATP, liberation of TCA- $^{32}\text{P}_i$  and free  $^{32}\text{P}_i$  occurred consecutively (Fig. 9). Even after that the fluorescence intensity still maintained its enhanced level. All these findings are easily explained by the proposed reaction scheme shown in Fig. 29.  $E_p^{\text{DNS-ADP}^*}$  is a TCA-unstable intermediate, and its formation is measured as TCA- $\text{P}_i$ . The rate of liberation of DNS-ADP from  $E^{\text{DNS-ADP}^*}$  is assumed to be very small, since the enhanced fluorescence level was maintained even after the release of free  $\text{P}_i$ .

The mechanism is supported by the following findings. (1) TCA- $\text{P}_i$  burst of 2 mol/mol  $F_1$  was observed with various concentrations of DNS-ATP (Fig. 10). The burst size agreed with the binding stoichiometry of 2 mol DNS-ATP/mol  $F_1$  obtained from the fluorometric titration of  $F_1$  (Fig. 5). (2) Boyer and coworkers (6) found  $^{18}\text{O}/\text{P}$  ratio of more than three for  $\text{P}_i$  formed during ATP hydrolysis by  $F_1$  at low concentrations of ATP, suggesting a rapid equilibrium of  $E^{\text{ATP}} \rightleftharpoons E_p^{\text{ADP}}$ . Notably the present reaction scheme resembles strikingly that of myosin ATPase (12-15). This similarity was originally pointed out by Boyer and coworkers (36). When  $\text{Ca}^{2+}$  was used as a divalent cation instead of  $\text{Mg}^{2+}$ , the release of DNS-ADP was accelerated (Fig. 12). This is also found with myosin ATPase.

There are several pieces of evidence to indicate the regulatory effect of ATP on ATP hydrolysis by  $F_1$  (6-10). Boyer and coworkers (6) found that an increase in the ATP concentration



-58-

### ADDITION OF ATP

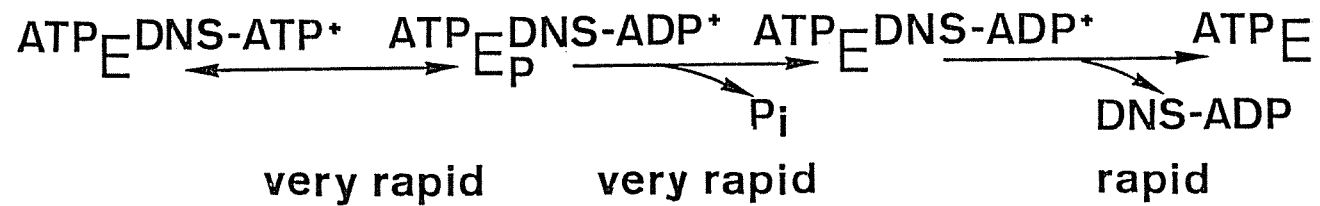
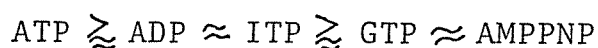


Fig. 29. The reaction mechanism of  $F_1$ -DNS-ATPase. Although two identical catalytic sites are postulated on  $F_1$ , only one of them is indicated here.

during ATP hydrolysis by  $F_1$  decreased the extent of water oxygen incorporated into each  $P_i$  formed, as if ADP and  $P_i$  were released at one site when ATP was bound to another. In this study, we found that ATP accelerated markedly the formation of  $E_P^{DNS-ADP^*}$  from  $E^{DNS-ATP^*}$  (Fig. 13), release of  $P_i$  from  $E_P^{DNS-ADP^*}$  (Fig. 15), and also release of DNS-ADP from  $E^{DNS-ADP^*}$  (Fig. 16). This acceleration will be explained by a mechanism that a conformational change is induced by binding of ATP to regulatory site(s) which are different from the catalytic site(s) binding DNS-ATP.

When ATP was added to  $F_1$ -DNS-nucleotide under conditions where most of the DNS-ATP was bound to  $F_1$ , all the DNS-ATP was liberated rapidly as TCA- $P_i$  (Fig. 13). However, when ATP was added at the initial phase of the  $F_1$ -DNS-ATPase reaction, the TCA- $P_i$  liberation was only slightly accelerated, and then stopped (Fig. 14). These findings indicate that the rate of the reverse reaction,  $E^{DNS-ATP^*} \longrightarrow E^{DNS-ATP}$ , is very small.

The rapid fluorescence decrease observed on addition of ATP, ADP, AMPPNP, ITP, or GTP to the reaction mixture containing DNS-ATP,  $F_1$ , and  $Mg^{2+}$  (Fig. 18) is suggested to be derived by the release of DNS-ADP induced by a conformational change of the catalytic site on  $F_1$ . The second slow phase will be due to the displacement of bound DNS-ADP by other nucleotides. ADP and AMPPNP also accelerated the TCA- $P_i$  liberation, although the extent of the acceleration was smaller than that by ATP. Thus, the effects of nucleotides to accelerate the TCA- $P_i$  liberation and to release DNS-ADP in the first rapid phase can be summarized as follows in the decreasing order of their efficiency:



CTP accelerated slightly the step,  $E^{\text{DNS-ATP}^*} \longrightarrow E_P^{\text{DNS-ADP}^*}$  (Fig. 19), and induced only a slow release of DNS-ADP from  $F_1$  (Fig. 18B). These findings suggest that the affinity of the regulatory site for CTP is very low or a conformational change of the catalytic site is not induced by the CTP binding to the regulatory site. AMP accelerated neither the TCA- $P_i$  liberation (Fig. 19) nor the DNS-ADP release (Fig. 22).

Recently, interactions of nucleotides with isolated subunits of  $F_1$ -ATPase from thermophilic bacteria were investigated by Kagawa and coworkers (37). They found that ATP were bound to both  $\alpha$  and  $\beta$ , the affinity of the former being higher than that of the latter. They also found that CTP was bound to  $\alpha$  subunit but not to  $\beta$  subunit, or that the conformational change of  $\beta$  subunit was not induced by CTP. Neither  $\alpha$  nor  $\beta$  subunit bound AMP. If we assume that beef heart  $F_1$  and thermophilic bacterial  $F_1$  have essentially the same structure and function, our results strongly suggest that the catalytic site and the regulatory site exist on  $\alpha$  and  $\beta$  subunits, respectively. This propose is apparently contrast to a widely accepted view that the catalytic site and the non-catalytic nucleotide binding site of  $F_1$ -ATPase are located on  $\beta$  and  $\alpha$  subunits, respectively (38-42). However, it should be noted that this hypothesis was derived mainly by analyzing the effects of chemical modifications of  $F_1$  only on the over-all reaction of  $F_1$ -ATPase. But this discrepancy will be removed by postulating that the hydrolysis of NTP by  $F_1$  occurs at different catalytic sites.

If we assume that hydrolysis of DNS-ATP occurs only through the pathway via  $E_P^{\text{DNS-ADP}^*}$  in the steady state,  $V_{\text{max}}$  has to be smaller than or equal to the maximum rate,  $V_f$ , for formation of  $E^{\text{DNS-ATP}^*}$ . However,  $V_f$  was  $0.34 \text{ s}^{-1}$  (Fig. 8), which is much smaller than  $V_{\text{max}}$  ( $\gg 1 \text{ s}^{-1}$ ) (Fig. 23). Therefore, another pathway is also suggested for hydrolysis of DNS-ATP. Furthermore, when ATP was added under the conditions where most of  $F_1$  was in the form of  $E^{\text{DNS-ADP}^*}$ , ATP hydrolysis occurred without a lag phase (Fig. 24). If ATP is mainly hydrolyzed via  $E^{\text{ADP}}$ , a lag phase corresponding to the release of DNS-ADP should be observed contrary to the present finding. Thus, it is highly probable that hydrolysis of NTP occurs via different catalytic pathways and at different catalytic sites in  $F_1$  as is observed with myosin ATPase (12,13).

$E_P^{\text{ADP}}$  is widely accepted as a key intermediate in the energy-transducing process of myosin ATPase, and the present investigation clearly demonstrated that this type of intermediate is involved in the  $F_1$ -ATPase reaction. Therefore, it is speculated that the reverse process of the present reaction mechanism functions in the ATP synthesis. Differential effects of inhibitors on ATP synthesis on hydrolysis have been interpreted by several workers (43,44) as showing that the catalytic route for ATP synthesis is separate from that involved in ATP hydrolysis, although this view has been disputed by Boyer (11) from several lines of consideration.

The fluorescence enhancement of  $F_1$ -DNS-nucleotide induced by  $P_i$  in the presence of  $\text{Mg}^{2+}$  suggests that the environment of the nucleotide-binding sites on  $F_1$  becomes more hydrophobic by

the action of  $P_i$ , thus diminishing the rate of the DNS-ADP release (Table I, Fig. 28). An apparent dissociation constant of this complex at pH 8 was  $195 \mu\text{M}$  (Fig. 25) and this value decreased on lowering the pH. These results are in good agreement with those of Kasahara and Penefsky (45) who obtained the dissociation constant of  $285 \mu\text{M}$ . Another interesting feature of the  $P_i$  effect is the distinction of the two DNS-ATP binding sites on  $F_1$  which otherwise seem to be equivalent; that is, the saturation of the fluorescence enhancement induced by  $P_i$  at 1 mol DNS-ATP/mol  $F_1$  implies the heterogeneity of the two binding sites, at least with respect to the interaction with  $P_i$ .



## REFERENCES

1. Senior, A.E. (1973) Biochim. Biophys. Acta 301, 249-277
2. Kagawa, Y., Sone, N., Hirata, H., & Yoshida, M. (1979) J. Bioenerg. Biomem. 11, 39-78
3. Futai, M. (1977) Biochem. Biophys. Res. Commun. 79, 1231-1237
4. Slater, E.C., Kemp, A., Van der Kraan, I., Muller, J.L.M., Roveri, O.A., Verschoor, G.J., Wagenvoord, R.J., & Wielders, J.P.M. (1979) FEBS Lett. 103, 7-11
5. Harris, D.A. (1978) Biochim. Biophys. Acta 463, 245-273
6. Hutton, R.L. & Boyer, P.D. (1979) J. Biol. Chem. 254, 9990-9993
7. Roveri, O.A., Muller, J.L.M., Wilms, J., & Slater, E.C. (1980) Biochim. Biophys. Acta 589, 241-255
8. Vasilyeva, E.A., Fitin, A.F., Minkov, I.B., & Vinogradov, A.D. (1980) Biochem. J. 188, 807-815
9. Penefsky, H.S. (1977) J. Biol. Chem. 252, 2891-2899
10. Schuster, S.M., Ebel, R.E., & Lardy, H.A. (1975) J. Biol. Chem. 250, 7848-7853
11. Boyer, P.D. (1979) Membrane Bioenergetics (Lee, C.P., Schatz, G., & Ernster, L. eds.) pp. 461-479, Addison-Wesley Publishing Company Inc., London
12. Inoue, A., Takenaka, H., Arata, T., & Tonomura, Y. (1979) Adv. Biophys. (Kotani, M. ed.) Vol. 13, pp. 1-194, Japan Sci. Soc. Press and University Park Press, Tokyo and Baltimore
13. Tonomura, Y. (1972) Muscle Proteins, Muscle Contraction and Cation Transport, University of Tokyo Press and University Park Press, Tokyo and Baltimore

14. Trentham, D.R., Eccleston, J.F., & Bagshaw, C.R. (1976) Quart. Rev. Biophys. 9, 217-281
15. Taylor, E.W. (1979) CRC Crit. Rev. Biochem. 6, 103-164
16. Watanabe, T., Inoue, A., Tonomura, Y., Uesugi, S., Ohtsuka, E., & Ikehara, M. (1981) submitted to J. Biochem.
17. Glynn, I.M. & Chappell, J.B. (1964) Biochem. J. 90, 147-149
18. Tietz, A. & Ochoa, S. (1958) Arch. Biochem. Biophys. 78, 477-494
19. Furukawa, K.-I., Ikebe, M., Inoue, A., & Tonomura, Y. (1980) J. Biochem. 88, 1629-1641
20. Beyer, R.E. (1967) Methods in Enzymology (Colowick, S.P. & Kaplan, N.O., eds.) Vol. 10, pp. 186-194, Academic Press, New York
21. Beechey, R.B., Hubbard, S.A., Linnett, P.E., Mitchell, A.D., & Munn, E.A. (1975) Biochem. J. 148, 533-537
22. Gornall, A.G., Bardwill, C.S., & David, M.M. (1949) J. Biol. Chem. 177, 751-766
23. Weber, K. & Osborn, M. (1969) J. Biol. Chem. 244, 4406-4412
24. Nakamura, H. & Tonomura, Y. (1968) J. Biochem. 63, 279-294
25. Yamaguchi, M. & Tonomura, Y. (1979) J. Biochem. 86, 509-523
26. Fiske, C.H. & Subbarow, Y. (1925) J. Biol. Chem. 66, 375-400
27. Pullman, M.E. & Monray, G.C. (1963) J. Biol. Chem. 238, 3762-3769
28. Ebel, R.E. & Lardy, H.A. (1975) J. Biol. Chem. 250, 191-196
29. Takashi, R., Tonomura, Y., & Morales, M.F. (1977) Proc. Natl. Acad. Sci. USA 74, 2334-2338
30. Karlisch, S.J.D., Yates, D.W., & Glynn, I.M. (1976) Nature 263, 251-253

31. Shoshan, V., Shavit, N., & Chipman, D.M. (1978) Biochim. Biophys. Acta 504, 108-122
32. Verschoor, G.J., van de Sluis, P.R., & Slater, E.C. (1977) Biochim. Biophys. Acta 462, 422-437
33. Each, F.S. & Allison, W.S. (1979) J. Biol. Chem. 254, 10740-10746
34. Wagenvoord, R.J., Kemp, A., & Slater, E.C. (1980) Biochim. Biophys. Acta 593, 204-211
35. Harris, D.A., Gomez-Fernandez, J.C., Klungsoyr, L., & Radda, G.K. (1978) Biochim. Biophys. Acta 504, 364-383
36. Boyer, P.D., Cross, R.L., & Momsen, W. (1973) Proc. Natl. Acad. Sci. USA 70, 2837-2839
37. Ohta, S., Tsuboi, M., Oshima, T., Yoshida, M., & Kagawa, Y. (1980) J. Biochem. 87, 1609-1617
38. Esch, F.S. & Allison, W.S. (1978) J. Biol. Chem. 253, 6100-6106
39. Ferguson, S.J., Lloyd, W.J., Lyons, M.H., & Radda, G.K. (1975) Eur. J. Biochem. 54, 117-126
40. Pougeois, R., Satre, M., & Vignais, P.V. (1979) Biochemistry 18, 1408-1413
41. Drutsa, V.L., Kozolov, I.A., Milgrom, Y.M., Shabarova, Z.A., & Sokolova, N.I. (1979) Biochem. J. 182, 617-619
42. Kozlov, I.A. & Milgrom, Y.M. (1980) Eur. J. Biochem. 106, 457-462
43. Penefsky, H.S. (1972) J. Biol. Chem. 249, 3579-3585
44. Steinmeier, R.C. & Wang, J.H. (1979) Biochemistry 18, 11-18
45. Kasahara, M. & Penefsky, H.S. (1978) J. Biol. Chem. 253, 4180-4187

PART II.

Reactions of a Fluorescent ATP Analog, 2'-(5-Dimethylamino-naphthalene-1-Sulfonyl) Amino-2'-DeoxyATP, with E. coli F<sub>1</sub>-ATPase and Its Subunits: Evidence Suggesting the High Affinity Catalytic Site in  $\alpha$  Subunit and Low Affinity Regulatory Site in  $\beta$  Subunit.

## SUMMARY

We performed kinetic studies on the reactions of fluorescent ATP analog, 2'-(5-dimethyl-aminonaphthalene-1-sulfonyl) amino-2'-deoxyATP (DNS-ATP), with E. coli  $F_1$ -ATPase ( $EF_1$ ) and its subunits, to clarify the role of each subunit in the ATPase reaction. The following results were obtained.

1. In the presence of  $Mg^{2+}$ , 3 mol of DNS-ATP binds to 1 mol of  $EF_1$  with an apparent dissociation constant of  $0.23 \mu M$ . Upon binding, the fluorescence intensity of DNS-ATP at 520 nm increased exponentially with  $t_{1/2}$  of 35 s and reached 3.5 times the original fluorescence level. Following the fluorescence increase, DNS-ATP was hydrolyzed, and the fluorescence intensity maintained its enhanced level.
2. The addition of an excess of ATP over  $EF_1$ -DNS-nucleotide complex in the presence of  $Mg^{2+}$  decreased the fluorescence intensity rapidly, indicating the acceleration of DNS-nucleotide release from  $EF_1$ . ADP and GTP also decreased the fluorescence intensity.
3. DCCD inhibited markedly the accelerating effect of ATP on DNS-nucleotide release from  $EF_1$  and the  $EF_1$ -ATPase activity at steady state. On the other hand, DCCD inhibited only slightly the fluorescence increase of DNS-ATP due to its binding to  $EF_1$  and the rate of single turnover of DNS-ATP hydrolysis catalyzed by  $EF_1$ .
4. In the presence of  $Mg^{2+}$ , 0.65-0.82 mol of DNS-ATP binds to 1 mol of isolated  $\alpha$  subunit of  $EF_1$  with an apparent dissociation constant of  $0.06-0.07 \mu M$ . Upon binding, the fluorescence intensity of DNS-ATP at 520 nm increased 1.55 fold very rapidly ( $t_{1/2} < 1$  s). The fluorescence intensity of DNS-ATP was unaffected by the addition of the isolated  $\beta$  subunit.

5. The kinetic properties of the fluorescence change of DNS-ATP's reaction with  $EF_1$ -ATPase reconstituted from  $\alpha$ ,  $\beta$  and  $\delta$  subunits were quite similar to that of native  $EF_1$ .

These findings strongly support the previous proposal that the high affinity catalytic site and low affinity regulatory site exist in the  $\alpha$  and  $\beta$  subunit, respectively

## INTRODUCTION

$F_1$ -ATPase [EC 3.6.1.3] is composed of five subunits, designated  $\alpha$  through  $\epsilon$  in order of decreasing molecular weight (1,2). The stoichiometry of either  $\alpha_3\beta_3\gamma$  or  $\alpha_2\beta_2\gamma$  is proposed for the major subunits of  $F_1$  (3-5). Recent reconstitution studies on  $F_1$ 's from thermophilic bacterium PS3 ( $TF_1$ ) (6,7) and *E. coli* ( $EF_1$ ) (8,9) shed light on the role of each subunit of  $F_1$ . The complex of  $\alpha$  with  $\beta$  and  $\gamma$  subunits possesses the ATPase activity, and the  $\delta$  and  $\epsilon$  subunits are essential for the binding of the  $\alpha\beta\gamma$  complex to the membranous component,  $F_0$ . The  $\alpha$  and  $\beta$  subunits each have nucleotide-binding sites, which are different in their affinity and specificity for nucleotides (9,10), and the total number of nucleotide-binding site in  $F_1$  is 4-7 (11,12). The different nucleotide-binding sites in  $F_1$  have been revealed by steady-state kinetics of the ATPase reaction (13), binding measurements (11,14), and the affinity labelling of nucleotide-binding sites (15-17). The  $F_1$ -ATPase activity was found to be inhibited by the modification of the  $\beta$  subunit which has a low affinity binding site for nucleotides (15,16,18-23). This finding suggests that the low affinity binding site in  $\beta$  subunit is the catalytic site. This suggestion is supported by the finding that the steady-state  $F_1$ -ATPase activity has a high  $K_m$  value for ATP (13,24).

Recently, we have synthesized a fluorescent ATP analog DNS-ATP, 2'-(5-dimethyl-aminonaphthalene-1-sulfonyl) amino-2'-deoxyATP (25), and studied the mechanism of the DNS-ATPase reaction of beef heart  $F_1$  (26). We found that the reaction mechanism of  $F_1$ -ATPase is very similar to that of myosin ATPase, and that the nucleotides at high

concentrations accelerate the rates of three elementary steps in  $F_1$ -ATPase (26). These findings were interpreted as showing the existence of low affinity regulatory site(s) as well as high affinity catalytic sites (26). Together with the results on the direct nucleotide binding measurements of the isolated  $\alpha$  and  $\beta$  subunit (9,10), this view can be extended to the subunit localization of the high affinity catalytic site in the  $\alpha$  subunit and the low affinity regulatory site in the  $\beta$  subunit. However, this view is quite opposite to the widely accepted hypothesis as mentioned above.

To determine whether the catalytic site exists in the  $\alpha$  or  $\beta$  subunit, we performed kinetic studies on the reactions of DNS-ATP with  $EF_1$  and isolated active subunits. The results obtained strongly supported our hypothesis that the high affinity catalytic site and low affinity regulatory site exist in the  $\alpha$  and  $\beta$  subunits, respectively.



## MATERIALS AND METHODS

Materials — DNS-ATP, DNS-ADP and [ $\gamma$ - $^{32}$ P]DNS-ATP (DNS-AT $^{32}$ P) were synthesized as described previously (25). Pyruvate kinase [EC 2.7.1.40] was prepared according to the method of Tietz and Ochoa (27). ATP, ADP and AMP were purchased from Khojin Ltd. (Tokyo). AMPPNP, ITP, GTP, CTP and phosphoenolpyruvate were purchased from Sigma Chemicals Co. (St. Louis, MO). All other chemicals were of reagent grade purity.

Preparation of EF<sub>1</sub>,  $\alpha$  and  $\beta$  Subunit, and Reconstituted EF<sub>1</sub>-ATPase — EF<sub>1</sub> was purified as described previously (28) from *E. coli* KY7485 ( $\lambda$ asn -5) after thermoinduction of the transducing phage carrying a set of structural genes for the proton translocating ATPase (29). Purified EF<sub>1</sub> was precipitated by 55% ammonium sulfate and dissolved in 50mM Tris-acetate (pH 7.0) and 2mM EDTA, at a concentration of 5-10 mg/ml. The EF<sub>1</sub> solution was dialyzed against the same buffer solution at 20°C for 20 h before use. The  $\alpha$ ,  $\beta$  and  $\delta$  subunits were purified from EF<sub>1</sub> as described previously (9). Reconstituted EF<sub>1</sub>-ATPase was prepared from a mixture of the  $\alpha$ ,  $\beta$  and  $\delta$  subunits as described previously (8), and concentrated to 2 mg/ml by Diaflo XM-100A membrane purchased from Amicon Ltd. (Lexington, MA). The concentrated enzyme was dialyzed against the above buffer solution at 20°C for 20 h before use. The protein concentration was determined by biuret method (30) or by the method of Bradford (31) with bovine serum albumin as a standard. The molecular weights of EF<sub>1</sub>,  $\alpha$ ,  $\beta$  subunits, and reconstituted EF<sub>1</sub>-ATPase were taken as 376,000, 58,000, 52,000, and 364,000, respectively (9,28).

Fluorescence Measurements — Measurement solutions were prepared by addition of reagents in 5-20  $\mu$ l portions to 2 ml of 2 mM EDTA, 100 mM NaCl and 50 mM Tris-acetate at pH 7.0 and 30°C. The fluorescence intensity of DNS-ATP at 520 nm with excitation at 340 nm was measured as described previously (26).

DNS-ATPase and ATPase Activity —  $EF_1$  at 0.87-1.6  $\mu$ M was allowed to react with 2.8  $\mu$ M DNS-AT<sup>32</sup>P in 2 mM EDTA, 100 mM NaCl and 50 mM Tris-acetate at pH 7.0 and 30°C for 1 min. Then, the hydrolysis was started by the addition of 5 mM MgCl<sub>2</sub>. The amount of <sup>32</sup>P<sub>i</sub> liberated when the reaction was terminated by TCA (TCA-<sup>32</sup>P<sub>i</sub>) was measured as described previously (26). The steady-state ATPase activity of  $EF_1$  was measured in the presence of an ATP-feeder system (0.1 mg/ml pyruvate kinase and 5 mM phosphoenolpyruvate) at pH 8.0 and 30°C (26). The amount of TCA-P<sub>i</sub> liberated was measured by the method of Fiske and Subbarow (32).

Binding of DNS-AT<sup>32</sup>P to  $\alpha$  Subunit — To measure the binding of DNS-AT<sup>32</sup>P to  $\alpha$  subunit, the equilibrium dialysis was performed at room temperature using chambers consisting of two wells separated by a layer of dialysis membrane (9). One side of the chamber contained subunit and both wells contained 2 mM EDTA, 100 mM NaCl and 50 mM Tris-acetate at pH 7.0.

## RESULTS

Fluorescence Change of DNS-ATP on Its Binding to  $EF_1$  — Figure 1(A) shows a typical time course of change in the fluorescence intensity of DNS-ATP at 520 nm during its reaction with  $EF_1$  in the presence of 3 mM free  $Mg^{2+}$ . The fluorescence intensity of 1.1  $\mu M$  DNS-ATP in the presence of 2 mM EDTA increased only slightly on addition of 0.99  $\mu M$   $EF_1$  [arrow a in Fig. 1(A); compare curves a and b in Fig. 2]. On further addition of 5 mM  $MgCl_2$  [arrow b in Fig. 1(A)], the fluorescence increased exponentially with a  $t_{1/2}$  of 35 s, and reached a plateau level, which was 3.2 fold the fluorescence intensity of free DNS-ATP. Being observed only in the presence of  $EF_1$ , the  $Mg^{2+}$ -dependent fluorescence increase of DNS-ATP reflects the binding of DNS-ATP to the nucleotide-binding sites in  $EF_1$  (cf. DISCUSSION). On a further addition of 2 mM  $P_i$  [arrow c in Fig. 1(A)], the fluorescence intensity increased rapidly to the level of 5.1 fold that of free DNS-ATP. When 2 mM ATP was added to the reaction mixture [arrow d in Fig. 1(A)], the fluorescence intensity decreased rapidly to about 50% of the original level, then decreased slowly. When a small amount of DNS-ATP was added to  $EF_1$  ( $\ll 0.5$  mol/mol  $EF_1$ ), the fluorescence intensity decreased to a level almost identical to that of free DNS-ATP within 5 min after the addition of ATP. However, when a large amount of DNS-ATP was used, the second phase of the decrease occurred very slowly, and even 10 min after the addition of ATP, the fluorescence intensity was not the same as that of free DNS-ATP.

Figure 1(B) shows a time course of change in the fluorescence intensity of DNS-ATP in the presence of 3 mM  $Ca^{2+}$ . When 5 mM  $CaCl_2$

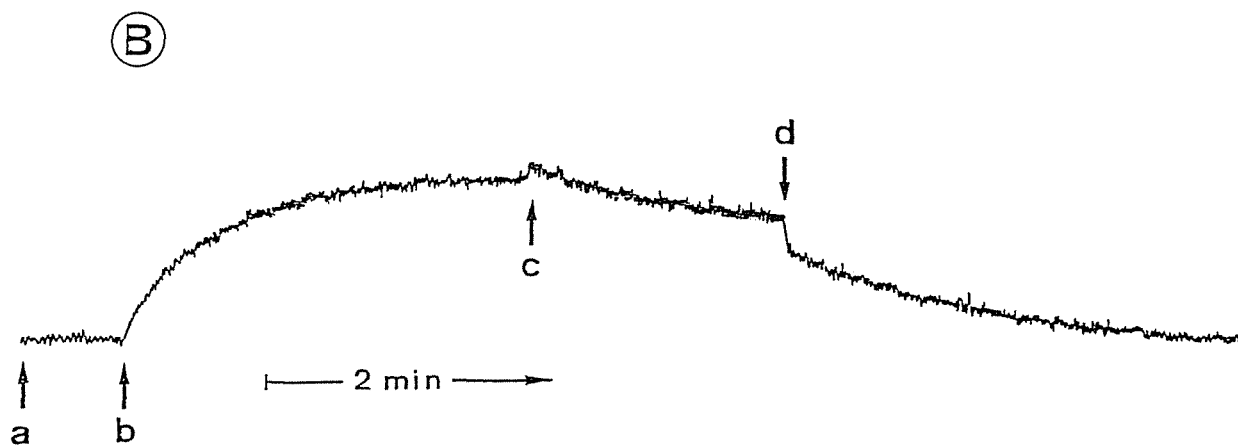
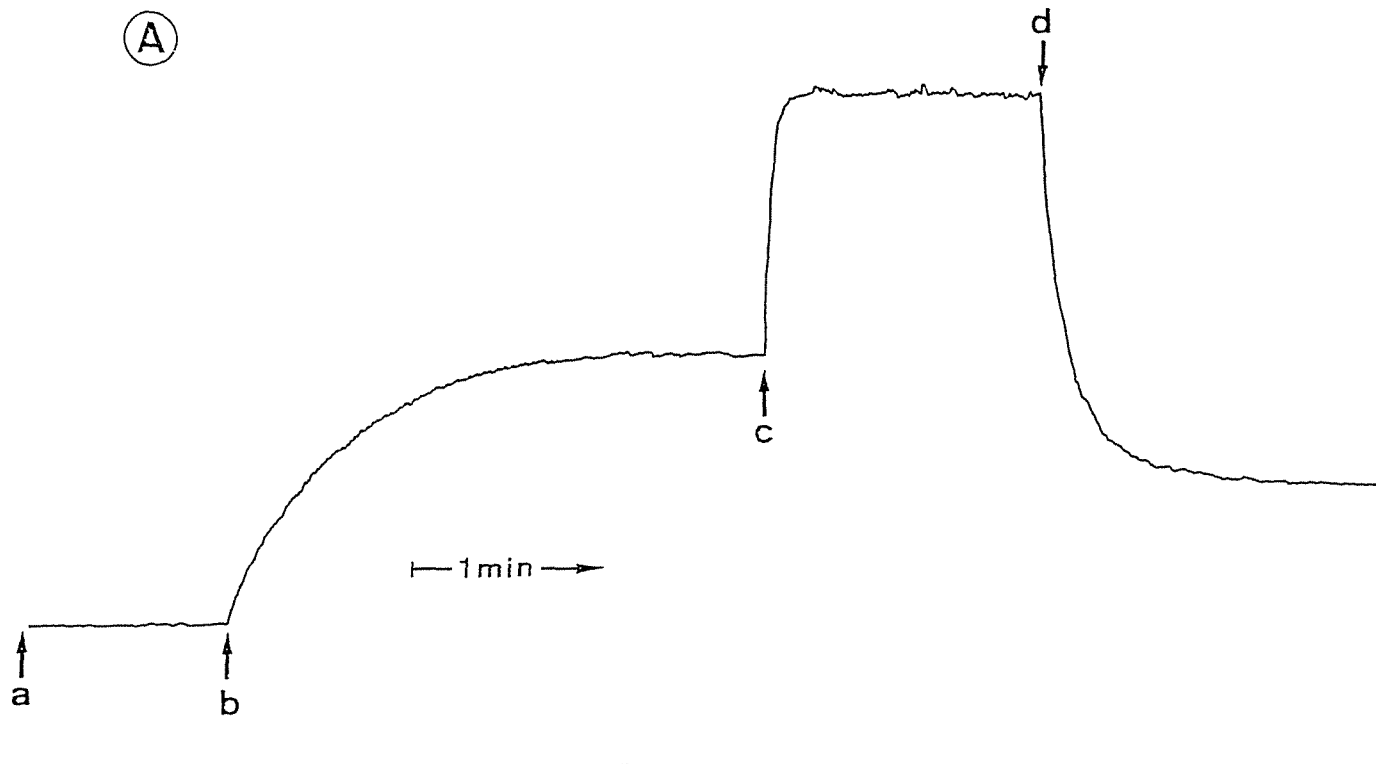


Fig. 1. Time course of fluorescence intensity change of DNS-ATP in the presence of  $EF_1$ . To a mixture containing  $1.1 \mu\text{M}$  DNS-ATP,  $2 \text{ mM}$  EDTA,  $0.1 \text{ M}$  NaCl and  $50 \text{ mM}$  Tris-acetate at pH 8.0 and  $30^\circ\text{C}$ , the following additions were made at time indicated by arrows (a-d). (A): a,  $0.99 \mu\text{M}$   $EF_1$ ; b,  $5 \text{ mM}$   $\text{MgCl}_2$ ; c,  $2 \text{ mM}$   $\text{K-P}_i$ ; d,  $2 \text{ mM}$  ATP. (B): a,  $0.94 \mu\text{M}$   $EF_1$ ; b,  $5 \text{ mM}$   $\text{CaCl}_2$ ; c,  $2 \text{ mM}$   $\text{K-P}_i$ ; d,  $2 \text{ mM}$  ATP. The emission and excitation wavelengths were 520 and 340 nm, respectively.

was added to a reaction mixture containing 1.1  $\mu\text{M}$  DNS-ATP, 0.94  $\mu\text{M}$   $\text{EF}_1$  and 2 mM EDTA (b), the fluorescence intensity of DNS-ATP increased exponentially with almost the same value of  $t_{1/2}$  as that in the case of 5 mM  $\text{MgCl}_2$  addition. The plateau level of fluorescence in the presence of  $\text{Ca}^{2+}$  was 2 fold that of free DNS-ATP. Further addition of 1 mM  $\text{P}_i$  (c) did not cause any fluorescence increase, but caused a slow decrease. On further addition of 2 mM ATP (d), the fluorescence intensity decreased rapidly by about 10%, then approached slowly to the level of free DNS-ATP.

Figure 2 shows the fluorescence emission spectra of free DNS-ATP and various complexes of DNS-ATP with  $\text{EF}_1$ . As previously described (25), DNS-ATP had an emission peak at 555 nm (trace a). On addition of  $\text{EF}_1$ , the emission peak shifted to around 550 nm with a slight increase in the fluorescence intensity (trace b). Addition of 5 mM  $\text{MgCl}_2$  markedly increased the fluorescence intensity, and the maximum shifted to 530 nm (trace c). Further addition of 2 mM  $\text{P}_i$  caused a further increase of the fluorescence and the shift of the maximum to around 520 nm (trace d). Addition of 2 mM ATP reversed these fluorescence changes almost backward to the state of free DNS-ATP (trace e). These fluorescence changes of DNS-ATP on its reactions with  $\text{EF}_1$  are almost equal to those observed for beef heart  $\text{F}_1$ .

Stoichiometry of DNS-ATP Binding to  $\text{EF}_1$  — The stoichiometry of DNS-ATP binding to  $\text{EF}_1$  was determined by fluorometric titration of 1.1  $\mu\text{M}$  DNS-ATP with  $\text{EF}_1$  in the presence of 3 mM free  $\text{Mg}^{2+}$  (Fig. 3). Several kinds of reaction intermediates are produced by the reaction of  $\text{EF}_1$  with DNS-ATP, as will be mentioned in "DISCUSSION." However, we (26) previously found that in the case of beef heart  $\text{F}_1$ , the fluorescence intensity of one intermediate is only slightly higher

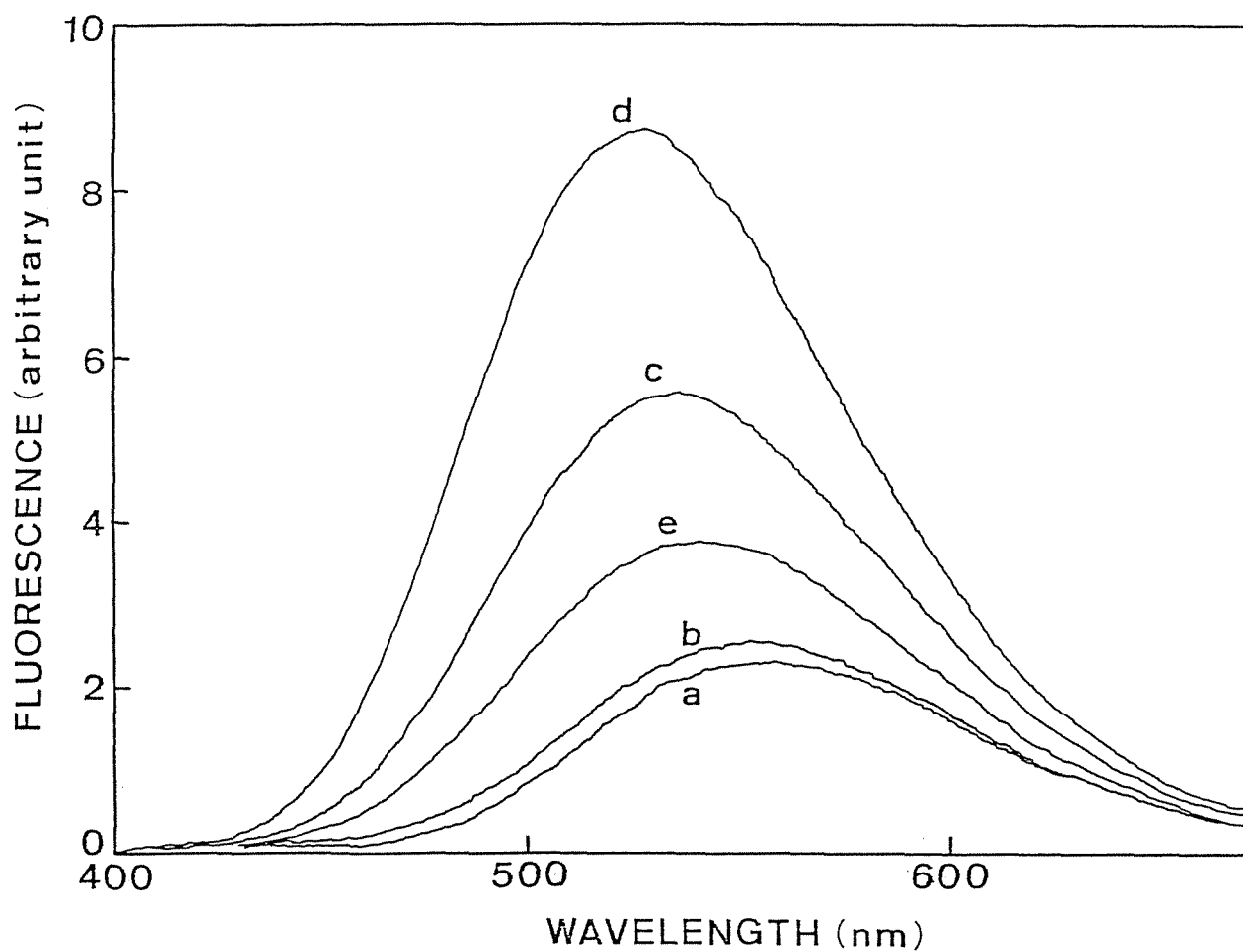


Fig. 2. Fluorescence emission spectra recorded during the course of reaction of DNS-ATP with  $EF_1$ . Spectra were recorded in the following order; curve a, 1.1  $\mu\text{M}$  DNS-ATP alone; curve b, 1 min after addition of 1.6  $\mu\text{M}$   $EF_1$ ; curve c, 2 min after addition of 5 mM  $\text{MgCl}_2$ ; curve d, 1 min after addition of 2 mM  $\text{K-P}_i$ ; curve e, 1 min after addition of 2 mM ATP. Other conditions were the same as described in Fig. 1 or in the text.

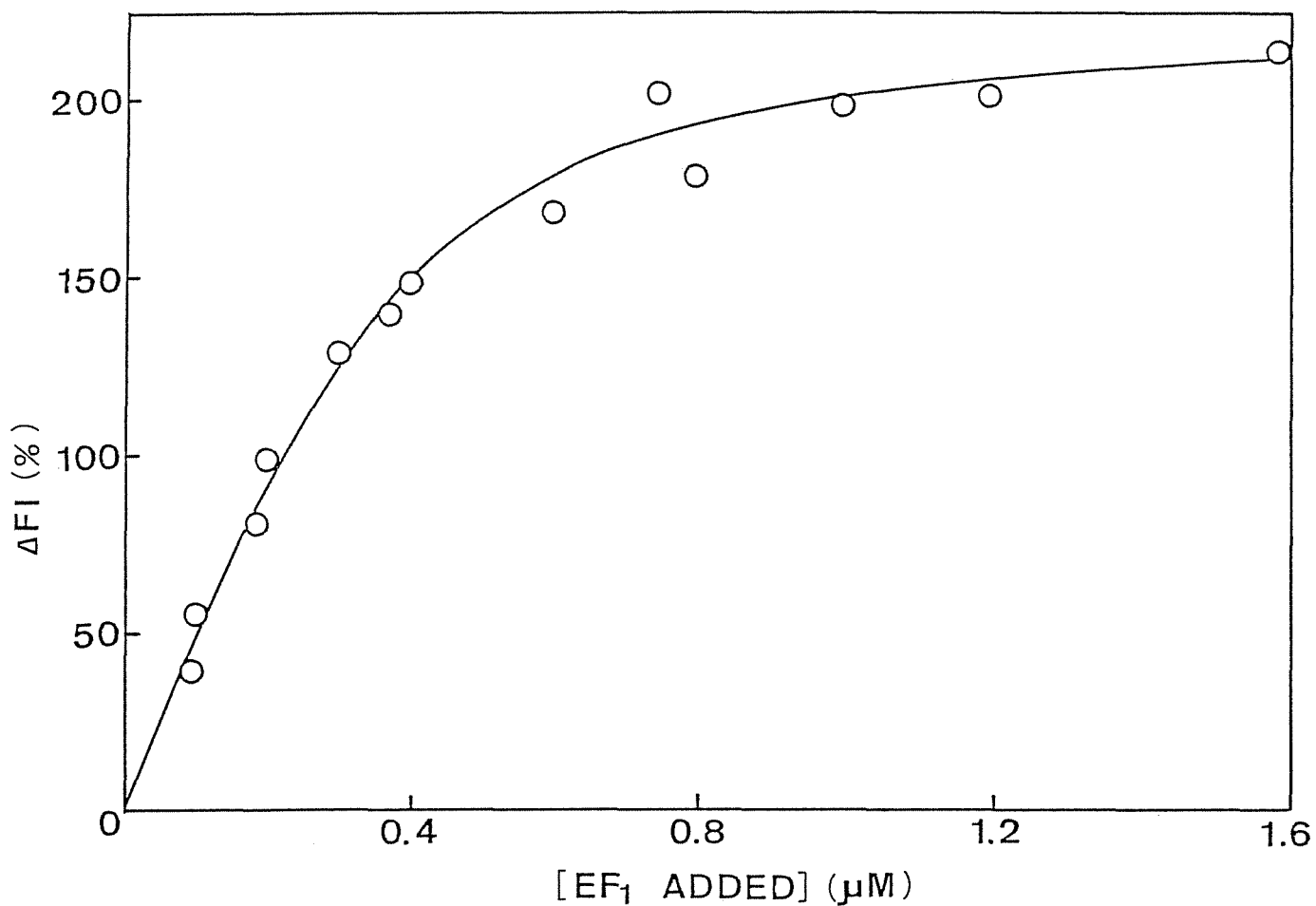


Fig. 3. Fluorometric titration of DNS-ATP with EF<sub>1</sub> in the presence of MgCl<sub>2</sub>. The extent of fluorescence increase 2 min after addition of 5 mM MgCl<sub>2</sub> was plotted against the amount of EF<sub>1</sub> added. The reaction mixture contained 1.1 μM DNS-ATP in 2 mM EDTA, 0.1 M NaCl and 50 mM Tris-acetate at pH 7.0 and 30°C. The solid line is the theoretical curve (see the text).

than that of free DNS-ATP and the intensities of other intermediates are much higher than that of free DNS-ATP and are equal to each other. Therefore, the data were analyzed based on the quadratic equation:

$$\Delta F = \frac{\Delta F_{\max}}{2} \left\{ (nE_0 + S_0 + \phi_{\text{DNS-ATP}}) - [(nE_0 + S_0 + \phi_{\text{DNS-ATP}})^2 - 4nE_0S_0]^{\frac{1}{2}} \right\} \quad (\text{Eq. 1})$$

where  $\Delta F$  is the extent of fluorescence increase, and is assumed to be proportional to the amount of  $EF_1$ -DNS-nucleotide complex.

$\Delta F_{\max}$  is the maximum value of  $\Delta F$ , and is obtained when all the DNS-ATP binds to  $EF_1$ . Both the  $\Delta F$  and  $\Delta F_{\max}$  values are expressed as percentage of the fluorescence intensity of free DNS-ATP in the absence of  $Mg^{2+}$ .  $E_0$  and  $S_0$  are the total concentrations of  $EF_1$  and DNS-ATP, respectively.  $n$  is the number of independent and equivalent binding sites of DNS-ATP in  $EF_1$ , and  $\phi_{\text{DNS-ATP}}$  is their dissociation constant. The solid line in Fig. 3 is the best fit of the data to Eq. 1 with  $\Delta F_{\max} = 250\%$ ,  $n = 3$ , and  $\phi_{\text{DNS-ATP}} = 0.23 \mu\text{M}$ . With  $n$  values other than 3, the fit was poor.

Hydrolysis of DNS-ATP by  $EF_1$  — We found that in the absence of free  $Mg^{2+}$ , DNS-ATP is not hydrolyzed by  $EF_1$ . Therefore, we measured the time course of TCA- $^{32}\text{P}_i$  liberation after addition of 5 mM  $\text{MgCl}_2$  to a reaction mixture containing 2.8  $\mu\text{M}$  DNS-AT $^{32}\text{P}$ , 1.6  $\mu\text{M}$   $EF_1$  and 2 mM EDTA (Fig. 4). The amount of TCA- $^{32}\text{P}_i$  liberated at 120 s was 0.47 mol/mol  $\alpha$ . The amount of DNS-nucleotide bound to  $EF_1$  under the conditions used was estimated to be 0.53 mol/mol  $\alpha$  by using  $n = 3$  and  $\phi_{\text{DNS-ATP}} = 0.23 \mu\text{M}$ . Under these conditions the fluorescence increase was found to be almost completed after 120 s of reaction. When ATP at 2 mM was added 60 s after starting the reaction (arrow in Fig. 4),



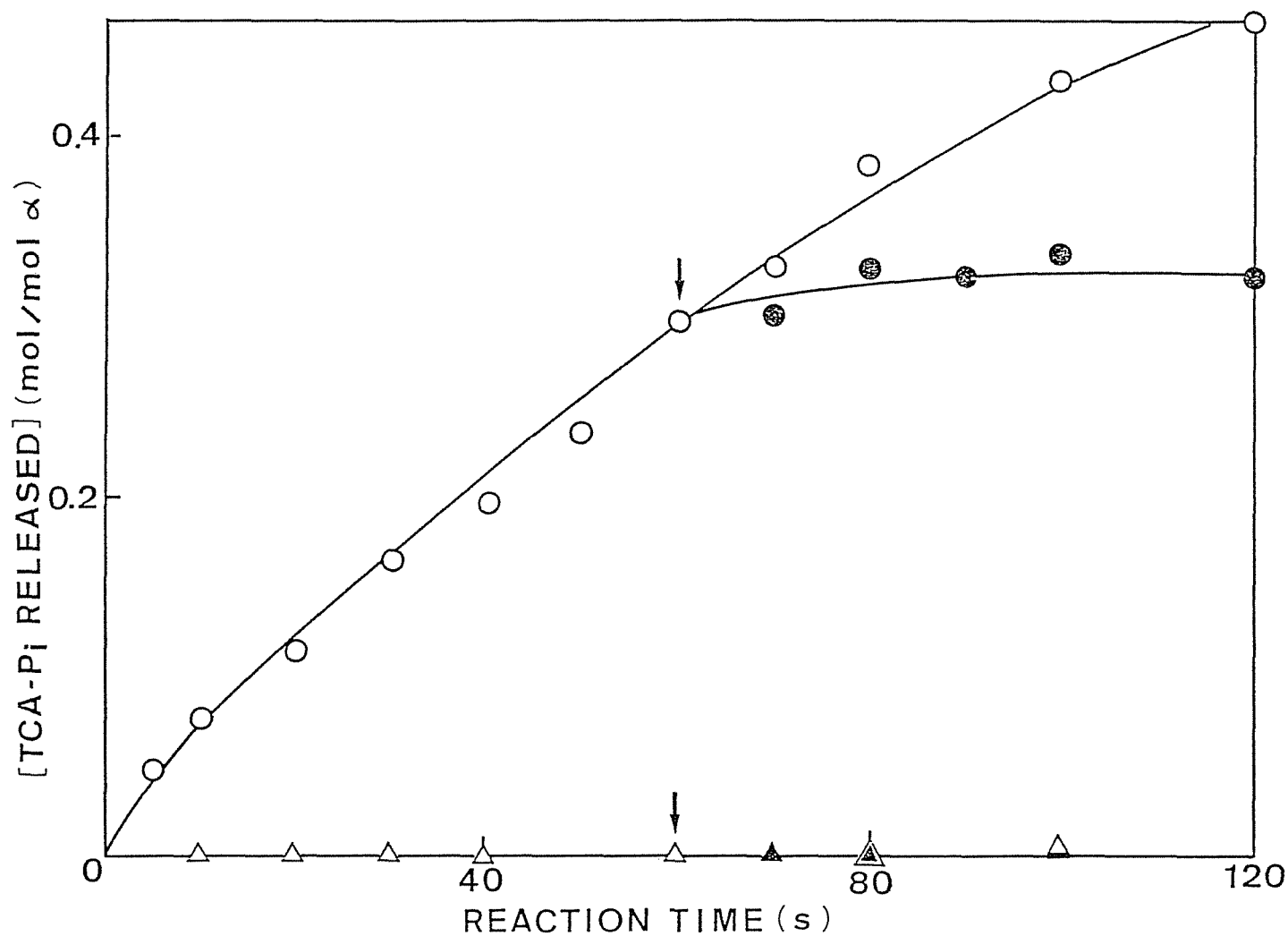


Fig. 4. Initial phase of TCA- $^{32}\text{P}_i$  liberation from DNS-AT $^{32}\text{P}$  catalyzed by EF<sub>1</sub> or purified  $\alpha$  subunit. The reaction mixture contained 2.8  $\mu\text{M}$  DNS-AT $^{32}\text{P}$  and 1.6  $\mu\text{M}$  EF<sub>1</sub> (O, ●) or 2.3  $\mu\text{M}$   $\alpha$  subunit ( $\Delta$ ,  $\blacktriangle$ ) in 2 mM EDTA, 0.1 M NaCl and 50 mM Tris-acetate at pH 7.0 and 30°C. The reaction was started by the addition of 5 mM MgCl<sub>2</sub>. At the time indicated by an arrow (60 s after addition of MgCl<sub>2</sub>), 2 mM ATP was added (●,  $\blacktriangle$ ).

the TCA- $^{32}\text{P}_i$  liberation ceased immediately, showing no acceleration such as observed on beef heart  $F_1$  (26).

Acceleration of DNS-Nucleotide Release from  $\text{EF}_1$ -Nucleotide Complex by Addition of Nucleotides and Pyrophosphate — The fluorescence intensity of  $\text{EF}_1$ -DNS-nucleotide complex maintained its enhanced level after liberation of TCA- $^{32}\text{P}_i$ . Because of a very small rate of release of DNS-ADP from the complex, it is clear that DNS-ADP formed by hydrolysis of DNS-AT $^{32}\text{P}$  was still bound to  $\text{EF}_1$ . In the presence of 3 mM  $\text{Mg}^{2+}$ , DNS-ATP at 1.1  $\mu\text{M}$  was allowed to react with 0.98  $\mu\text{M}$   $\text{EF}_1$  for 2 min. Then, various nucleotides (0.2 mM) or pyrophosphate (2 mM) were added, and the following decrease in the fluorescence intensity was measured (Fig. 5). The addition of ATP caused a fluorescence decrease with first rapid and second slow phases (trace a). In the case of beef heart  $F_1$ , we found that the time course of the fluorescence decrease after addition of ATP was identical to that of the release of DNS-ADP from  $F_1$ -DNS-nucleotide in both rapid and slow phases (26). Therefore, we assumed that the fluorescence decrease after addition of ATP corresponds to the release of DNS-nucleotide from  $\text{EF}_1$ -DNS-nucleotide in the case of  $\text{EF}_1$  as well. ADP (trace b) and GTP (trace c) also induced a fluorescence decrease, but the rates of the decrease were smaller than that induced by ATP. The rates of the fluorescence decrease on addition of AMPPNP (trace d),  $\text{PP}_i$  (trace e), and CTP (trace f) became smaller in this order. AMP (trace g) had no effect on the fluorescence intensity of  $\text{EF}_1$ -DNS-nucleotide.

Effects of DCCD on the Reaction of DNS-ATP with  $\text{EF}_1$  — Figure 6 shows the time course of the change in the fluorescence intensity of

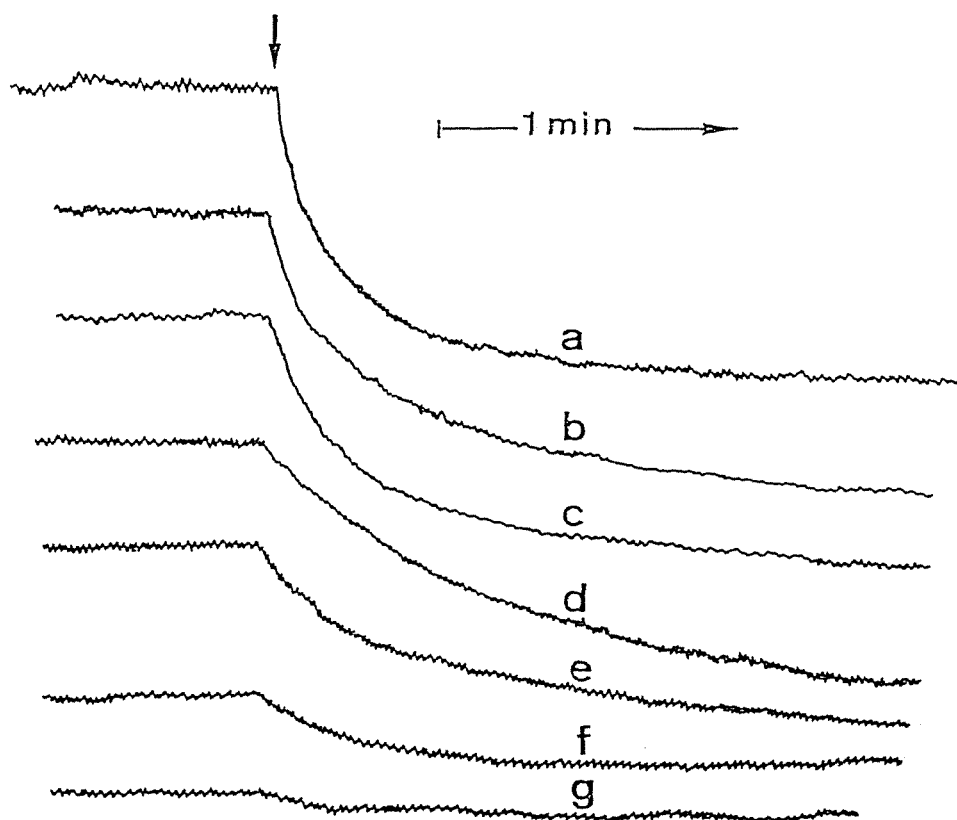


Fig. 5. Fluorescence decrease on addition of various phosphate compounds to  $EF_1$ -DNS-nucleotide complex. DNS-ATP at  $1.1 \mu\text{M}$  was allowed to react with  $0.98 \mu\text{M}$   $EF_1$  in the presence of  $3 \text{ mM Mg}^{2+}$  for 2 min, then at the time indicated by an arrow, the following additions were made; a,  $0.2 \text{ mM ATP}$ ; b,  $0.2 \text{ mM ADP}$ ; c,  $0.2 \text{ mM GTP}$ ; d,  $0.2 \text{ mM AMPPNP}$ ; e,  $2 \text{ mM PP}_i$ ; f,  $0.2 \text{ mM CTP}$ ; g,  $0.2 \text{ mM AMP}$ . Other conditions were the same as described in Fig. 1.

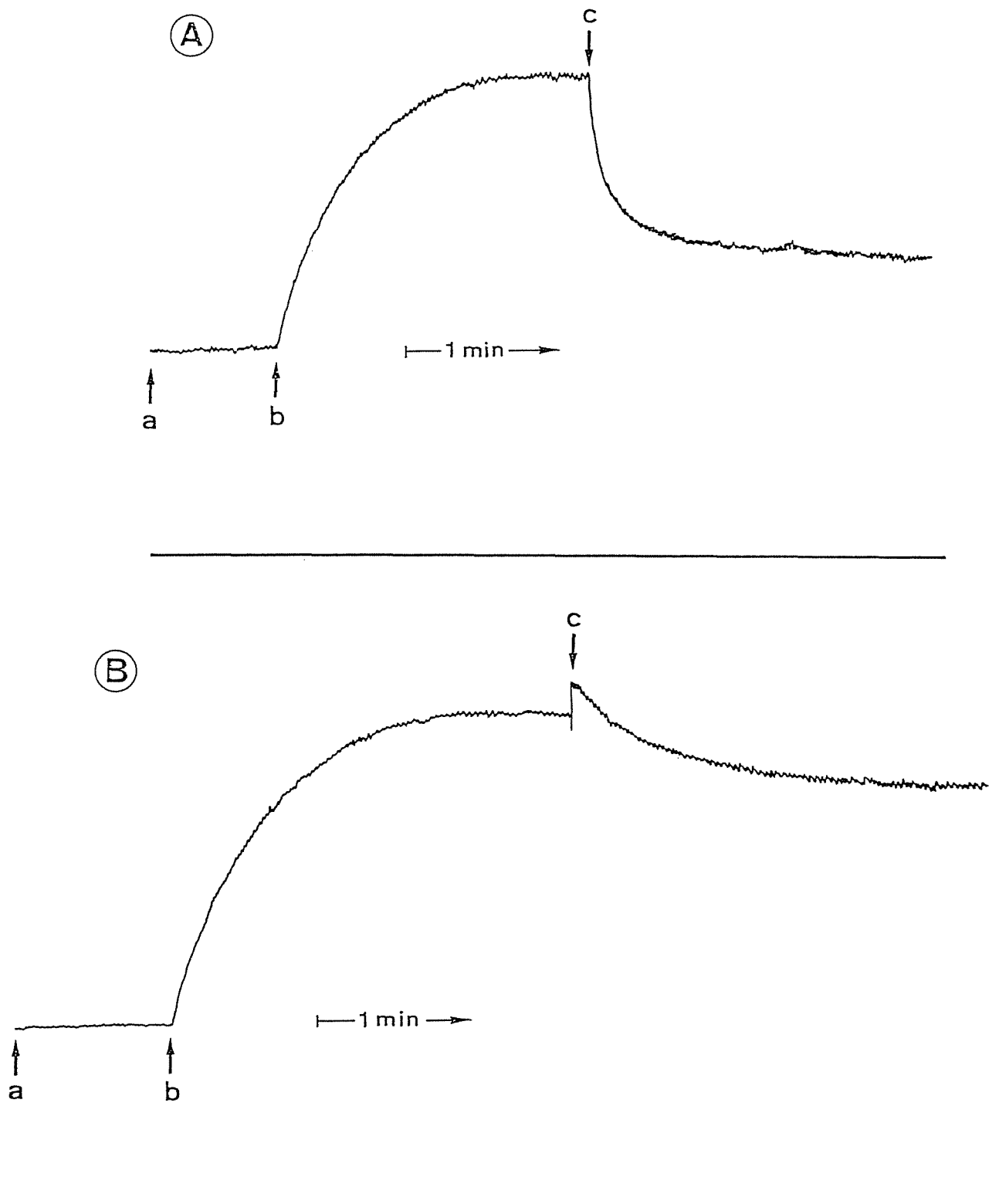


Fig. 6. Inhibition by DCCD-treatment of decrease in the fluorescence intensity of  $EF_1$ -DNS-nucleotide upon addition of ATP. After incubation of  $0.98 \mu\text{M}$   $EF_1$  without (A) or with (B)  $0.2 \text{ mM}$  DCCD in  $2 \text{ mM}$  EDTA,  $100 \text{ mM}$  NaCl and  $50 \text{ mM}$  Tris-acetate at pH 7.0 and  $30^\circ\text{C}$  for 20 min, the following additions were made at the time indicated by arrows (a-c) a,  $1.1 \mu\text{M}$  DNS-ATP; b,  $5 \text{ mM}$   $\text{MgCl}_2$ ; c,  $2 \text{ mM}$  ATP.

1.1  $\mu\text{M}$  DNS-ATP during its reaction with 0.98  $\mu\text{M}$   $\text{EF}_1$ , which was preincubated with 0 (A) or 0.2 mM DCCD (B) at pH 7.0 and 30°C for 20 min. The time course of increase in the fluorescence intensity after addition of 5 mM  $\text{MgCl}_2$  (b) was almost unaffected by the DCCD-treatment. On the other hand, the decrease of the fluorescence intensity upon subsequent addition of 2 mM ATP (c) was inhibited markedly by the DCCD-treatment (Fig. 6B).

Figure 7 shows the effects of DCCD on the steady-state rate of  $\text{EF}_1$ -ATPase and the initial rate of  $\text{EF}_1$ -DNS-ATPase. The steady-state rate of the  $\text{Mg}^{2+}$ -ATPase reaction of  $\text{EF}_1$  was inhibited almost completely by the DCCD-treatment [Fig. 7(A)], as already reported by Satre *et al.* (21). The initial rate of TCA- $^{32}\text{P}_i$  liberation in the presence of a low concentration of DNS-ATP was only slightly inhibited by the DCCD-treatment of  $\text{EF}_1$  [Fig. 7(B)]. It must be noted that in both experiments  $\text{EF}_1$  of the same concentration range was preincubated with DCCD (legend of Fig. 7).

Fluorescence Change of DNS-ATP on Its Binding to  $\alpha$  Subunit of  $\text{EF}_1$  — Fig. 8(A) shows a typical time course of change in the fluorescence intensity of DNS-ATP at 520 nm during its reaction with  $\alpha$  subunit of  $\text{EF}_1$ . The fluorescence intensity of 1.1  $\mu\text{M}$  DNS-ATP in the presence of 2 mM EDTA did not change on addition of 0.8  $\mu\text{M}$   $\alpha$  subunit [arrow a in Fig. 8(A), *cf.* Fig. 9]. On further addition of 5 mM  $\text{MgCl}_2$  [arrow b in Fig. 8(A)], the fluorescence intensity increased very rapidly ( $t_{1/2} < 1$  s) by 19%. No fluorescence increase was observed in the absence of this subunit or in the presence of an excess amount of ATP with the subunit. On further addition of 2 mM  $\text{P}_i$  [arrow c in Fig. 8(A)], the fluorescence intensity changed only slightly and maintained its level. When 2 mM ATP was finally added [arrow d in

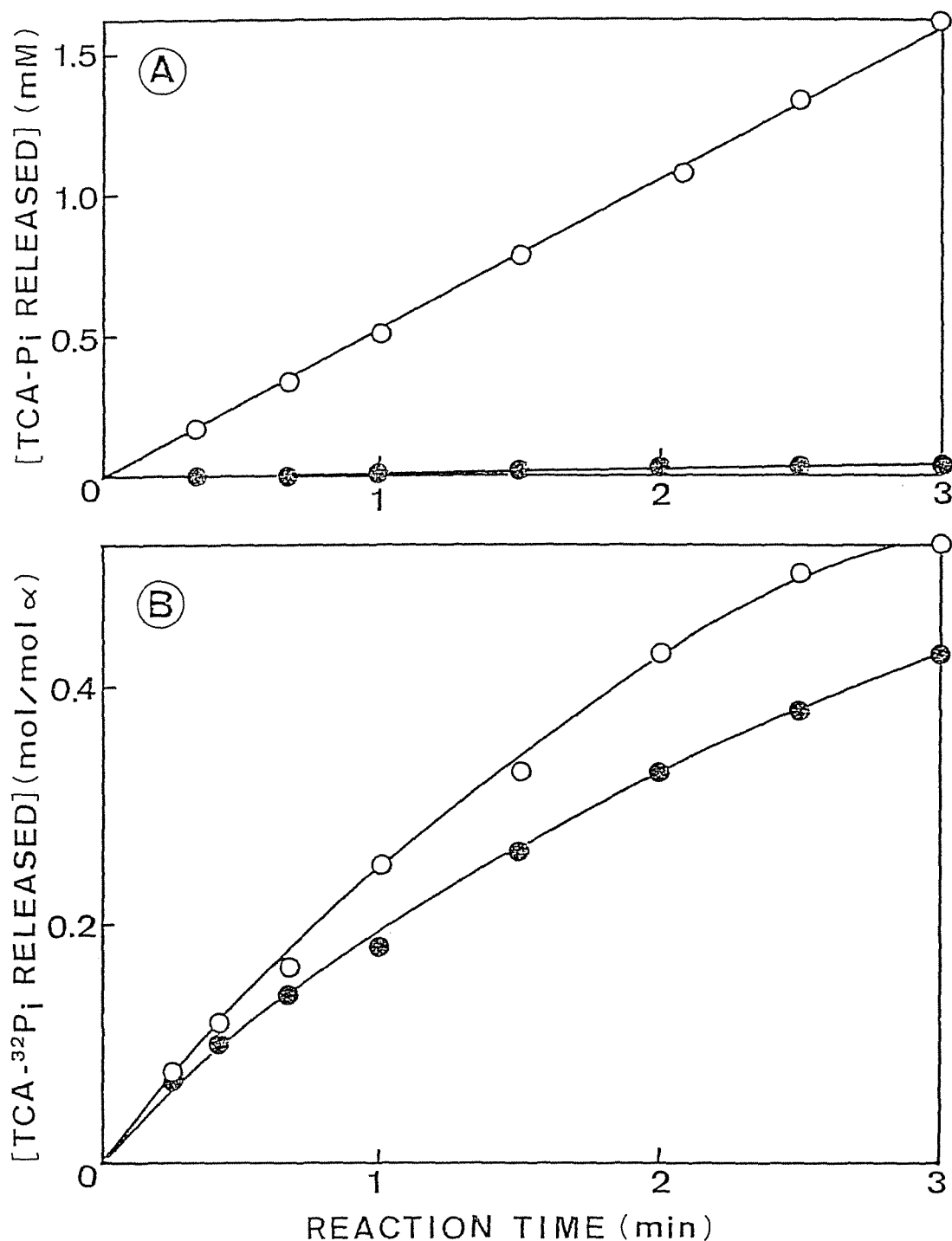


Fig. 7. Effects of DCCD-treatment of EF<sub>1</sub> on its steady-state ATPase and single turnover of DNS-ATP hydrolysis. (A) EF<sub>1</sub> at 0.87  $\mu$ M was preincubated with (●) or without (○) 0.2 mM DCCD in 2 mM EDTA and 50 mM Tris-acetate at pH 7.0 and 30°C for 20 min. Then, EF<sub>1</sub> solution was diluted to 0.087  $\mu$ M in 5 mM phosphoenolpyruvate, 0.11 mg/ml pyruvate kinase, 2.5 mM MgCl<sub>2</sub>, 0.2 mM EDTA and 50 mM Tris-HCl at pH 8.0 and 30°C. The reaction was started by addition of 5 mM ATP. (B) EF<sub>1</sub> at 1.6  $\mu$ M was preincubated with (●) or without (○) 0.2 mM DCCD under the same conditions as A, then allowed to react with 2.8  $\mu$ M DNS-AT<sup>32</sup>P for 1 min. The reaction was started by addition of 3 mM Mg<sup>2+</sup>.

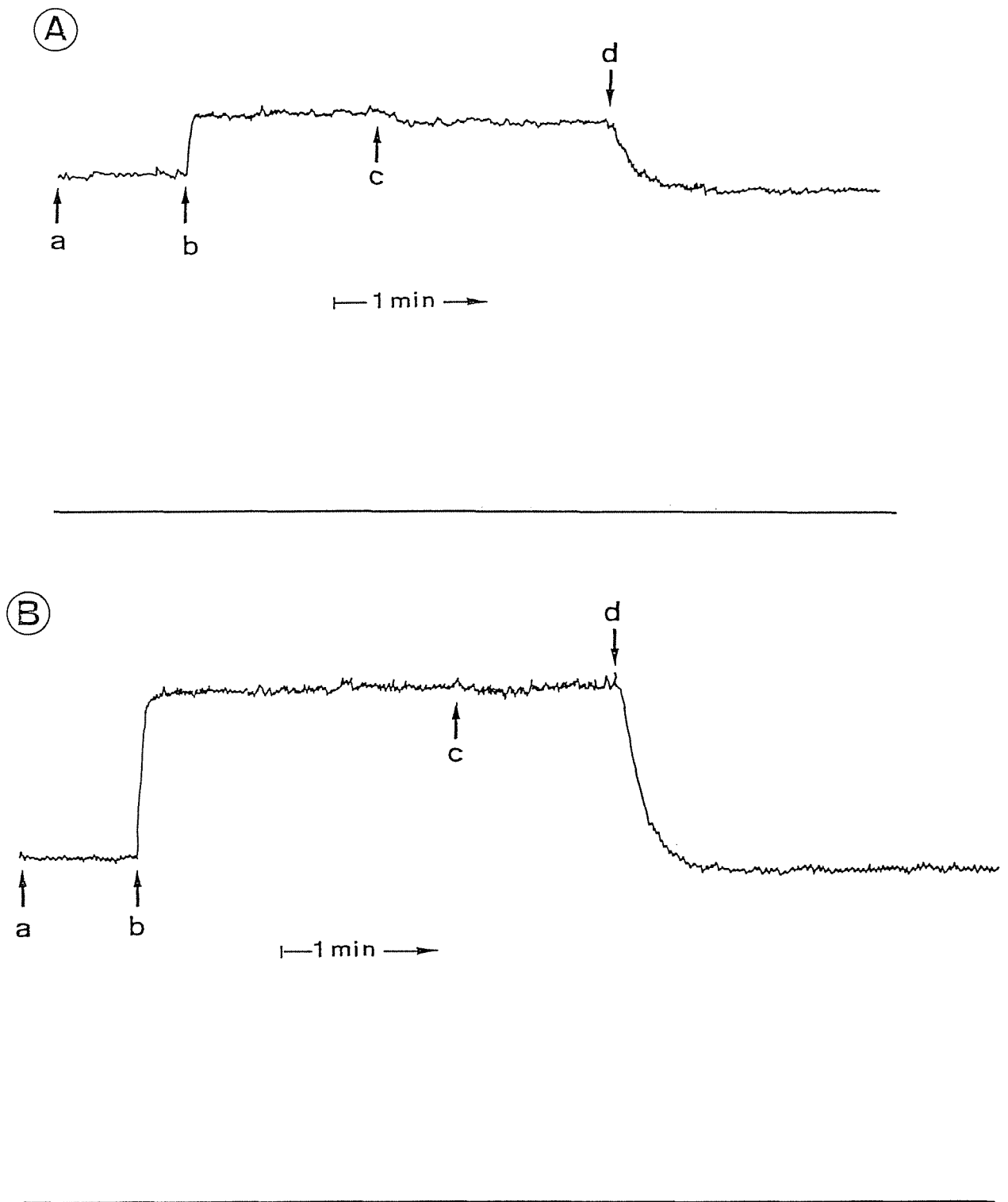


Fig. 8. Time course of fluorescence intensity change of DNS-ATP in the presence of  $\alpha$  subunit. (A) To a reaction mixture containing  $0.8 \mu\text{M}$   $\alpha$  subunit in a buffer solution (2 mM EDTA, 0.1 M NaCl and 50 mM Tris-acetate at pH 7.0 and  $30^\circ\text{C}$ ), the following additions were made at the time indicated by arrows (a-d); a,  $1.1 \mu\text{M}$  DNS-ATP; b, 5 mM  $\text{MgCl}_2$ ; c, 2 mM  $\text{K-P}_i$ ; d, 2 mM ATP. (B) To a reaction mixture containing  $4 \mu\text{M}$   $\alpha$  subunit in the buffer solution, the following additions were made at the time indicated by arrows (a-d); a,  $1.1 \mu\text{M}$  DNS-ATP; b, 5 mM  $\text{MgCl}_2$ ; c, 0.2 mM AMP; d, 0.2 mM ATP.

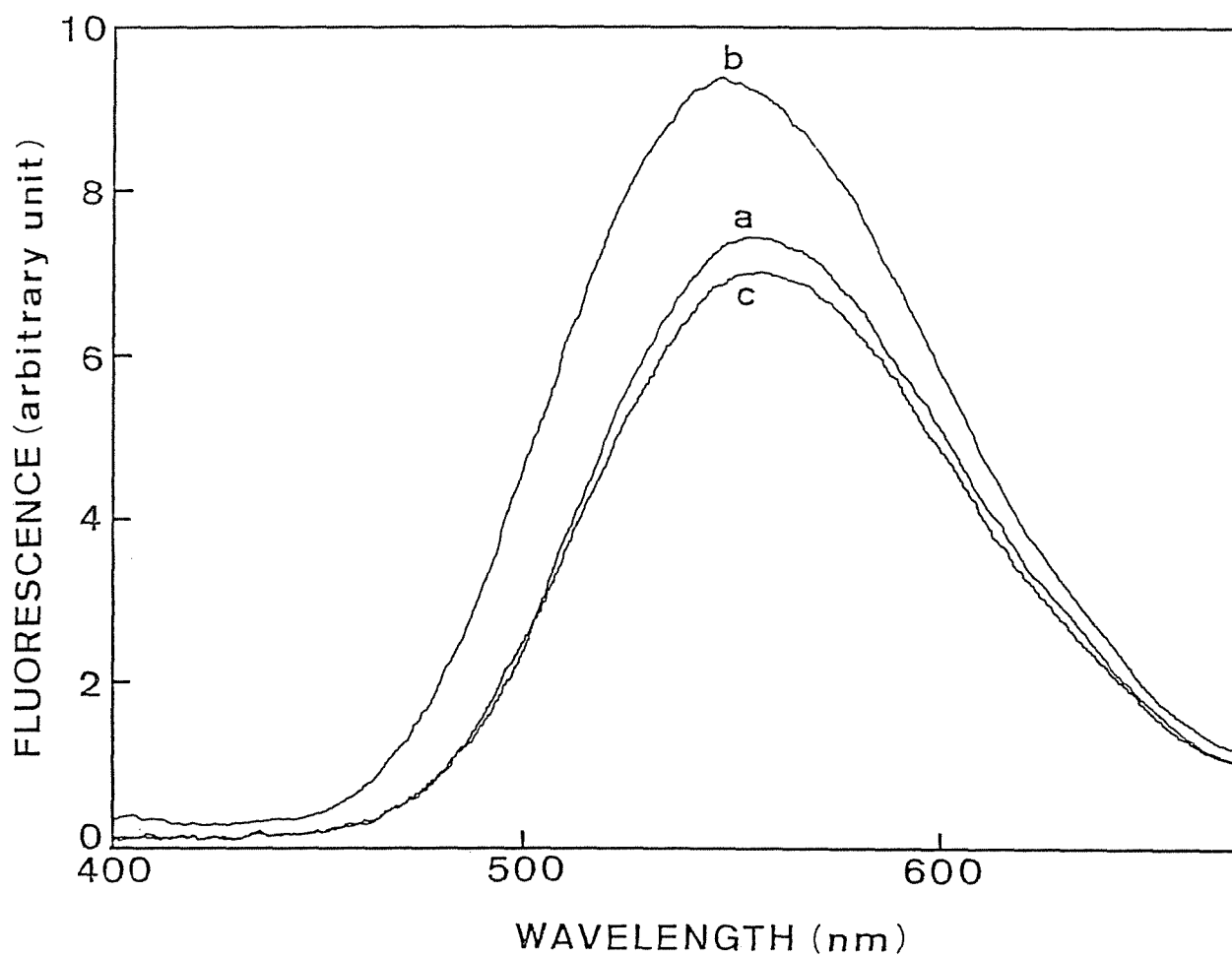


Fig. 9. Fluorescence emission spectra recorded during the course of reaction of DNS-ATP with  $\alpha$  subunit. Spectra were recorded in the following order; curve a, 1 min after addition of  $4 \mu\text{M}$   $\alpha$  subunit to  $1.1 \mu\text{M}$  DNS-ATP; curve b, 1 min after addition of  $5 \text{ mM}$   $\text{MgCl}_2$ ; curve c, 1 min after addition of  $2 \text{ mM}$  ATP. The fluorescence emission spectra of  $1.1 \mu\text{M}$  DNS-ATP alone in  $2 \text{ mM}$  EDTA and in  $2 \text{ mM}$  EDTA +  $5 \text{ mM}$   $\text{MgCl}_2$  were the same as the curve a and c, respectively. Other conditions are the same as described in Fig. 8.



Fig. 8(A)], the fluorescence intensity decreased exponentially with a  $t_{1/2}$  of 8 s to a level which was about 5% lower than that before the addition of 5 mM  $MgCl_2$ . The final level was found to be equal to that of free DNS-ATP in the presence of free  $Mg^{2+}$ .

Essentially the same experiment was carried out with 4.0  $\mu M$   $\alpha$  subunit; as shown in Fig. 8(B) the fluorescence intensity increased very rapidly by 50% upon addition of 5 mM  $MgCl_2$  [arrow b in Fig. 8(B)]. Addition of 0.2 mM AMP [arrow c in Fig. 8(B)] had no effect on the fluorescence intensity, whereas subsequent addition of 0.2 mM ATP [arrow d in Fig. 8(B)] decreased the intensity as observed in Fig. 8(A). When 5 mM  $CaCl_2$ , instead of  $MgCl_2$ , was added to the reaction mixture, no change of the fluorescence intensity was observed (data not shown).

Fluorescence emission spectra were recorded during the course of reaction of DNS-ATP with  $\alpha$  subunit (Fig. 9). Addition of 4.0  $\mu M$   $\alpha$  subunit to 1.1  $\mu M$  DNS-ATP in the presence of 2 mM EDTA did not change the fluorescence emission spectrum of the free DNS-ATP (trace a). Further addition of 5 mM  $MgCl_2$  increased the fluorescence intensity, and the emission maximum shifted to around 530 nm (trace b). Addition of 2 mM ATP decreased the fluorescence intensity to the level of free DNS-ATP in the presence of  $Mg^{2+}$  (trace c), which was slightly lower than that in the absence of  $Mg^{2+}$  (trace a).

Stoichiometry of DNS-ATP Binding to  $\alpha$  Subunit — The stoichiometry of DNS-ATP binding to  $\alpha$  subunit was determined by fluorometric titration of 1.1  $\mu M$  DNS-ATP with  $\alpha$  subunit in the presence of 3 mM  $Mg^{2+}$  at 4° or 30°C (Fig. 10). Data were analyzed based on Eq. 1, where the parameters for  $EF_1$  were taken as those for  $\alpha$  subunit. The solid lines in Fig. 10 are the best fits of the data of the DNS-ATP titration with  $\alpha$  subunit at 4° (●) and 30°C (○). The parameters

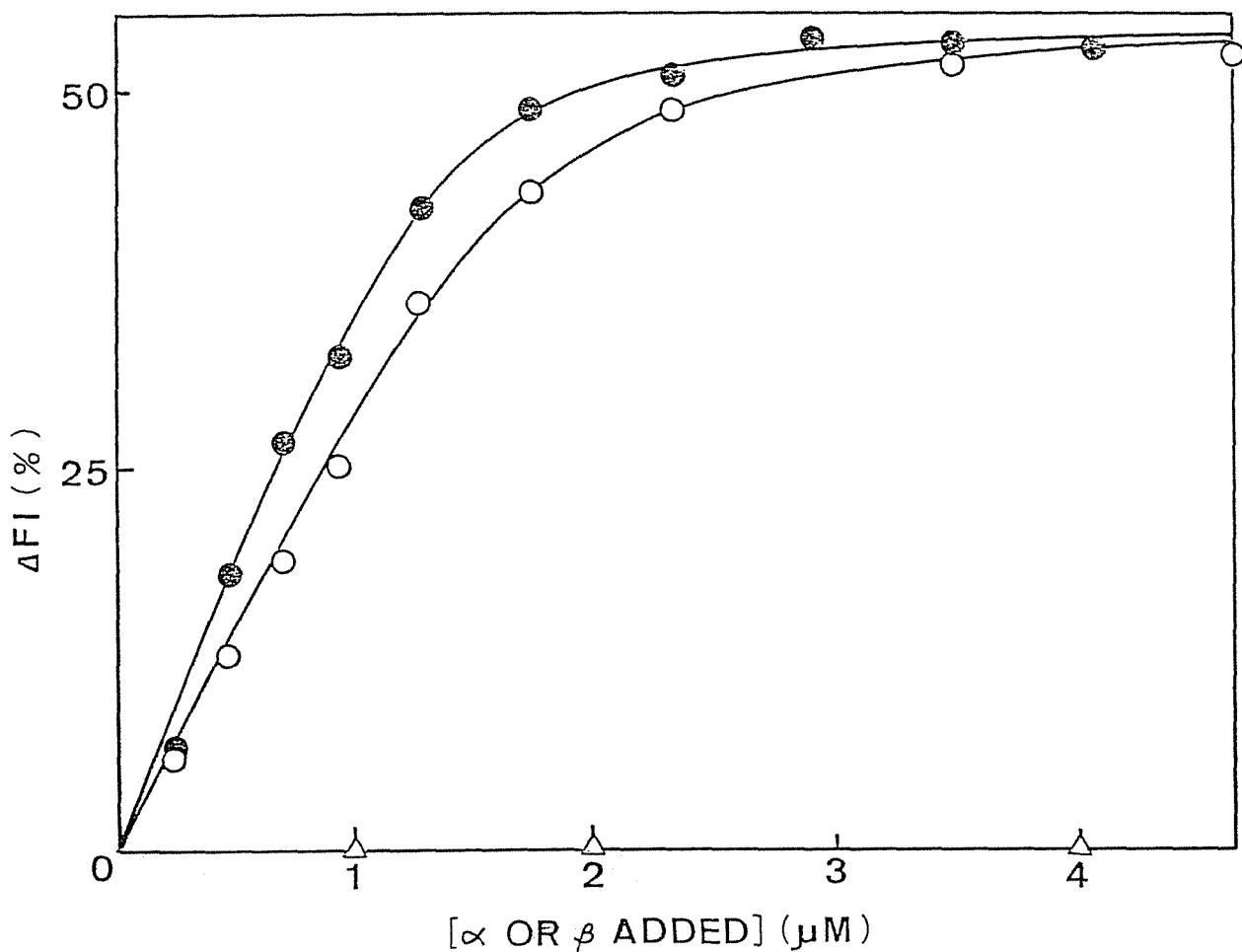


Fig. 10. Fluorescence titration of DNS-ATP with  $\alpha$  subunit in the presence of  $Mg^{2+}$ . The extent of fluorescence increase of  $1.1 \mu M$  DNS-ATP after addition of  $3 mM Mg^{2+}$  was plotted against the amount of  $\alpha$  subunit at  $30^\circ$  (O) or  $4^\circ C$  (●). Other conditions are the same as described in Fig. 8. The extent of fluorescence decrease of free DNS-ATP in the presence of free  $Mg^{2+}$  (cf. Fig. 9, curve c) was corrected. The solid lines are the theoretical curves (see the text). When  $1.1 \mu M$  DNS-ATP was allowed to react with  $\beta$  subunit in the presence of  $Mg^{2+}$  at  $30^\circ C$ , no fluorescence change was observed ( $\Delta$ ).

obtained from the data are  $n = 0.82$ , and  $\phi_{\text{DNS-ATP}} = 0.06 \mu\text{M}$  at  $4^\circ\text{C}$ , and  $n = 0.65$  and  $\phi_{\text{DNS-ATP}} = 0.07 \mu\text{M}$  at  $30^\circ\text{C}$ . The value of  $\Delta F_{\text{max}}$  was 55% at both temperatures. When  $\beta$  subunit up to  $4 \mu\text{M}$  was added to  $1.1 \mu\text{M}$  DNS-ATP, no  $\text{Mg}^{2+}$ -dependent fluorescence increase was observed ( $\Delta$ ).

The DNS-ATP binding to  $\alpha$  subunit was also measured at room temperature by the equilibrium dialysis. We found that even in the absence of  $\text{Mg}^{2+}$ , DNS-ATP can bind to  $\alpha$  subunit with an apparent dissociation constant of about 5 times higher than that in the presence of  $\text{Mg}^{2+}$ . However, during the equilibration we noticed some denaturation of  $\alpha$  subunit, and therefore could not analyze the data quantitatively.

Effects of Nucleotides and Pyrophosphate on DNS-ATP Bound to  $\alpha$  Subunit — The fluorescence intensity of DNS-ATP increased by addition of  $5 \text{ mM MgCl}_2$  to the mixture containing  $1.1 \mu\text{M}$  DNS-ATP,  $0.8 \mu\text{M}$   $\alpha$  subunit and  $2 \text{ mM EDTA}$ . Then, ADP, AMPPNP, GTP, ITP, CTP at  $0.2 \text{ mM}$  or  $\text{PP}_i$  at  $2 \text{ mM}$  was added. All these compounds decreased the fluorescence intensity exponentially with  $t_{1/2} = 7\text{-}8 \text{ s}$  to a level almost equal to that of free DNS-ATP (data not shown), as was observed upon the addition of  $0.2 \text{ mM ATP}$  (Fig. 8).

DCCD inhibited the steady-state rate of  $\text{EF}_1\text{-ATPase}$  activity at high ATP concentrations, but did not inhibit  $\text{EF}_1\text{-DNS-ATPase}$  activity at low DNS-ATP concentrations, as mentioned above (Fig. 7). On the contrary we found that DCCD at  $2 \text{ mM}$  did not affect the  $\text{Mg}^{2+}$ -dependent fluorescence increase and the ATP-dependent fluorescence decrease of DNS-ATP in the presence of  $\alpha$  subunit (data not shown), suggesting that the results obtained above (Figs. 6 & 7) were not due to the reaction of DCCD to this subunit.

Inability of  $\alpha$  Subunit to Hydrolyze DNS-ATP and ATP — No TCA- $^{32}\text{P}_i$  liberation was observed on either addition of 5 mM  $\text{MgCl}_2$  to the reaction mixture containing 2.8  $\mu\text{M}$  DNS-AT $^{32}\text{P}$ , 2.3  $\mu\text{M}$   $\alpha$  subunit and 2 mM EDTA ( $\Delta$ ), or subsequent addition of 2 mM ATP ( $\blacktriangle$ ) (Fig. 4). Even when 5 mM  $\text{MgCl}_2$  was added to the mixture containing 7.6  $\mu\text{M}$  AT $^{32}\text{P}$  and 1.6  $\mu\text{M}$   $\alpha$  or 1.8  $\mu\text{M}$   $\beta$  subunit in 2 mM EDTA, no TCA- $^{32}\text{P}_i$  liberation was observed (data not shown). These results are in agreement with the previous finding that the isolated  $\alpha$ ,  $\beta$  or  $\delta$  subunit did not have ATPase activity (7,8).

Fluorescence Change of DNS-ATP on Its Binding to Reconstituted  $\text{EF}_1$ -ATPase — To determine what kind of subunit interactions are needed for the  $\text{EF}_1$ -ATPase activity, we further investigated the reaction of DNS-ATP with the reconstituted  $\text{EF}_1$ -ATPase. Figure 11 shows the time course of change in the fluorescence intensity of DNS-ATP at 520 nm during its reaction with reconstituted  $\text{EF}_1$ -ATPase. The fluorescence intensity of 1.1  $\mu\text{M}$  DNS-ATP in the presence of 2 mM EDTA increased slightly on addition of 0.36 mg/ml reconstituted  $\text{EF}_1$ -ATPase [arrow a in Fig. 11. compare curves a and b in Fig. 12]. On further addition of 5 mM  $\text{MgCl}_2$  [arrow b in Fig. 11], the fluorescence intensity increased very rapidly ( $t_{1/2} < 1$  s), then slowly with  $t_{1/2}$  of about 30 s. The plateau level was 1.83 fold the intensity of free DNS-ATP. On further addition of 2 mM  $\text{P}_i$  [arrow c in Fig. 11], the fluorescence increased rapidly to a level of 2.4 fold that of free DNS-ATP. On addition of 2 mM ATP [arrow d in Fig. 11], the fluorescence intensity decreased to the level of free DNS-ATP.

When 5 mM  $\text{CaCl}_2$  was added to the mixture containing 1.1  $\mu\text{M}$  DNS-ATP and 0.36 mg/ml reconstituted  $\text{EF}_1$ -ATPase in the presence of 2 mM EDTA, the fluorescence intensity increased exponentially with

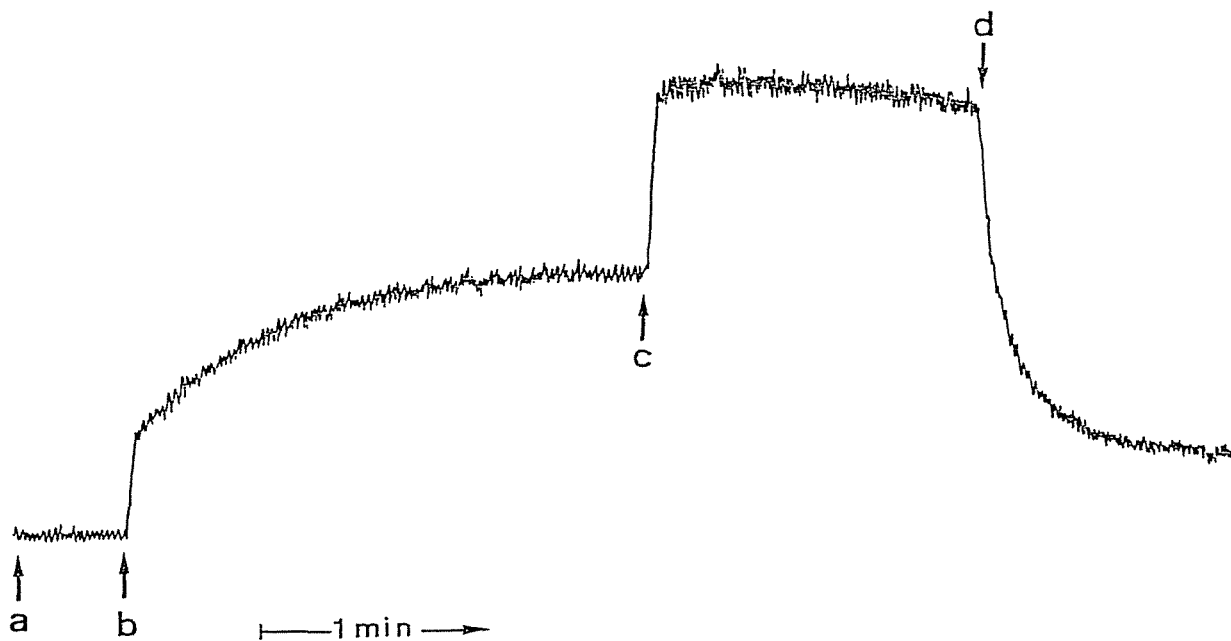


Fig. 11. Time course of fluorescence intensity change of DNS-ATP in the presence of reconstituted  $EF_1$ -ATPase. To a mixture containing 0.36 mg/ml reconstituted  $EF_1$ -ATPase in 2 mM EDTA, 100 mM NaCl and 50 mM Tris-acetate at pH 7.0 and 30°C, the following additions were made at the time indicated by arrows (a-d); a, 1.1  $\mu$ M DNS-ATP; b, 5 mM  $MgCl_2$ ; c, 2 mM  $K-P_i$ ; d, 2 mM ATP. Specific activity of the reconstituted  $EF_1$ -ATPase was 30 U/mg protein. The concentration of the reconstituted  $EF_1$ -ATPase was shown by the protein concentration, because the reconstitution was not complete [note that the specific activity of purified  $EF_1$  is about 100 U/mg protein (28)].

$t_{1/2}$  of 40 s to reach a plateau level, which was 1.5 fold the intensity of free DNS-ATP. Further addition of 2 mM  $P_i$  induced a small increase (6%) in the fluorescence intensity (data not shown).

Figure 12 shows the fluorescence emission spectra of free DNS-ATP (trace a) and complexes of DNS-ATP with reconstituted  $EF_1$ -ATPase. When 0.53 mg/ml reconstituted  $EF_1$ -ATPase was added to 1.1  $\mu$ M DNS-ATP in the presence of 2 mM EDTA, the fluorescence intensity increased slightly with a shift of the emission maximum from 555 to 550 nm (trace b). Further addition of 5 mM  $MgCl_2$  markedly increased the fluorescence intensity, and the maximum shifted to 535 nm (trace c). The addition of 2 mM ATP reversed these fluorescence changes backward to the state of free DNS-ATP (trace d).

Figure 13 shows the result of fluorescence titration of DNS-ATP with reconstituted  $EF_1$ -ATPase in the presence of 3 mM  $Mg^{2+}$ . The extent of the  $Mg^{2+}$ -dependent fluorescence increase of 1.1  $\mu$ M DNS-ATP increased with increase in the amount of reconstituted  $EF_1$ -ATPase added. When the amount of reconstituted  $EF_1$ -ATPase added was 1.5  $\mu$ M (0.54 mg/ml), the extent of the  $Mg^{2+}$ -dependent fluorescence increase was 88% of the intensity of free DNS-ATP. However, we could not obtain a good fit to the data based on Eq. 1, since we could not measure the saturation level of the fluorescence increase.

Acceleration of DNS-Nucleotide Release from Reconstituted  $EF_1$ -ATPase-DNS-Nucleotide Complex by Nucleotides and Pyrophosphate — DNS-ATP at 1.1  $\mu$ M was allowed to react with 0.42 mg/ml reconstituted  $EF_1$ -ATPase for 2 min in the presence of 3 mM  $Mg^{2+}$ . Then, 0.2 mM of nucleotide or 2 mM pyrophosphate was added [arrow  $\underline{c}$  in Fig. 14], and the following decrease in the fluorescence intensity was measured

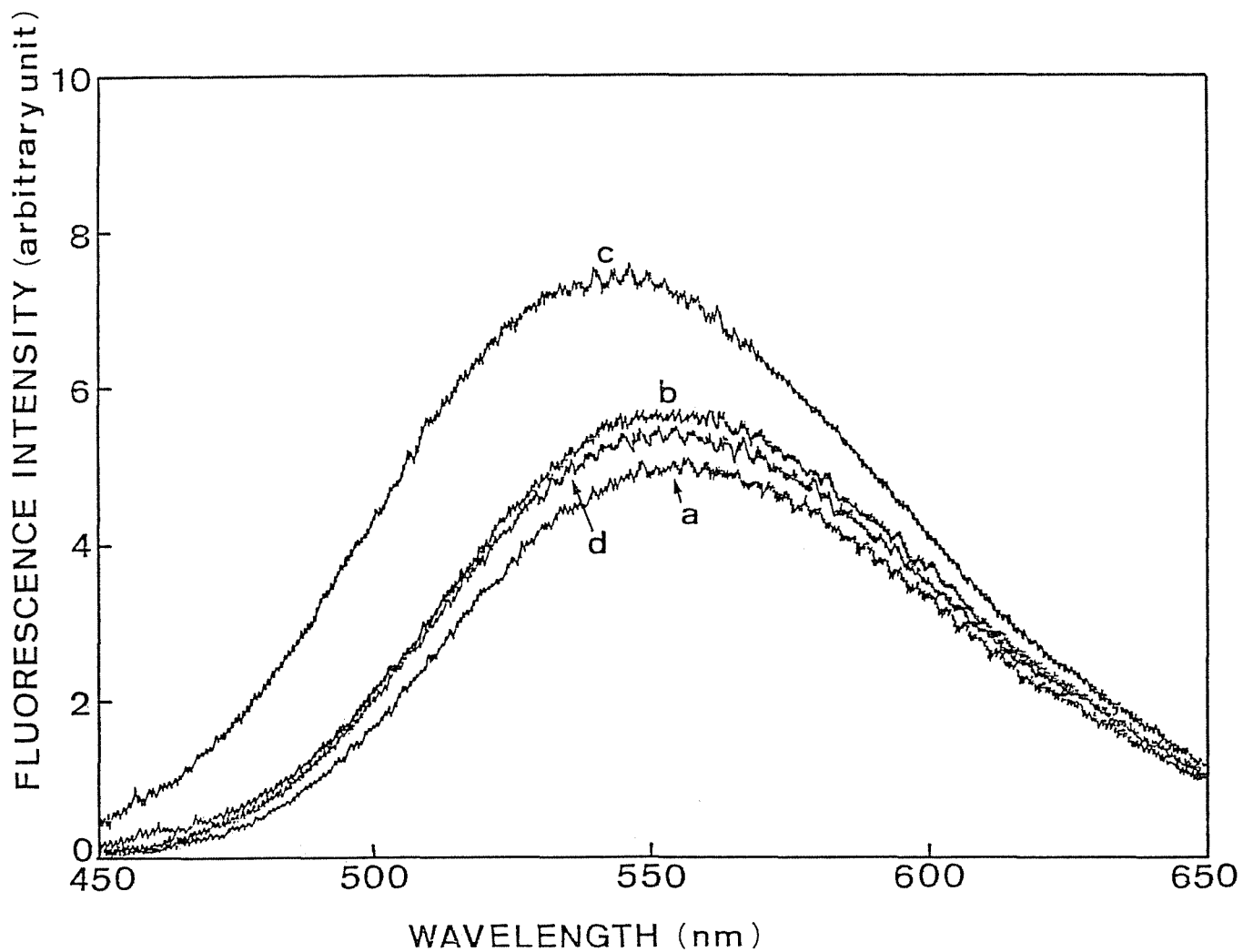


Fig. 12. Fluorescence emission spectra recorded during the course of reaction of DNS-ATP with reconstituted  $EF_1$ -ATPase. Spectra were recorded in the following order; curve a, 1.1  $\mu$ M DNS-ATP; curve b, 1 min after addition of 0.53 mg/ml reconstituted  $EF_1$ ; curve c, 2 min after addition of 3 mM  $Mg^{2+}$ ; curve d, 1 min after addition of 2 mM ATP. Other conditions are the same as described in Fig. 11.

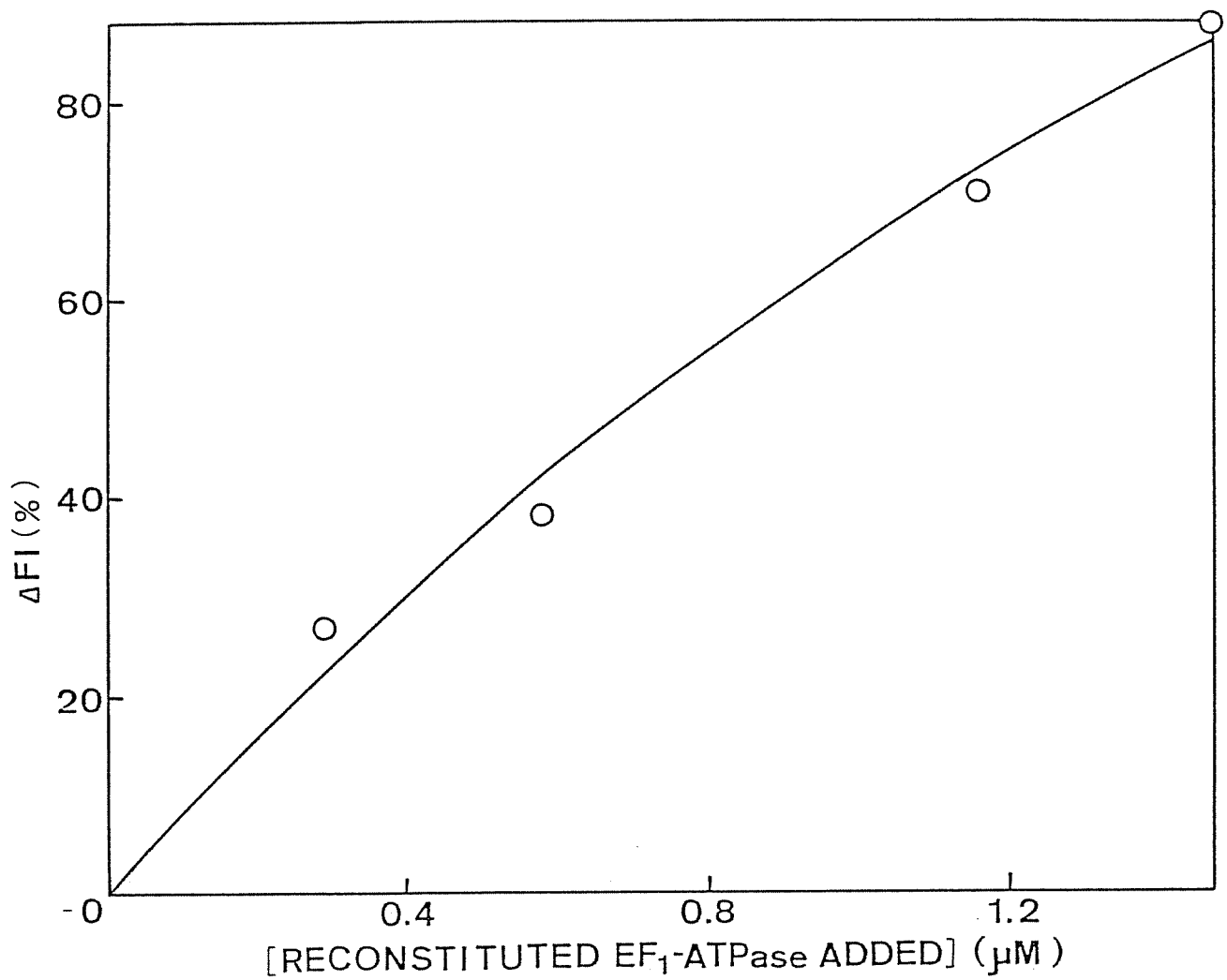


Fig. 13. Fluorometric titration of DNS-ATP with reconstituted EF<sub>1</sub>-ATPase in the presence of Mg<sup>2+</sup>. The extent of fluorescence enhancement of 1.1 μM DNS-ATP 2 min after addition of 3 mM Mg<sup>2+</sup> was plotted against the amount of reconstituted EF<sub>1</sub>-ATPase added. Other conditions are the same as described in Fig. 11.



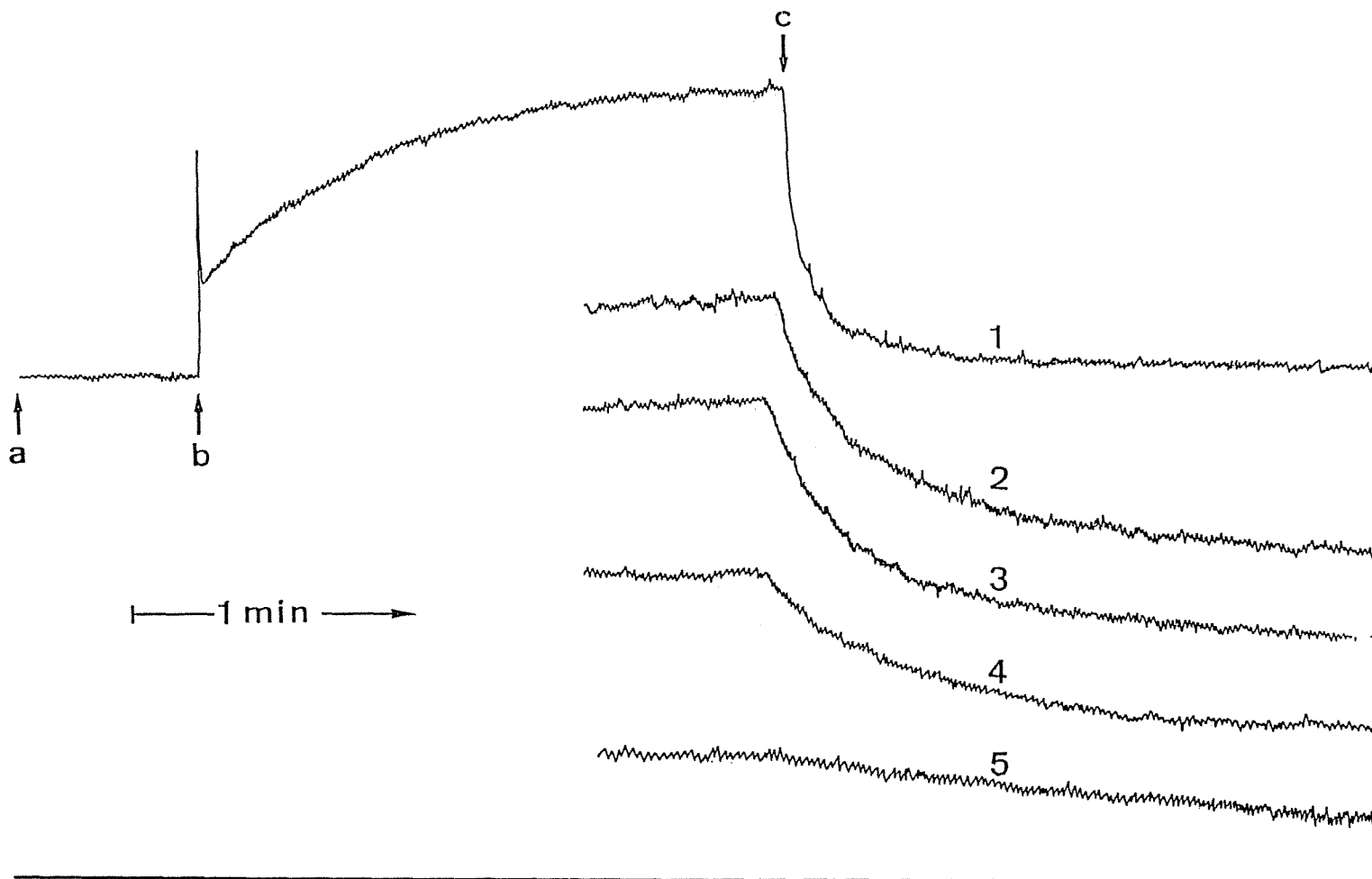
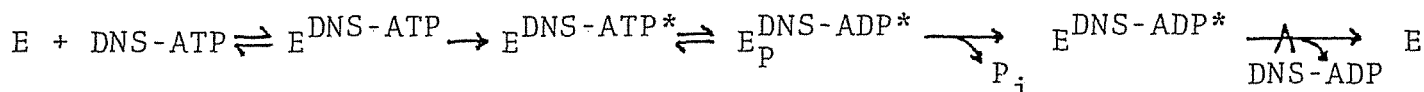


Fig. 14. Fluorescence decrease on addition of various phosphate compounds to reconstituted  $EF_1$ -ATPase-DNS-nucleotide. DNS-ATP at  $1.1 \mu\text{M}$  was added to  $0.42 \text{ mg/ml}$  reconstituted  $EF_1$ -ATPase (indicated by arrow a), then  $3 \text{ mM Mg}^{2+}$  was added (indicated by arrow b). At the time indicated by arrow c, the following additions were made;  $0.2 \text{ mM ATP}$  (1),  $0.2 \text{ mM ADP}$  (2),  $2 \text{ mM PP}_i$  (3),  $0.2 \text{ mM CTP}$  (4) or  $0.2 \text{ mM AMP}$  (5). Other conditions are the same as described in Fig. 11.

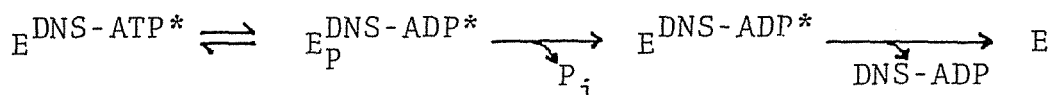
(Fig. 14). The addition of ATP caused a fluorescence decrease, first rapidly ( $t_{1/2} < 1$  s) and then slowly, and the final level was almost equal to that of free DNS-ATP (trace 1). When ADP (trace 2),  $PP_i$  (trace 3) or CTP (trace 4) was added, the fluorescence decreased almost exponentially. The rate of the fluorescence change decreased in the order of  $ATP > ADP \approx PP_i > CTP$ . AMP (trace 5) had no effect on the fluorescence intensity of the reconstituted  $EF_1$ -ATPase-DNS-nucleotide.

## DISCUSSION

We have previously performed kinetic studies on the single turnover of DNS-ATPase of beef heart  $F_1$  (26), and proposed the following reaction scheme for the  $F_1$ -DNS-ATPase reaction:



The asterisk designates the reaction intermediate with enhanced fluorescence intensity of DNS-nucleotide. In the presence of  $\text{Mg}^{2+}$ , DNS-ATP binds to the high affinity site of  $F_1$  to form a loose complex without enhanced fluorescence ( $E^{\text{DNS-ATP}}$ ). The loose complex is converted to a tight complex with enhanced fluorescence ( $E^{\text{DNS-ATP}^*}$ ), then bound DNS-ATP is cleaved on the enzyme ( $E_P^{\text{DNS-ADP}^*}$ ). The apparent affinity of DNS-ATP to the enzyme is very high. Nucleotides such as ATP at high concentrations markedly accelerate the following three steps in the reaction sequence:



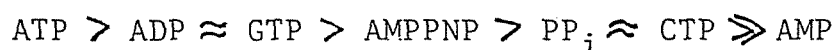
Therefore, we suggested that there are low affinity regulatory site(s) as well as the high affinity catalytic sites in  $F_1$ . The purified  $EF_1$  contained 2 mol ATP and 0.5 mol ADP per mol enzyme (33). These bound adenine nucleotides were found to be nonexchangeable with nucleotides in the medium (33). Therefore, in analyzing the results on the reaction of  $EF_1$  with DNS-ATP, we neglected the effect of these tightly bound adenine nucleotides.

The first issue investigated in this study is the similarity of the reaction mechanism of  $EF_1$ -DNS-ATPase to that of  $F_1$ -DNS-ATPase. In the presence of  $\text{Mg}^{2+}$ , DNS-ATP reacted with  $EF_1$  to induce a

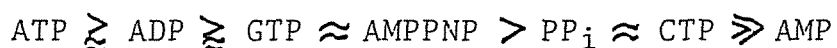
fluorescence increase similar to that observed on beef heart  $F_1$  (Figs. 1 & 2). This finding suggests that the environment of DNS-ATP binding sites in  $EF_1$  is hydrophobic as is the case for  $F_1$ . The fluorescence intensity of  $EF_1$ -DNS-nucleotide complex increased on further addition of  $P_i$ , again as is the case for  $F_1$ -DNS-nucleotide complex. The fluorescence increase by  $P_i$  was observed even in the presence of excess amounts of DNS-ATP to  $EF_1$ . Furthermore, we (26) previously found that in the case of beef heart  $F_1$ , the affinity of DNS-ATP was unaffected by the addition of  $P_i$ . These findings indicate that the DNS-ATP binding site in  $EF_1$  is made more hydrophobic by the action of  $P_i$ . The fluorometric titration of DNS-ATP with  $EF_1$  in the presence of  $Mg^{2+}$  indicated that 3 mol of DNS-ATP was bound to 1 mol of  $EF_1$  with an apparent dissociation constant of  $0.23 \mu M$  (Fig. 3). Using the same method of fluorometric titration, we previously found that 2 mol of DNS-ATP binds to 1 mol of beef heart  $F_1$  with an apparent dissociation constant of  $0.44 \mu M$  (26). The stoichiometry of 3 mol DNS-ATP bound/mol  $EF_1$  is consistent with the  $\alpha_3 \beta_3 \gamma \delta \epsilon$  stoichiometry of  $EF_1$  subunits (34). When  $Mg^{2+}$  was added to a reaction mixture containing  $EF_1$  and a low concentration of DNS-ATP, the fluorescence intensity was increased ( $E^{DNS-ATP^*}$ ; Fig. 1), and the increase was followed by liberation of  $P_i$  on termination of the reaction with TCA ( $E_P^{DNS-ADP^*}$  &  $E^{DNS-ADP^*}$ ; Fig. 4). The fluorescence intensity maintained its increased level after liberation of TCA- $P_i$ , indicating that the rate of liberation of DNS-ADP from  $E^{DNS-ADP^*}$  is very small. These findings are quite similar to those of beef heart  $F_1$  (26).

The mechanism of acceleration of  $EF_1$ -DNS-ATPase by high

concentrations of nucleotide was investigated using the same procedures as in the case of beef heart  $F_1$ . A biphasic decrease in the fluorescence intensity of  $EF_1$ -DNS-nucleotide complex was observed upon addition of high concentrations of ATP (Fig. 5). Therefore, it was suggested that ATP binding to low affinity regulatory site(s) in  $EF_1$  induced a conformational change around the catalytic sites and accelerated the release of DNS-nucleotide, as in the case of beef heart  $F_1$  (26). The rapid phase of the fluorescence decrease observed on addition of ATP, ADP, or GTP to  $EF_1$ -DNS-nucleotide complex (Fig. 5) is suggested to be due to the release of DNS-nucleotide induced by a conformational change of catalytic site on  $EF_1$ . The second slow phase will be due to the displacement of bound DNS-nucleotide by other nucleotide. This slow release of DNS-nucleotide was also observed in the case of addition of  $PP_i$  or CTP. Thus, the ability of phosphate compounds to release DNS-nucleotide from  $EF_1$  was found to follow in the order of



This order was similar to that observed on beef heart  $F_1$  (26):



In the case of beef heart  $F_1$ , ATP at high concentrations accelerated markedly the  $TCA-P_i$  liberation from  $E^{\text{DNS-ATP}^*}$  (26), whereas no acceleration of the  $TCA-P_i$  liberation by ATP was observed in the case of  $EF_1$ -DNS-ATPase (Fig. 4). This may suggests that the reaction mechanism of  $EF_1$ -DNS-ATPase is essentially different from that of  $F_1$ -DNS-ATPase. However, if we assume the reaction mechanisms of these ATPases are essentially the same, we can explain the discrepancy between the results of the two enzymes as due to the larger rate constant of the cleavage step ( $E^{\text{DNS-ATP}^*} \longrightarrow E_p^{\text{DNS-ADP}^*}$ ) than the rates of the following steps in the case of  $EF_1$ -DNS-ATPase. Then, the

acceleration of TCA-P<sub>i</sub> liberation due to acceleration of the cleavage step is not observed, since the amount of E<sup>DNS-ATP\*</sup> at steady state is small.

The second issue is the subunit localization of the high affinity catalytic site and low affinity regulatory site. We previously suggested that the high affinity catalytic site and low affinity regulatory site exist in the  $\alpha$  and  $\beta$  subunit, respectively (26). This suggestion is based on the information that the isolated  $\alpha$  subunit of thermophilic F<sub>1</sub> or EF<sub>1</sub> and  $\beta$  subunit of thermophilic F<sub>1</sub> have high affinity and low affinity nucleotide-binding site, respectively (9,10). In this study, we found that the fluorescence intensity of DNS-ATP increased markedly on its reaction with  $\alpha$  subunit but not with  $\beta$  subunit of EF<sub>1</sub> in the presence of Mg<sup>2+</sup> (Figs. 8-10). The fluorometric titration of DNS-ATP with  $\alpha$  subunit in the presence of Mg<sup>2+</sup> indicated that 0.65-0.82 mol of DNS-ATP bound to 1 mol of  $\alpha$  subunit very tightly (Fig. 10). This finding suggests that properties of DNS-ATP binding to  $\alpha$  subunit are very similar to those of DNS-ATP binding to EF<sub>1</sub>.

We investigated the possibility of the existence of a low affinity regulatory site in  $\beta$  subunit by using DCCD, a potent inhibitor of F<sub>1</sub>-ATPase activity specific to  $\beta$  subunit (20-23). DCCD had no effect on the binding of DNS-ATP with  $\alpha$  subunit. It inhibited only slightly the fluorescence increase of DNS-ATP by its binding to EF<sub>1</sub> (Fig. 6) and the single turnover of DNS-ATP hydrolysis by EF<sub>1</sub> [Fig. 7(B)]. DCCD inhibited markedly both the accelerating effect of ATP on DNS-nucleotide release from EF<sub>1</sub> (Fig. 6) and the EF<sub>1</sub>-ATPase activity in the steady state [Fig. 7(A)]. These findings indicate that the modification of  $\beta$  subunit by DCCD blocks the function of the low affinity regulatory site, without affecting the binding of DNS-ATP to the high affinity catalytic site.

Thus, our findings strongly suggest that the high affinity catalytic site and the low affinity regulatory site exist in  $\alpha$  and  $\beta$  subunits, respectively. This concept is apparently opposite to a widely accepted view that the catalytic site and the non-catalytic nucleotide binding site are located in  $\beta$  and  $\alpha$  subunits, respectively (15,16,18-23). It should be mentioned that the latter view has been derived mainly from the inhibition of  $F_1$ -ATPase activity in the steady state by chemical modification of  $\beta$  subunit. However, we cannot determine the subunit localization of the catalytic site and regulatory site by measuring the effect of the modification of  $\alpha$  or  $\beta$  subunit on the steady-state ATPase. This is because the low affinity nucleotide-binding to the regulatory site accelerates markedly the release of product bound to the catalytic site (26), and the  $F_1$ -ATPase activity in the steady state is markedly inhibited by the modification of the regulatory site as well.

In the previous paper, it was suggested that hydrolysis of nucleosidetriphosphate in the steady state occurs via different catalytic pathways and at different catalytic sites in  $F_1$  because of the following two reasons (26). (a) The value of  $V_f$  ( $0.34 \text{ s}^{-1}$ ) for the formation of  $E^{\text{DNS-ATP}^*}$  was smaller than that of  $V_{\text{max}}$  ( $\gg 1 \text{ s}$ ) for the steady-state rate of  $F_1$ -DNS-ATPase. (b) When ATP was added under conditions where most of  $F_1$  was in the form of  $E^{\text{DNS-ADP}^*}$ , ATP hydrolysis occurred without lag phase. For  $EF_1$ , the modification of  $\beta$  subunit by DCCD blocks both catalytic pathways, because DCCD inhibited the  $EF_1$ -ATPase in the steady state almost completely [Fig. 7(A)].

The third issue investigated in this paper is the difference between the structure and function of the isolated  $\alpha$  subunit and those of integrated  $\alpha$  in  $EF_1$ . Recently, Dunn and Futai (7), and Dunn

(35) reported that the isolated  $\alpha$  subunit of  $EF_1$  binds ATP in the absence of  $Mg^{2+}$  with very high affinity ( $K_D = 0.1 \mu M$  at  $4^\circ C$ ). In this study, we found that the structure and function of the  $\alpha$  subunit are altered when isolated from  $EF_1$  in the following two respects: (a) In the presence of  $Ca^{2+}$ , DNS-ATP showed the fluorescence increase on its reaction with  $EF_1$  [Fig. 1(B)], but not with isolated  $\alpha$  subunit. The apparent dissociation constant of isolated  $\alpha$  subunit for DNS-ATP in the presence of  $Mg^{2+}$  was  $0.07 \mu M$ , which was about 1/3 of the value found with  $EF_1$  (Figs. 3 & 10). The extent of the fluorescence increase of DNS-ATP bound to the isolated  $\alpha$  subunit in the presence of  $Mg^{2+}$  was 55% of the fluorescence intensity of free DNS-ATP, which was about 1/5 of the value found with  $EF_1$  (Figs. 3 & 10). These differences suggest that on isolation of  $\alpha$  subunit, its affinity for DNS-ATP increased and the environment of the nucleotide-binding site became less hydrophobic. (b)  $P_i$  had no effect on the fluorescence intensity of DNS-ATP bound to the isolated  $\alpha$  subunit [Fig. 8(A)], whereas  $P_i$  enhanced markedly the fluorescence intensity in the case of  $EF_1$  [Fig. 1(A)]. This finding is consistent with the report that the  $P_i$  binding site exists in the  $\beta$  subunit (36), and it also suggests an interaction between the  $\alpha$  and  $\beta$  subunits in  $EF_1$ .

We found that the properties of the reaction of DNS-ATP with the isolated  $\alpha$  subunit was unaffected by the addition of the  $\beta$  subunit, and that the fluorescence changes of DNS-ATP on its reaction with  $EF_1$ -ATPase reconstituted from  $\alpha$ ,  $\beta$  and  $\delta$  subunit were quite similar to those on its reaction with native  $EF_1$ . On addition of  $Mg^{2+}$  to a reaction mixture containing DNS-ATP and the reconstituted  $EF_1$ -ATPase, the fluorescence intensity increased in two phases (Fig. 11). The



rapid phase ( $t_{1/2} < 1$  s) of the increase was suggested to be due to the contamination by free  $\alpha$  subunit, since the rapid phase was not observed on addition of  $\text{Ca}^{2+}$  instead of  $\text{Mg}^{2+}$ . It is suggested that the hydrophobicity of the nucleotide binding site is recovered to the level of native  $\text{EF}_1$ , since the extent of the  $\text{Mg}^{2+}$ -dependent fluorescence increase was larger than 88% of the intensity of free DNS-ATP (Fig. 13). Furthermore, the decrease in the fluorescence intensity of reconstituted  $\text{EF}_1$ -DNS-nucleotide complex after adding a phosphate compound showed a specificity quite similar to that of native  $\text{EF}_1$ : which is  $\text{ATP} > \text{ADP} \approx \text{PP}_i > \text{CTP} \gg \text{AMP}$  (Fig. 14). These findings clearly indicate that the subunit interactions in reconstituted  $\text{EF}_1$ -ATPase are similar to those in the native  $\text{EF}_1$ .

## REFERENCES

1. Kagawa, Y., Sone, N., Hirata, H., & Yoshida, M. (1979) J. Bioenerg. Biomem. 11, 39-78
2. Penefsky, H.S. (1979) Adv. Enzymol. 49, 223-280
3. Baird, B.A. & Hammes, G.G. (1977) J. Biol. Chem. 252, 4743-4748
4. Verschoor, G.J., van de Sluis, P.R., & Slater, E.C. (1977) Biochim. Biophys. Acta 462, 422-437
5. Esch, F.S. & Allison, W.S. (1979) J. Biol. Chem. 254, 10740-10746
6. Yoshida, M., Okamoto, H., Sone, N., Hirata, H., & Kagawa, Y. (1977) Proc. Natl. Acad. Sci. U.S.A. 74, 936-940
7. Yoshida, M., Sone, N., Hirata, H., & Kagawa, Y. (1977) J. Biol. Chem. 252, 3480-3485
8. Futai, M. (1977) Biochem. Biophys. Res. Commun. 79, 1231-1237
9. Dunn, S.D. & Futai, M. (1980) J. Biol. Chem. 255, 113-118
10. Ohta, S., Tsuboi, M., Oshima, T., Yoshida, M., & Kagawa, Y. (1980) J. Biochem. 87, 1609-1617
11. Garret, N.E. & Penefsky, H.S. (1975) J. Biol. Chem. 250, 6640-6647
12. Slater, E.C., Kemp, A., Van der Kraan, I., Muller, J.L.M., Roveri, O.A., Verschoor, G.J., Wagenvoord, R.J., & Wielders, J.P.M. (1979) FEBS Lett. 103, 7-11
13. Schuster, S.M., Ebel, R.E., & Lardy, H.A. (1975) J. Biol. Chem. 250, 7848-7853
14. Wielders, J.P.M., Slater, E.C., & Muller, J.L.M. (1980) Biochim. Biophys. Acta 589, 231-240
15. Budker, V.G., Kozlov, I.A., Kurbatov, V.A., & Milgrom, Y.M. (1977) FEBS Lett. 83, 11-14

16. Drutsa, V.L., Kozlov, I.A., Milgrom, Y.M., Shabarova, Z.A., & Sokolova, N.I. (1979) Biochem. J. 182, 617-619
17. Wagenvoord, R.J., Kemp, A., & Slater, E.C. (1980) Biochim. Biophys. Acta 593, 204-211
18. Ferguson, S.J., Lloyd, W.J., & Radda, G.K. (1975) Eur. J. Biochem. 54, 127-133
19. Esch, F.S. & Allison, W.S. (1978) J. Biol. Chem. 253, 6100-6106
20. Pougeois, R., Satre, M., & Vignais, P.V. (1979) Biochemistry 18, 1408-1413
21. Satre, M., Lunardi, J., Pougeois, R., & Vignais, P.V. (1979) Biochemistry 18, 3134-3140
22. Shoshan, V. & Selman, B.R. (1980) J. Biol. Chem. 255, 384-389
23. Yoshida, M., Poser, J.W., Allison, W.S., & Esch, F.S. (1981) J. Biol. Chem. 256, 148-153
24. Hammes, G.G. & Hilborn, D.A. (1971) Biochim. Biophys. Acta 233, 580-590
25. Watanabe, T., Inoue, A., Tonomura, Y., Uesugi, S., Ohtsuka, E., & Ikehara, M. (1981) J. Biochem. 90, 956-965
26. Matsuoka, I., Watanabe, T., & Tonomura, Y. (1981) J. Biochem. 90, 967-989
27. Tietz, A. & Ochoa, S. (1958) Arch. Biochem. Biophys. 78, 477-494
28. Futai, M., Sternweis, P.C., & Heppel, L.A. (1974) Proc. Natl. Acad. Sci. U.S.A. 71, 2725-2729
29. Kanazawa, H., Miki, T., Tamura, F., Yura, T., & Futai, M. (1979) Proc. Natl. Acad. Sci. U.S.A. 76, 1126-1130
30. Gornall, A.G., Bardwill, C.S., & David, M.M. (1949) J. Biol. Chem. 177, 751-766

31. Bradford, M.M. (1976) Anal. Biochem. 72, 248-254
32. Fiske, C.H. & Subbarow, Y. (1925) J. Biol. Chem. 66, 375-400
33. Maeda, M., Kobayashi, H., Futai, M., & Anraku, Y. (1976)  
Biochem. Biophys. Res. Commun. 70, 228-234
34. Bragg, P.D. & Hou, C. (1975) Arch. Biochem. Biophys. 167, 311-321
35. Dunn, S.D. (1980) J. Biol. Chem. 255, 11857-11860
36. Lauquin, G., Pougeois, R., & Vignais, P.V. (1980) Biochemistry  
19, 4620-4626

## ACKNOWLEDGMENTS

I would like to express my great appreciation to Professor Y. Tonomura, Faculty of Science, Osaka University, and Professor M. Futai, Faculty of Pharmaceutical Sciences, Okayama University, and Dr. T. Nakamura, National Cardiovascular Center Research Institute, for their guidances, many valuable suggestions, and continuous encouragements during the course of this work.

I am greatly indebted to Dr. T. Watanabe, Faculty of Science, Osaka University, who performed the synthesis of DNS-ATP with his great ability in organic chemistry.

I am grateful to Dr. H. Kanazawa, Faculty of Pharmaceutical Sciences, Okayama University, and Dr. Y. Fukumori and Professor T. Yamanaka, Faculty of Science, Osaka University, for large scale culture of E. coli. Ms. K. Takeda, Faculty of Pharmaceutical Sciences, Okayama University, kindly supplied me the preparations of  $EF_1$  and its subunits.

I am also grateful to many members of Professor Tonomura's laboratory for their help in the preparation of beef heart mitochondria.

Finally, I want to extend my thanks to Professor Y. Orii, Medical School, Kyoto University, and Dr. R. E. Yantorno, Faculty of Science, Osaka University, for their valuable discussion and help in the preparation of this thesis in English.

## LIST OF PUBLICATIONS

1. Calorimetric studies of heat of respiration of mitochondria.  
Nakamura, T. & Matsuoka, I. (1978) J. Biochem. 84, 39-46
2. Calorimetric studies of the heat of respiration of mitochondria.  
Matsuoka, I., Watanabe, T., & Nakamura, T. (1978) Frontiers of Biological Energetics Vol. 1, pp. 689-697, Academic Press, Inc., New York
3. Reversible effects of fatty acids on respiration, oxidative phosphorylation, and heat production of rat liver mitochondria.  
Matsuoka, I. & Nakamura, T. (1979) J. Biochem. 86, 675-681
4. Comparative studies on the effects of linoleate and methyl linoleate and their hydroperoxides on the respiration and reactivities of rat heart mitochondria. Shiotani, A.  
Watanabe, T., Matsuoka, I., & Nakamura, T. (1980) J. Biochem. 88, 677-683
5. Reaction mechanism of the ATPase activity of mitochondrial  $F_1$ , studied by using a fluorescent ATP analog, 2'-(5-dimethylaminonaphthalene-1-sulfonyl) amino-2'-deoxyATP. Matsuoka, I., Watanabe, T., & Tonomura, Y. (1981) J. Biochem. 90, 967-989
6. Reactions of fluorescent ATP analog, 2'-(5-dimethylaminonaphthalene-1-sulfonyl) amino-2'-deoxyATP with E. coli  $F_1$ -ATPase and its subunits. Matsuoka, I., Takeda, K., Futai, M., & Tonomura, Y. submitted to J. Biochem.